THESIS

NUMERICAL SIMULATION DIAGNOSTICS OF A FLASH FLOOD EVENT IN JEDDAH, SAUDI ARABIA

Submitted by

Ahmad Samman

Department of Atmospheric Science

In partial fulfillment of the requirements

For the Degree of Master of Science

Colorado State University

Fort Collins, Colorado

Spring 2014

Master's Committee:

Advisor: William R. Cotton

Russ Schumacher
Darrell G. Fontane

ABSTRACT

NUMERICAL SIMULATION DIAGNOSTICS OF A FLASH FLOOD EVENT IN JEDDAH, SAUDI ARABIA

On 26 January 2011, a severe storm hit the city of Jeddah, the second largest city in the Kingdom of Saudi Arabia. The storm resulted in heavy rainfall, which produced a flash flood in a short period of time. This event caused at least eleven fatalities and more than 114 injuries. Unfortunately, the observed rainfall data are limited to the weather station at King Abdul Aziz International airport, which is north of the city, while the most extreme precipitation occurred over the southern part of the city. This observation was useful to compare simulation result even though it does not reflect the severity of the event.

The Regional Atmospheric Modeling System (RAMS) developed at Colorado State University was used to study this storm event. RAMS simulations indicted that a quasi-stationary Mesoscale convective system developed over the city of Jeddah and lasted for several hours. It was the source of the huge amount of rainfall. The model computed a total rainfall of more than 110 mm in the southern part of the city, where the flash flood occurred. This precipitation estimation was confirmed by the actual observation of the weather radar. While the annual rainfall in Jeddah during the winter varies from 50 to 100 mm, the amount of the rainfall resulting from this storm event exceeded the climatological total annual rainfall.

The simulation of this event showed that warm sea surface temperature, combined with high humidity in the lower atmosphere and a large amount of convective available potential

energy (CAPE) provided a favorable environment for convection. It also showed the presence of a cyclonic system over the north and eastern parts of the Mediterranean Sea, and a subtropical anti-cyclone over Northeastern Africa that contributed to cold air advection bringing cold air to the Jeddah area. In addition, an anti-cyclone (blocking) centered over east and southeastern parts of the Arabian Peninsula and the Arabian Sea produced a low level jet over the southern part of the Red Sea, which transported large water vapor amounts over Jeddah. The simulation results showed that the main driver behind the storm was the interaction between these systems over the city of Jeddah (an urban heat island) that produced strong low-level convergence.

Several sensitivity experiments were carried out showed that other variables could have contributed to storm severity as well. Those sensitivity experiments included several simulations in which the following variables were changed: physiographic properties were altered by removing the water surfaces, removing the urban heat island environment from the model, and changing the concentration of cloud condensation nuclei. The results of these sensitivity experiments showed that these properties have significant effects on the storm formation and severity.

ACKNOWLEDGMENT

I would like to acknowledge and greatly thank the following people who have made the completion of this thesis possible:

I thank my advisor, Dr. William R. Cotton for giving me the opportunity to work with one of the best scientists in our field. I also thank him for his helpful discussion and valuable support during the entire process of writing this thesis. I thank him for making me look at life from a bright and sunny side. I would also like to thank Dr. Russ Schumacher for his valuable instructions and comments, and for agreeing to review my work and offer valuable feedback. I would like to thank Dr. Darrell G. Fontane for agreeing to be in my committee and for his encouragement and his precious insights.

Outside of my committee members, I would like to thank Dr. Gustavo Carrio for helping me develop some of the code used in this research, and for the very helpful and valuable discussions. Similarly, I thank Dr. Steven Miller for support with satellite products used in the study as well as my colleague Ayman Albar from the Presidency of Meteorology and Environment for supporting me with the radar observations. I additionally would like to thank Theodore Letcher, Michal Clavner, and Vandana Jha for their valuable discussions. I also would like to acknowledge any one who has helped me move toward writing this thesis including professors, computer technicians, colleagues, and friends.

Finally, but most importantly, I would like to thank my wife, Wijdan, and my sons, Osaid and Owais, for their absolute support during this endeavor. I could not have accomplished this without them.

TABLE OF CONTENTS

LIST OF TABLES

LIST OF FIGURES

CHAPTER 1: INTRODUCTION

1.1. Motivation

The city of Jeddah, the second largest city in the Kingdom of Saudi Arabia (KSA), was afflicted twice in less than two years by severe storms that resulted in flash floods. The first storm was on 25 November 2009, which was declared a national disaster in the country. In this event, 122 people were killed and about 350 were reported missing. The property damages from this storm is estimated to be about four billion Saudi Riyals (one billion U.S. Dollars). More than 90 millimeters (3.5 inches) of rain fell over Jeddah in four hours.

The second storm occurred on 26 January 2011, when the total rainfall exceeded the 90 mm recorded during the 25 November 2009 flash flood, where the recorded rainfall was about 111 millimeters (4.3 inches) in about five hours. This event caused at least 11 fatalities and more than 114 were injured. The losses in this event were estimated to be about seventeen billion Saudi Riyals (five billion U. S. Dollars). In both events, the precipitation amount exceeded the total annual rainfall for Jeddah for the entire year (about 50 mm), and these events were the heaviest rainfall events in KSA in the last and the current decade.

Jeddah (study area) is considered the economic capital of the country and the largest seaport along the west coast with a population of about 5.1 million and an estimated area of 5,460 square kilometers. Jeddah is a destination for many Saudi tourists year around because it is a hub of businesses and finance, in addition to the availability of merchandise and goods. Jeddah is the principal gateway to Makkah, Islam's holiest city located 80 km east of Jeddah, which Muslims are required to visit at least once in their life to perform a pilgrimage.

Flash floods have become the main fatality producer from convective storm related events in the world (Doswell et al., 1996). Flash flood events caused more fatalities than any other severe weather phenomena, including tornadoes, hurricanes, and lightning in the United States (the National Oceanic and Atmospheric Administration [NOAA 2012]). In addition, flash floods can cause harsh damage to main roads, infrastructures, and properties. Figure 1.1 shows an example of a severe flash flood impact on a main highway in Jeddah.

Flash floods can be produced from a quasi-stationary, or slow moving, high-intensity thunderstorm over an area in a short period of time. It usually occurs suddenly and the duration is a few hours to half day, and rarely for more than one day, while the time of the peak of the storm varies from ten minutes to a few hours (Lin, 1999). Although the probability of floods occurrence in arid and semi-arid lands, such as KSA, is indeed very small (Lin, 1999), still there is a chance for them to occur (Maddox et al., 1980). Flash floods are usually related to the local physiography, as well as mesoscale, and small synoptic scale weather systems. Thus, forecasting flash floods is considered a difficult mission.

When factors such as severe storms, steep slope catchments, and poor vegetation cover exist, this combination will result in a high-velocity flow and rapidly rising water (Smith and Ward, 1998). In KSA, many different places have these factors and are subjected to flash flood events. This includes Jeddah and most of the areas along the west coast that extends from north to south, west of the mountains, especially in the winter season. Therefore, it is important to study, conduct research, and be able to improve forecasts of flash floods, and be able to warn people to minimize deaths and avoid disasters.

A couple of previous studies were conducted to analyze the severe storm that occurred on November 25, 2009 (AlKhalaf and Abdel Basset, 2013; Haggag and El-Badry, 2013). This study

will present a diagnostic analysis of the heavy rainfall of the severe storm that occurred on January 26, 2011, and the result of a numerical simulation of the event using the Regional Atmospheric Modeling System (RAMS). This severe storm event produced heavy rainfall and resulted in large economic losses and loss of life, if it is better understood then future events may be better predicted.

Fig. 1.1: Main road destroyed by Jeddah's flood. From Alateeq (2011)

1.2. The position and physiography of Saudi Arabia and Jeddah

The Kingdom of Saudi Arabia has an estimated area of approximately 2.25 million square kilometers and occupies nearly eighty percent of the Arabian Peninsula. Its geographical limits are from 34 degrees east to 58 degrees east and from 15 degrees north to 32 degrees north (figure 1.2). The main geographic features of the Arabian Peninsula are the plateau that rises rapidly from the Red Sea and then falls away to the Arabian Gulf, as well as the highlands along the western edge. In the north, the western highlands exceed 1,500 meters in elevation, and then decrease to about 1,200 meters near Medina, and then rise again to more than 3,000 meters in the

southwest. The watershed of the peninsula is quite narrow (40 to 130 kilometers) along the west coast. Regional geography and topography are shown in figure 1.3.

In the interior, the land surface gradually descends into a broad plateau of average elevation of about 1,200 meters. Here, drainage is more dendritic and much more extensive than on the west and gentle slopes on the east. This area is 1,200 kilometers long and curves eastwards from north to south. The greatest of the ridges is Jebal Tuwayq (850 meters above sea level), which reaches some 1,100 meters in elevation, south of the capital of KSA (Riyadh). Throughout the interior are extensive desert sand surfaces, one of which is the world's largest continuous sand area, the Al-Rub Al-Khali (Empty Quarter). The Al-Rub Al-Khali dominates the southern part of KSA and covers about 650,000 square kilometers. It slopes from 1,100 meters in elevation near the border with Yemen, and goes northeastwards and down to almost sea level near the Arabian Gulf. A smaller sand area of about 57,000 square kilometers, called the Al-Nafud, is located in the northcentral part of the kingdom, and a great arc of sand (Al-Dahna) of about 1,400 kilometers in length joins Al-Nafud with al-Rub al-Khali. In the eastern parts, the plateau slopes down to the Arabian Gulf where there are numerous salt flats and marshes.

There are almost no permanent rivers or surface streams in the kingdom, but Wadis (Valleys) are numerous. Those leading to the Red Sea are short and steep, but those draining eastwards are longer and more developed, except in Al-Nafud and Al-Rub Al-Khali.

Jeddah is located in the western region of KSA, along the east coast of the Red Sea and west of the Al-Hejaz plateau. This location has steep-sloped mountains, a very narrow coastal plain, and shallow coastal water (Haggag and El-Badry 2013). The Al-Hejaz escarpment rises above 2,100 m, and the mountain wall drops on the western side of the plateau toward the Red Sea, where Jeddah is located on the narrow coastal plain. Based on these topographic factors,

Jeddah is located in an area consisting of 80 natural drainage systems (Qari, 2009), which make it susceptible to floods in the case of heavy precipitation resulting from a severe storm. Figure (1.4) shows a satellite image of the city of Jeddah and the mountains to the east.

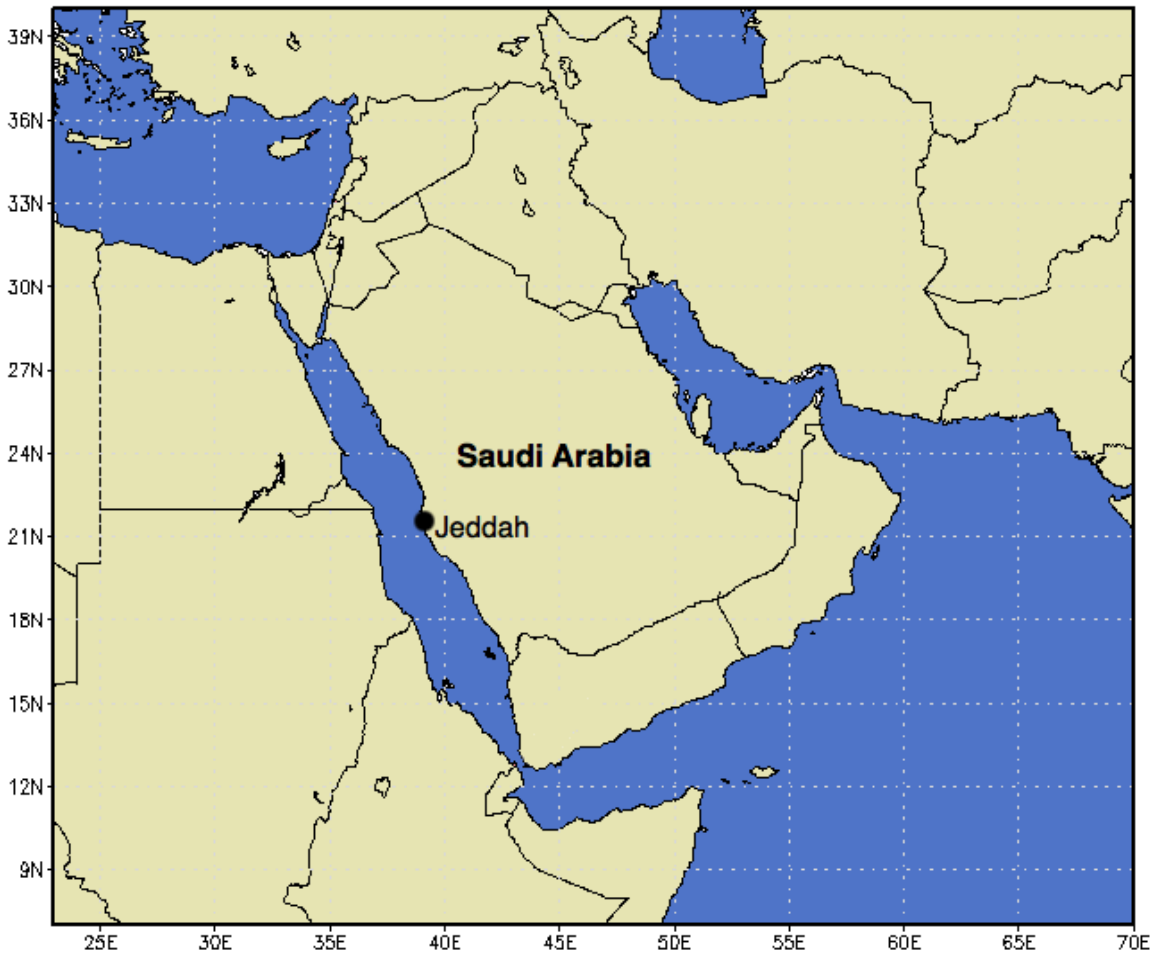

Fig. 1.2: The geographical limits of Saudi Arabia.

Fig. 1.3: The topography of Saudi Arabia. From http://www.ezilon.com/maps/asia/saudi-arabia-physical-maps.html

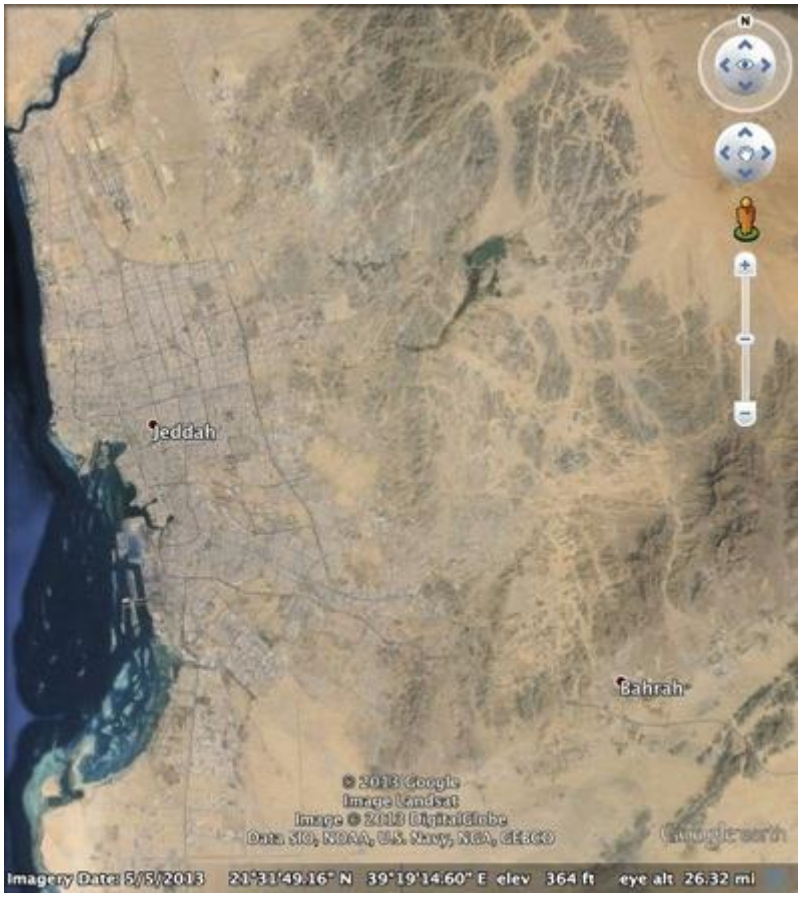

Fig. 1.4: Satellite image of Jeddah and the mountains to the east. Source "Jeddah." 21°31'49.16" N and 39°19'14.60" E. **Google Earth**. May 5, 2013. September 23, 2013.

1.3. The climate of Saudi Arabia and the area of study

Due to the complex topography and the extensive area of KSA, the climate of the country is diverse. These variable climatic characteristics are mainly based on the spatial and temporal temperature variability. In addition, the climate of the country is characterized by an inter-annual variability in temperature. In general, the climate of KSA is categorized as an arid (extreme desert and true desert) and semi-arid climate identified by hot and dry weather in the summer and cold and somewhat wet in the winter (Shmida, 1985). The weather is affected by many different air masses during the year. These air masses are polar continental, polar maritime, tropical

maritime and tropical continental described by Ghazanfar and Fisher (1998). Figure 1.5 illustrates these four basic air masses that affect the weather in the country.

The climate of KSA is generally warm with an average annual temperature of about 20°C (68°F) (De Pauw 2002). However, the average temperature in the summer reaches 45°C (113°F) and the temperature drops below 0°C (32°F) in the north and the southwestern parts of the country in the winter. The average temperature in the spring and autumn is about 29°C (84.2°F). In summer, the dominant synoptic feature over most of KSA is the thermal low that is considered an extension of the Indian low located over Asia, except for the southwestern region which is under the influence of the Red sea (monsoon) trough (Abdullah and Al-Mazroui, 1998). In winter, Abdullah and Al-Mazroui (1998) indicated that an interaction between the Mediterranean cyclones, Siberian high pressure, and the Red Sea trough control the climate of the northern part of the country. They mentioned that the main rain-producing synoptic systems in the northern part of the country are Mediterranean cyclones that move eastward associated with upper level troughs during an active phase of the subtropical and polar jets. The ridge of the Siberian high advects cold and dry air to the eastern and northeastern part of the country. The warm humid air that is advected from the Sudan low affects the southwestern part. Precipitation in this region usually occurs when warm moist air that is advected over the Red Sea interacts with cold air associated with the Siberian high. The general synoptic patterns that controls KSA climate in summer and winter are illustrated in Figure 1.6.

Rainfall in KSA generally occurs in winter and spring, usually from October to March, due to the Indian monsoon. However, it is anomalous, somewhat difficult to forecast, and low with an exception of the southwestern region of the country (Asir), which receives high rainfall. This part of the country receives more rainfall compared to the rest of the country due to its

orographic nature. Direct interaction of the moist westerly flow and the slopes of the mountains contribute to the total rainfall. Consequently, unique climatic features characterize the climate of this part of the country. Abdullah and Al-Mazroui (1998) has investigated and analyzed the rainfall in this region.

Regarding the precipitation mechanisms in KSA, generally the rain-producing synoptic system in the north of the country is associated with Mediterranean cyclones that move easterly (Abdullah and Al-Mazroui, 1998). The efficiency of these systems in rainfall production reduces southward. The rain-producing synoptic system in the southwestern region of the country is the Sudan cyclone and the Red Sea trough, when the moist, westerly flow interacts with the slopes of the mountains. The western region of the country is considered one of the regions that receive the lowest rainfall compared with the rest of the regions in the country. This lack of precipitation is generally caused by its location, which is not affected by either Mediterranean cyclones nor by the Sudan low.

The climate of Jeddah, which is located in the western region, is characterized by high temperatures and humidity in the summer due to its geographic location. These temperatures are about 40°C (104°F) when the city is affected by warm and dry air masses, usually when the whole country is under the influence of a thermal low extending from the Indian low located over Asia (Figure 1.6). The high humidity results from the high sea surface temperatures of the Red Sea. Qari (2009) indicated that a maximum temperature for the ten year period from 1990 to 1999 reached 49°C (120°F) between March and August, and the minimum temperature of 17.3°C (63.14°F) between January and February. He also indicated that relative humidity ranged between 100% during August through November, and 5% during January through March. In the

period between 2000 and 2011, the maximum temperature reached 52°C (125.6°F) in June, and the humidity range was between 100% and 5% for the same period.

Jeddah has experienced high precipitation amounts several times in the last four decades. Figure (1.7) shows rain gauge data (located at King Abdulaziz International Airport north of Jeddah) of these amounts. These events varied in occurrence between the months of November, December, and January. The city experienced relatively high precipitation in November in 1972, 1992, 2000, 2003 and 2009, while about 260 mm (10.2 inches) was also recorded in 1996, when the precipitation event lasted for about five days. Moreover, relatively high precipitation was recorded in December between 40 (1.5 inches) to 60 mm (2.4 inches) in 1977, 1989, 1993, and 2010. For January, Jeddah had a high precipitation amount of 100 mm (3.93 inches) in 1979, and precipitation ranged between 40 mm (1.5 inches) to 80 mm (3.1 inches) in 1970, 1992, 1998, and 1999. In the case of the 2011 flash flood event, the rain gauge at the airport recorded 76 mm (3 inches), but this does not reflect the range of severity of the precipitation, which occurred in the southern part of the city.

Precipitation in Jeddah is very sensitive to the synoptic regime. It generally occurs in winter, as mentioned before, when the interaction between the Mediterranean cyclones, the Siberian anticyclone, Sudan cyclone, and the Red Sea trough are in place. The topography of the region also plays an important role in precipitation. Subyani (2009) indicates that the topography influences the spatial variation of rainfall over Jeddah and its surroundings. He stated that based on observed rainfall rates from 1970 to 2005, the coastal part received about 100 mm (3.93 inches) per year, while the eastern part over the mountains received less than 220 mm (8.6 inches) per year.

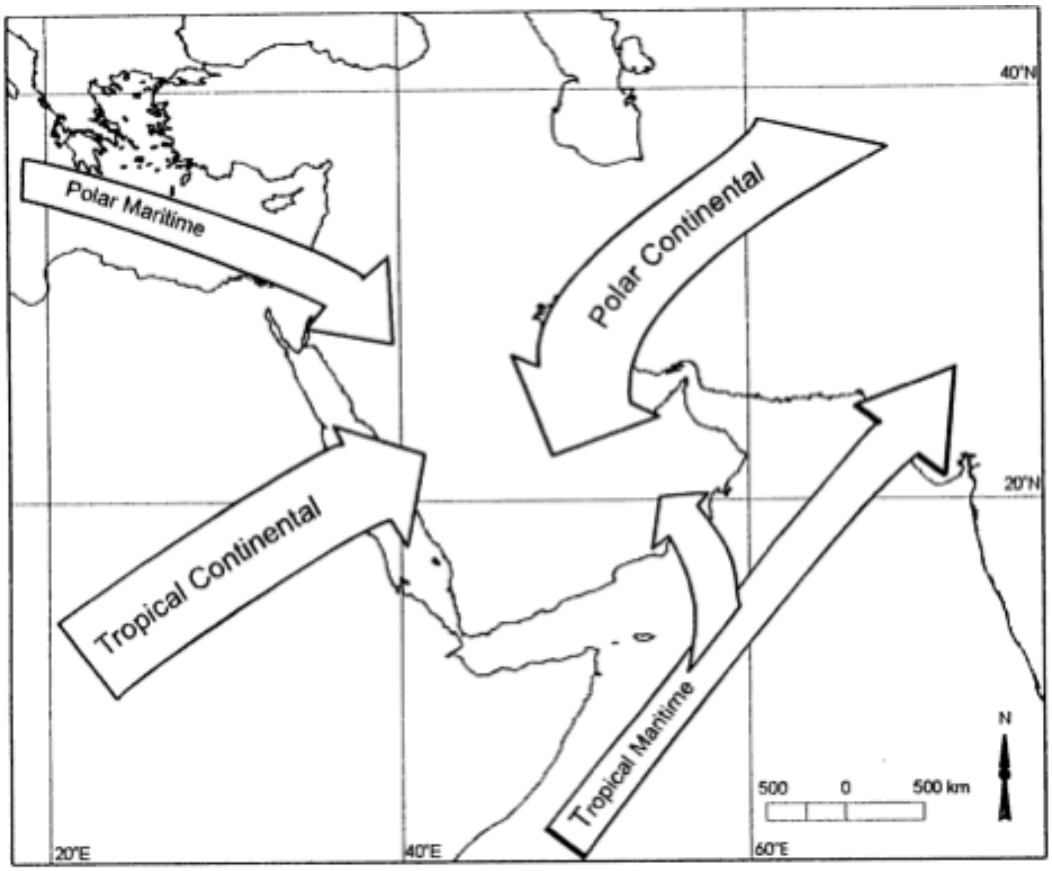

Fig. 1.5: Air masses affecting the Arabian Peninsula. From Ghazanfar and Fisher (1998).

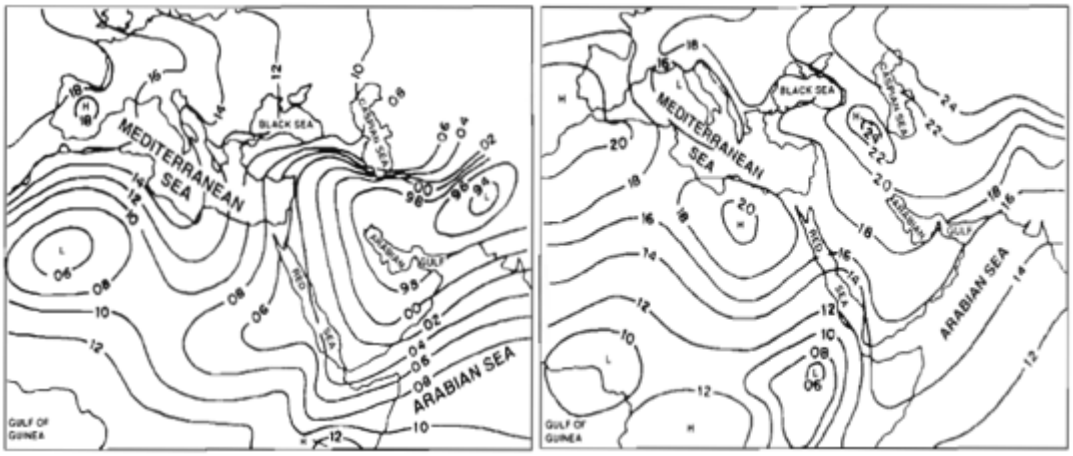

Fig. 1.6: The distribution of mean sea level pressure in summer (Left). The distribution of mean sea level pressure in winter (Right). From Abdullah and Al-Mazroui (1998).

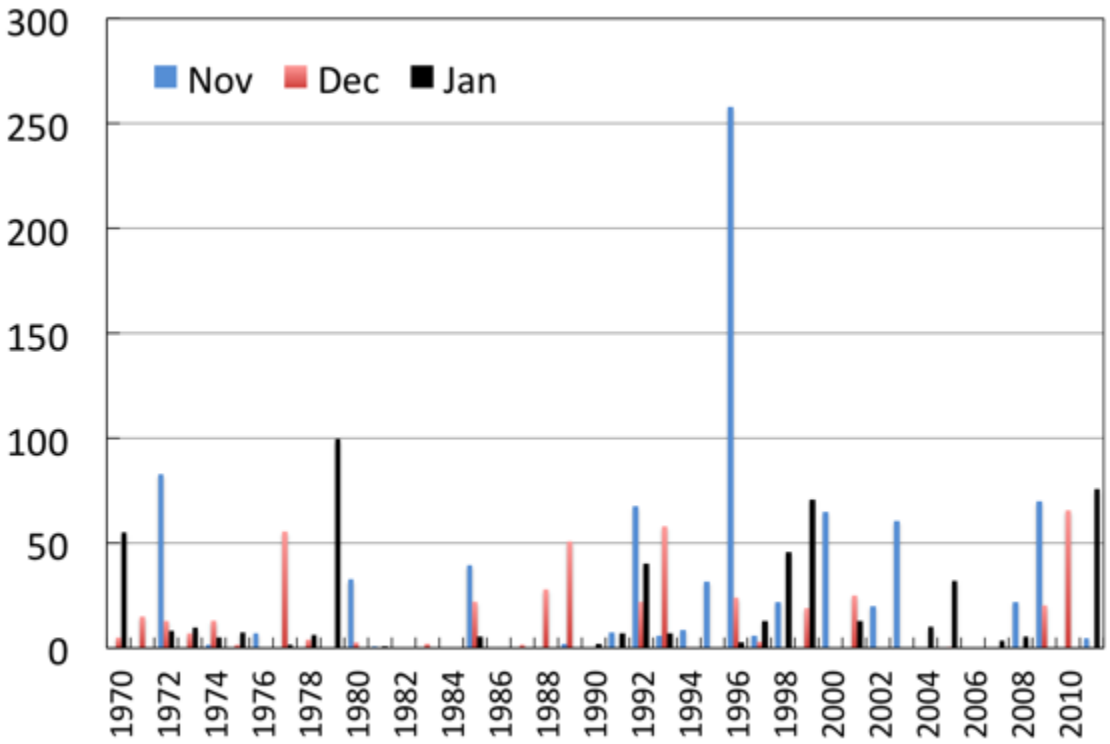

Fig. 1.7: Total rainfall in Jeddah for winter months, December, January, and February.

1.4. Objectives and aim of this thesis

The goal of this study is to investigate and examine the factors that led to the formation and the development of the severe storm that produced flash floods over Jeddah on 26 January 2011. This was accomplished by conducting numerical simulations using the Regional Atmospheric Modeling System (RAMS; Pielke et al., 1992; Cotton et al., 2003) in order to investigate the synoptic and mesoscale dynamics behind the storm formation, and to analyze and focus on: the mesoscale trigger mechanism, diagnosis of some physical quantities, and the effect of topography. This study also tests and examines the sensitivity of the storm severity and development to any change in various factors such as physiographic properties, synoptic dynamics, and aerosols concentration.

The thesis is organized as follows. Chapter 2 gives a detailed background about the previous studies related to flash floods and flash flood forecasting. Chapter 3 presents the description of the model, the data, and the domain that are used in the study. Synoptic and mesoscale analysis of the surface and the upper levels of the case study are presented in chapter 4. Chapter 5 will be concerned with the results of the numerical simulations and the sensitivity numerical experiments of the case study. Finally, the conclusions of this study as well as suggestions for future work will be presented in Chapter 6.

CHAPTER 2: BACKGROUND

Previous research related to flash floods and severe precipitation and their mechanisms are very limited in the Arabian Peninsula, although many studies have been conducted in the United States, Europe, and Asia. This could be due to the noticeable lack of precipitation in these areas, where deserts occupy a large percentage of its land. Even though the Arabian Peninsula has an arid to semi-arid climate, there is still a big chance for severe storms and extreme precipitation to occur. Previous generations in the country have spoken about many severe storms and heavy precipitation events that have occurred in the past and have caused destructive impacts in some places. But, due to the fact that weather data were not recorded until the early 1970s, people did not record their observations and scientists did not conduct research on them.

In general, flash flood forecasting has been the focus of much research for decades and it is considered a challenging mission. Doswell et al. (1996) developed an approach to forecasting the potential for a flash flood-producing storm. They argued that continuous heavy rainfall rates depend on the storm precipitation efficiency and involve rapid upward motion of very moist air, in addition to the speed of movement and the size of the system. Consequently, meteorological processes are considered for which these ingredients come together. For any given case, they found that the right mixture of the ingredients under variable synoptic and mesoscale situations controls the rainfall rates by determining which of the ingredients is most important. They concluded that the ingredients for flash floods are as follows. First, heavy precipitation, is generally the average rainfall rate (R) times the duration (D) of the rainfall $P = \bar{R}D$. High precipitation rate is a function of the precipitation efficiency (E), the rising air velocity (w), and the mixing ratio of the raising air (q), or $R = Ewq$. Second, it is necessary that conditions for

deep, moist convection occurs as well. Flash floods are generally a result of high rainfall rates associated with deep, moist convection. Deep, moist convection is associated with buoyancy, which is produced when a saturated air parcel lapse rate is less than the environment lapse rate rises, which means that the saturated parcel is warmer than the environment. Third, flash flood-producing storms must have a long duration. This depends on the system movement speed, the system size, and within-system variation in precipitation intensity. Finally, the storm type is important, such as whether a storm is multicell convection, supercell convection, squall lines, mesoscale convective systems, or non-convective precipitation systems combining these ingredients.

Many studies have been conducted regarding the dynamics and the mechanisms of flash flood-producing storms. Maddox et al. (1979) studied and examined quasi-stationary convective systems responsible for 150 flash flood events in the United States from the synoptic and mesoscale perspective. They were able to conclude from their analysis, some common features in many of the events. These features are for example, but not limited to, nighttime occurrence, the presence of an upper-level slow moving shortwave trough, and the presence of a large-scale ridge. A follow up study by Maddox et al. (1980) focused more on studying and analyzing the meteorological conditions of 61 flash flood events in the western United States. They concluded four characteristic synoptic patterns associated with the events, besides the presence of a strong 500 millibar (mb) trough and an intense surface cyclonic systems.

Three different studies examined a devastating flash flood in the Big Thompson canyon in Colorado on 31 July 1976 (Maddox et al. 1977; Caracena et al. 1979; and Cotton et al. 2003). Maddox et al. (1977) and Caracena et al. (1979) discussed the mesoscale processes of the storm development. They found that strong moist easterly low-level winds interacted with the

topography of the Front Range of the Rockies. Convective instability initiated with the orographic uplift, and south-southeasterly flow maintained the location of the system over the Big Thompson area.

Cotton et al. (2002) used the Regional Atmospheric Modeling System (RAMS) to simulate the event in addition to another five events (28 July 1997 Fort Collins storm, 31 July 1999 Dallas divide storm, 18-22 September 1997 storm in Park Range Storm, 4-6 September 1970 Southern San Juans storm, and 26 July 1999 Saguache Creek storm). The coarse resolution of the data used to initialize the model led to less successful simulations of the old events compared with more successful simulations for the more recent events. They found that convective storms are sensitive to the soil moisture field in addition to orography, while there were noticeable spatial and temporal errors in the simulations. It is important to note that in all cases extreme precipitation was simulated, but the resolution of physiography was not sufficient to place the storms in the observed watersheds for all cases.

In the Black Hills of South Dakota, a flash flood-producing storm was generated on 9-10 June 1972 and produced severe damage and deaths. Nair et al. (1997) studied this event by simulating the storm using RAMS. In their study, they conducted two different experiments, one using homogeneous initialization and the other using inhomogeneous initialization. Both simulations predicted the nature of the storm successfully, except that the inhomogeneous run was closer to the observation. The study indicated that the nature and the large-scale features of the storm were similar to the Big Thompson storm. They concluded that using inhomogeneous initialization enhanced the simulation and provided better flash flood forecasts and precipitation estimation.

Some other interesting research was conducted on flash flood events in Europe. Federico et al. (2008) conducted a numerical simulation to study and analyze a severe storm that occurred on 10-12 December 2003 over Calabria, southern Italy, where about 250 mm of precipitation was recorded over a large area. They used the RAMS numerical model, and they investigated the role of Calabrian orography, surface heat flux, and upper-level forcing. The synoptic forcing responsible for the event consisted of the presence of a deep surface low and an upper-level trough, which forced warm moist flow to rise over the Calabian orography. Their results showed that the orography of the area and the latent heat flux from the Mediterranean Sea played an important role in the storm intensity and the total precipitation amount. RAMS proved to be a suitable tool for flash flood forecasting in this case as well.

Romero et al. (2000) performed a study using the Pennsylvania State University – National Center for Atmospheric Research mesoscale model (MM5) on two extreme rainfall events over eastern Spain. The first event was on 3-4 November 1987, when the rainfall lasted for more than 30 hours and exceeded 800 mm in 24 hours, and the second event was on 20 October 1982, when the rainfall exceeded 400 mm and lasted for more than 12 hours. The model showed that both cases were characterized by a quasi-stationary mesoscale convective system. It also indicated the importance of latent heat release and the cyclogenesis generated due to topography that may have played an important role in producing low-level convergence and enhancing upslope winds. In both cases, the numerical model they used underestimated the total amount of precipitation, but it made a reasonable prediction of the spatial details of the field of precipitation and the duration of the events.

Another flash flood event occurred in the Llobregat basin in the Catalonia region of Spain on 10 June 2000 and was studied by Amengual et al. (2007). The researchers used the MM5

mesoscale model as well to force the Hydrologic Engineering Center's Hydrological Modeling System (HEC-HMS) in order to investigate and characterize the watershed hydrological response to this flash flood event. A reasonable reproduction of the discharge at the basin outlet demonstrated the mesoscale model capability of estimating the total precipitation.

In France, Ducrocq et al. (2002) conducted numerical simulations of five precipitation events. Two cases caused by a quasi-stationary system over southern France, and an extreme case of 12-13 November 1999 that produced a flood with recorded rainfall of above 100 mm and 500 mm respectively, and two convective systems produced localized flooding in the northern France. They evaluated the use of high-resolution grids in addition to advanced physical parameterization in the model in enhancing the result of the simulation for the extreme case. The study showed that using a high-resolution domain improved the results of the simulation for the extreme case, while there was no improvement in the other four cases. The authors attributed this failure to the initial conditions used in the model. They found that initializing the model using observational data resulted in better simulations. They also concluded that identifying the humidity fields made important differences in the quality of the simulations.

Senesi et al. (1996) studied a flash flood case that occurred in France on 22 September 1992, when the storm hit a city called Vaison-La-Romain in southern France in which 220 mm of rainfall was recorded in about three hours. They presented an analysis of the synoptic and complex mesoscale forcing that contributed to the storm development besides the orographic influences and its effects. The authors used two different models to simulate the storm and they predicted the severe storm successfully even though the spatial and temporal change was not realistic.

Akaeda et al. (1995) studied the evolution of a mesoscale convective system (MCS) that formed over Taiwan on 19 June 1987. In that event, the rainfall exceeded 100 mm. The study is interesting because the nature of the storm system is relatively similar to Jeddah's flash flood case in January 2011. They showed that the convective cells of the MCS formed repeatedly over the same area and produced stratiform rainfall that resulted in high precipitation totals. The interesting part in their study is the analysis of the factors contributing in the storm evolution and the heavy precipitation. The authors enumerated these factors and listed them as:

> 1) a moist, convectively unstable southerly flow of tropical origin, 2) a shallow convergence zone on the western side of the island dividing flow with northerly components from that with southerly components, 3) a quasi-stationary area of storm formation, 4) a mesoscale environment that produced a convective system with a favorable storm structure and movement.

The authors conducted a numerical simulation of the event and the main findings, in addition to the previous listed factors, were a quasi-stationary area of convergence near the observed convection, and the orographic role, which may have had a major role in maintaining the MCS.

Most of the research about flooding in the Arabian Peninsula, and specifically in the Jeddah area, is focused on the hydrological aspects of the watershed and the drainage systems. Subyani (2009) is an example, he studied the flood probability and the hydrological characteristic of some major wadis in western KSA, around and east of Jeddah. The paper presented a rainfall frequency analysis by using selected annual maximum 24-hour rainfall from 8 stations located in the wadis. However, the current study will focus on the meteorological aspects of the flood and give ample analysis of some previously conducted studies about the factors, characteristics, and properties on the formation and the development of the flash flood producing storms.

There are some other interesting meteorological studies that were conducted about flash flood storms in arid and semi-arid regions; three related events were conducted on the Arabian Peninsula region. Storms in these regions tend to be extremely intense and tragic due to their sudden occurrence in the early parts of the day, according to Li et al. (2003). They investigated a flash flood storm that hit Las Vegas, Nevada on 8 July 1999. The authors used RAMS to simulate this event and found that daytime surface heating along mountains slopes was the primary forcing mechanism of storm development in the simulation. However, the model did not do well in predicting the outflow from nighttime storms to the northeast of Las Vegas, which the authors believed was the main cause of the morning convection.

Another study of a flash flood event that took place in arid and semi-arid land was conducted by El-Sammany (2010). On 24 October 2008, a flash flood occurred over Wadi Watier in the Sinai Peninsula in Egypt. The author made a numerical simulation to investigate and analyze the event using The Weather Research and Forecast model (WRF). He wanted to test the reliability of the model in predicting flash floods in arid and semi-arid lands. His main finding was that the model proved that it is a reliable tool in flash flood prediction in an arid region, where the model forecast and the real measured rainfall were similar.

AlKhalaf and Abdel Basset (2013) investigated the storm that caused the flash flood over Jeddah in 25 November 2009 by studying the case in relation to isobaric absolute and relative vorticity and the isobaric potential vorticity. They concluded that upper level dynamics played a significant role in the initiation of the surface cyclogenesis responsible for this event. Their analysis indicated that an upper-level cold trough over the eastern Mediterranean and a warm high over southern Saudi Arabia, in addition to the availability of water vapor transported by a southerly low-level jet contributed to the heavy rainfall.

Another recent study conducted by Haggag and El-Badry (2013) also investigated the same flash flood event occurring over Jeddah in 25 November 2009. The authors studied the synoptic and mesoscale characteristics of the event and utilized the MM5 model to simulate the storm. Their simulation of the rainfall predicted over 400 mm and they attributed the heavy rainfall to a quasi-stationary MCS that formed over Jeddah and lasted for about 8 hours. Their synoptic analysis showed the synchronous presence of an anticyclone over the southeastern part of the Arabian Peninsula provided the moisture over the Red Sea and a Mediterranean cyclone centered over the eastern Mediterranean Sea, which produced a convergence zone over the central Red Sea. The authors conjectured, based on their simulation, that low-level convergence, atmospheric instability and topography played a role in enhancing the storm.

Many studied have agreed on combined synoptic and mesoscale features that could generate flash flood producing storms. The synoptic features can be summarized as a presence of an anticyclone that provides warm and moist flow and weak winds aloft, combined with the presence of a cyclonic system and an upper-level trough. The mesoscale features focus more on the vertical structure of the atmosphere, the storm duration, the storm propagation, and the orographic surfaces. Most numerical models used to simulate flash flood-producing storms were reliable tools, even though some models surpassed others in some of the physical properties and parameterization.

This research follows the same approach of Haggag and El-Badry (2013) to some extent in the first part, but will focus more on discovering the main factors that have played a role in the storm's evolution and severity in the second part. This study will run different simulations using RAMS to investigate and analyze the flash flood event occurred over Jeddah in 26 January 2011, since this event produced more rainfall and caused more economic losses and devastating

damages than the 2009 storm. This study will accurately analyze and classify the ingredients that contributed to this event. It will also conduct different numerical simulations to investigate the role of water surfaces, urban heat island effect, and cloud condensation nuclei (CCN) concentrations.

CHAPTER 3: DATA AND METHODOLOGY

3.1. Model overview

The model used in this study is the Regional Atmospheric Modeling system (RAMS) version 6.0 (Pielke et al., 1992; Cotton et al., 2003). This model has been developed in the Department of Atmospheric Science at Colorado State University (CSU), and, in its original configuration, was a combination of different numerical weather simulation models (Pielke et al., 1992). Cotton et al. (2003) mentioned that these models are the sea breeze mesoscale model (Mahrer and Pielke, 1977), the CSU cloud/mesoscale model (Tripoli and Cotton, 1982), and a hydrostatic version of the cloud model (Tremback, 1990).

RAMS has a wide variety of options, which make it designed to serve the researchers for a broad range of applications. Some of the variety of structures and features in the model include: a resolution ranging from less than a meter to a hundred kilometers, a domain ranging from a few kilometers to the entire globe, and a combination of physical options (Cotton et al., 2003).

RAMS is frequently used to simulate mesoscale phenomena, typically with a horizontal scale from 0.5 km to 50 km (Cotton et al., 2003). It has an interactive nested-grid capability, which is necessary to simulate phenomena that demand fine grid spacing (Nair et al., 1997). The model uses a sigma-z terrain-following coordinate in the vertical, and horizontally on the earth surface, grids are mapped using a polar stereographic projection (Cotton et al., 1994). At the lateral boundary of each grid, the basic radiative condition (Klemp and Wilhelmson, 1978a) is applied to the normal velocity components (Lerach, 2012). RAMS uses Harrington's (1997)

radiation scheme, which is a calculation of upwelling and downwelling radiative components using a two-stream structure (Lerach, 2012).

The model can be initialized from different large-scale historical and surface datasets, such as the National Center of Atmospheric Research (NCAR), National Center for Environmental Prediction (NCEP), National Climate Data Center (NCDC), or the European Center for Medium-Range Weather Forecasts (ECMWF). At the initialization step, the fields are interpolated from the coarse grid to the fine grids to complete the initialization process. Furthermore, the model has the ability for available sounding or surface data to be inputted by the user (Pielke et al., 1992).

Fine grid spacing is needed in order to resolve storm-scale processes and features (van den Heever and Cotton, 2004). Thus, for mesoscale cases such as the severe rainstorm event over Jeddah, high horizontal resolution grids are recommended at about 1 km to successfully resolve convection on the mesoscale (Bryan et al., 2003; Schwartz et al., 2009; Weisman et al., 1997). A large domain of coarse grid spacing is required to cover the entire region important to the synoptic dynamics. For the coarse grid spacing, convection parameterization must be used and there are two different schemes that can be utilized to apply convective parameterization. The first scheme is the Kuo scheme (Kuo, 1974), and the second scheme is the Kain-Fritsch (Kain and Fritsch, 1990). A detailed description on the model configuration used in this study will be discussed in the next sections.

3.2. Data

Previous sections have mentioned that RAMS can be initialized by using various different data sets. This study used the large-scale reanalysis data from NCEP/UCAR (Kalney et

al., 1996) and ECMWF ERA-40 for 26 January 0000 UTC to 1200 UTC. The data have a resolution of 2.5 X 2.5 degree latitude/longitude grid and was archived every six hours. The data are composed of seventeen pressure levels, and it includes three-dimensional variables of U and V wind components, geopotential heights, temperature, and relative humidity. In addition, the data includes the two-dimensional variable sea level pressure. This data set provided the initialization and the lateral boundary conditions for the coarse grid. Then, it was interpolated to the fine grid to complete the initialization process.

The Global Geological Survey (USGS) surface data were used. USGS data includes terrain height, sea surface temperature, vegetation type, soil textural class, and Normalized Difference Vegetation Index (NDVI) data.

Weather station data from the weather station at King Abdulaziz International Airport (21.42 N, 39.11 E) in Jeddah was provided from the Presidency of Meteorology and Environment (PME) in Saudi Arabia. This data included such variables as: the maximum and minimum temperatures, dew point temperature, pressure, wind speed and direction, relative humidity and total rainfall, were all used to calculate general climatic features for Jeddah.

Radar and satellite images of the event for the day of the storm (also obtained from PME) were used in the study to evaluate the model's performance, including the amount of precipitation on the day of the storm. In addition, Tropical Rainfall Measurement Mission (TRMM 3B42) data with a 0.25 X 0.25 resolution were likewise used to compare model-predicted and observed total rainfall on the day of the storm.

3.3. Model set up and experimental design

In this study, a multiple nested grid configuration was used. Coarse grid spacing is required in order to allow useful simulation of synoptic and mesoscale dynamics, while fine grid spacing is required to allow the simulation of convective scale features over the city of Jeddah. In order to successfully simulate the convective storm over Jeddah, three grids were used and centered over the area of Jeddah (21.50° N, 39.10° E) and it's surrounding. Figure 3.1 shows the domain of study that was utilized to simulate the storm over Jeddah. The model's domain spans Saudi Arabia, Jordan, Syria, Iraq, Iran, Egypt, Sudan, Ethiopia, Eastern Mediterranean, and the Gulf of Aden. Grid 1 covered the whole domain of the study and extended from 5° N to 37° N and from 23° E to 55° E. The horizontal grid spacing of grid 1 was 20 km with 200 X 200 grid points.

A finer grid (grid 2) extended from 17° N to 26° N and from 34° E to 44° E. It is nested within the coarse grid and had a grid spacing of 5 km in both X and Y and covered the central Red Sea and mostly the western region of Saudi Arabia. The latter nested grid had 198 X 198 grid points. The finest grid (grid 3) is nested within the second grid. It extends from 20.6° N to 22.3° N and from 38.1° E to 40.1° E. It covered an area of 4,000 km^2 and centered over Jeddah. The grid spacing in this fine grid was 1 km, with 200 X 200 grid points in the horizontal. The grid configuration used for this study is shown in Figure 3.2.

These simulations used 35 vertical levels extending from the surface to 13 km, using a stretching vertical grid with its lowest level at 100 m. A stretch ratio of 1.12 was used to stretch the vertical grid spacing until the vertical expansion of the grid spacing reached 750 m above, then the grid spacing was kept constant. The time steps for the simulations for grid 1, 2, and 3 were 10, 2, and 1 s, respectively. For all numerical experiments, the model was initialized and

nudged at the lateral boundary using NCEP and ECMWF data sets starting from 0000 UTC on 26 January and the simulation duration was 12 hours until 1200 UTC. It is worth mentioning that using the ECMWF data set resulted in under-estimation of the precipitation and did not initiate convection. Thus, the NCEP dataset was used for all of the simulations. The details of the model set up are shown in Table 1.

Several different experiments were conducted in order to test the sensitivity of the storm formation and severity to various factors. The first experiment was conducted to investigate the role of the sea in enhancing the storm by performing two runs. The first run was conducted using actual water surfaces, while the second run was conducted by removing the water surfaces from the model. Another experiment focused on investigating the role of the urban heat island effect on this event. The latter runs considered the city of Jeddah along with an urban model to examine the role of the city. By conducting the two runs, one using the urban model and another (*no city*) run, the urban environment influence on the storm formation and the precipitation was examined.

In addition, more experiments were conducted to test the sensitivity of the storm evolution and severity to the change in the number concentration of cloud condensation nuclei (CCN). This experiment included running four simulations for different CCN concentrations starting from inputting low values and increasing gradually to high values. A detailed discussion on the sensitivity of the storm formation and severity will be presented in chapter 4.

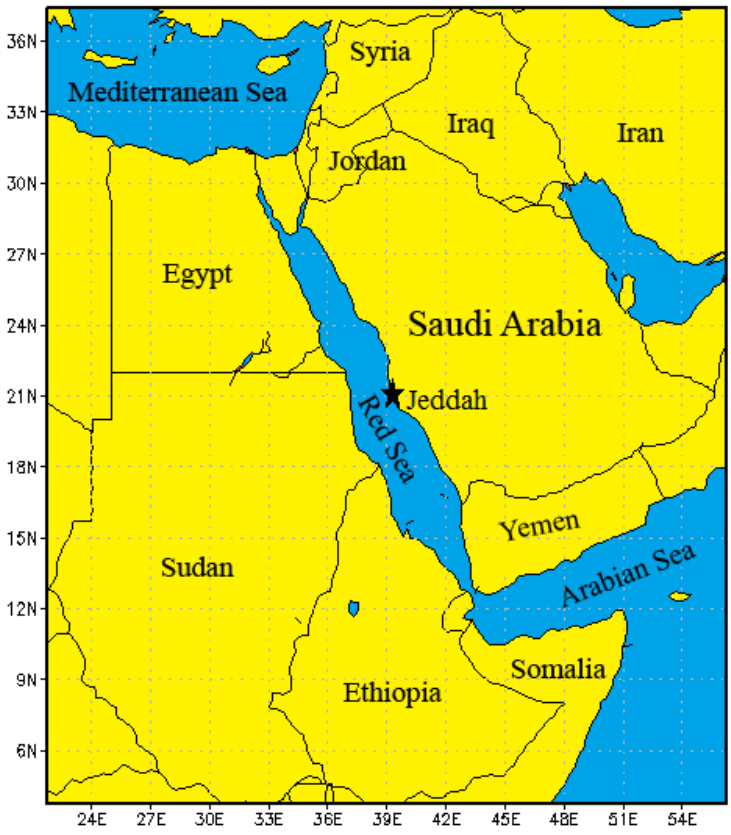

Fig. 3.1: The domain of study and the location of Jeddah.

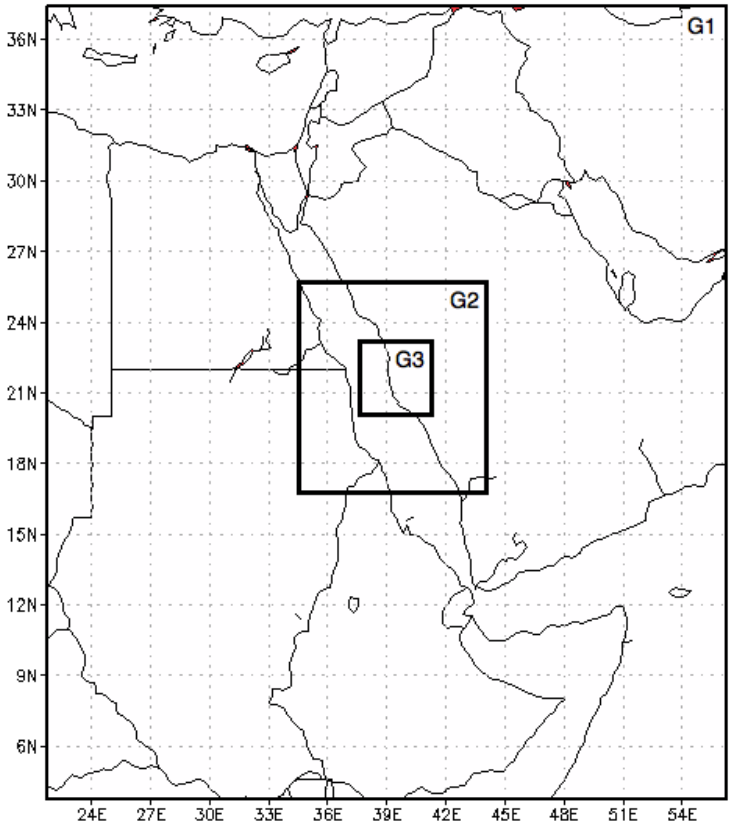

Fig. 3.2: RAMS nested grid configuration, from largest to smallest, grid1 to 3 (labeled in upper right of grid).

Table 1: RAMS model configuration

Model Aspect	Setting
Grids	Grid 1 200X200 Δx, Δy = 20000m Grid 2 198X198 Δx, Δy = 5000m Grid 3 200X200 Δx, Δy = 1000m
Domain Center (Lat, Lon)	21.5° N, 39.1° E
Vertical Structure	35 vertical-levels: Δz: 100m at the surface Stretched to a maximum of 750m Model top: 12000m
Initialization	NCEP, 26 January 2011, 0000 UTC
Nudging	NCEP, 26 January 2011, 0600 UTC NCEP, 26 January 2011, 1200 UTC
Time Steps	10, 2, 1 s, for Grid 1,2, and 3 respectively
Simulation Duration	12 h
Radiation	Harrington
Boundary Condition	Klemp-Wilhemson
Cumulus Parameterization	Kain-Fritsch for grids 1 and 2

CHAPTER 4: THE CASE STUDY

4.1. Synoptic overview

The precipitation over the city of Jeddah started on 26 January 2011 from about 03Z and lasted for about 6 hours. The rainfall started as light to moderate rain until the precipitation maximized in the morning time between 08Z and 11Z, prior the occurrence of the flood at about noontime. It was previously mentioned that the main synoptic pattern usually responsible for precipitation in the city of Jeddah is the presence of winter Mediterranean cyclogenesis associated with an anticyclone over the southeastern part of the Arabian Peninsula that is considered an extension of the Siberian High pressure system. This chapter will contain an analysis and discussion of the synoptic and mesoscale processes that were responsible for the storm formation and development.

4.1.1. Surface analysis

The synoptic pattern for the flash flood case occurred on 26 January 2011 which is similar to the prevalent winter pattern described previously. On 24 January at 06Z, a case of winter cyclogenesis started over the Mediterranean and went until 26 January at 12Z when it started decaying. Two anticyclones were present associated with the Mediterranean cyclogenesis. The first anticyclone was a quasi-stationary anticyclone dominating the weather of the Arabian Peninsula during the period between the 23rd and 27th of January 2011. The second anticyclone was a subtropical anticyclone over northern Africa, specifically over western Egypt. The mean sea level pressure charts are shown in Figure 4.1, and the 1000 hPa charts depict contours of heights with 30 geopotential meter (gpm) increments shown in Figure 4.5, determine the starting

time of the Mediterranean cyclone formation (growth) at 12Z on the 24th (Figures 4.1c and 4.5c). In addition, the charts show the presence of the quasi-stationary anticyclone over the eastern part of the Arabian Peninsula, and its continued existence continued for 24, 25 and 26 January.

Figure 4.2, 4.3, 4.6, and 4.7 show the deepening of the cyclonic system over the north of the Mediterranean Sea starting from 00Z on the 25th (Figure 4.2a and 4.6a). Then, the system evolved into its mature stage on 25 January at 12Z (Figure 4.2c and4.6c). This stage lasted for about 18 hours until the cyclone started to decay at 06Z on the 26th (Figure 4.3b and 4.7b). In addition, the figures show the domination of the subtropical anticyclone over northeastern Africa starting on 25 January at 12Z (Figure 4.2c and 4.6c) and lasting until 12Z on 26 January (Figure 4.3c and 4.7c). In addition, the inverted v-shaped Red Sea trough associated with the Sudan cyclone was present over the Red Sea area on 24 January at 00Z (Figure 4.1a and 4.5a) and started to oscillate northward to cover the entire Red Sea region the following two days (Figure 4.2 and 4.6).

To show specific locations of the three involved systems, Figure 4.4 shows charts of 1000 hPa heights and relative humidity for 24-26 of January at 00Z. These charts clearly describe how the Mediterranean cyclone deepened and shifted toward the northeastern Mediterranean Sea within the three-day period. At 00Z on the 24th (Figure 4.4a), the Mediterranean cyclone was not present over the eastern part of the Mediterranean and still did not yet have its impact on the Middle East. On the 25th at 00Z (Figure 4.4b), the Mediterranean cyclone started to shift toward the east until it began to deepen over Turkey in the area between 35°N and 40°N and 30°E and 35°E (Figure 4.4c), where the cyclone had a major influence in providing the cold air advection aloft in addition to the subtropical anticyclone over northeastern Africa.

The Mediterranean cyclone brought cold air from northern Europe (polar maritime) to the Mediterranean Sea area. The presence of the subtropical anticyclone over northeastern Africa also contributed in bringing some of the cold air in the Mediterranean area to the northern area of the Red Sea. On the other hand, the presence of the quasi-stationary anticyclone contributed to advecting warm and moist air (tropical maritime) from the Indian Ocean and Arabian Sea toward the southern Red Sea area. Interaction between the cold air advection from the north toward the south, and the warm moist air from the south toward the north over the central Red Sea area, is basically the main mechanism responsible for this storm's formation and development, taking into account that any shifting in one of the three systems could obstruct the storm formation. These three synoptic pressure systems contributed to the Jeddah's storm formation and severity.

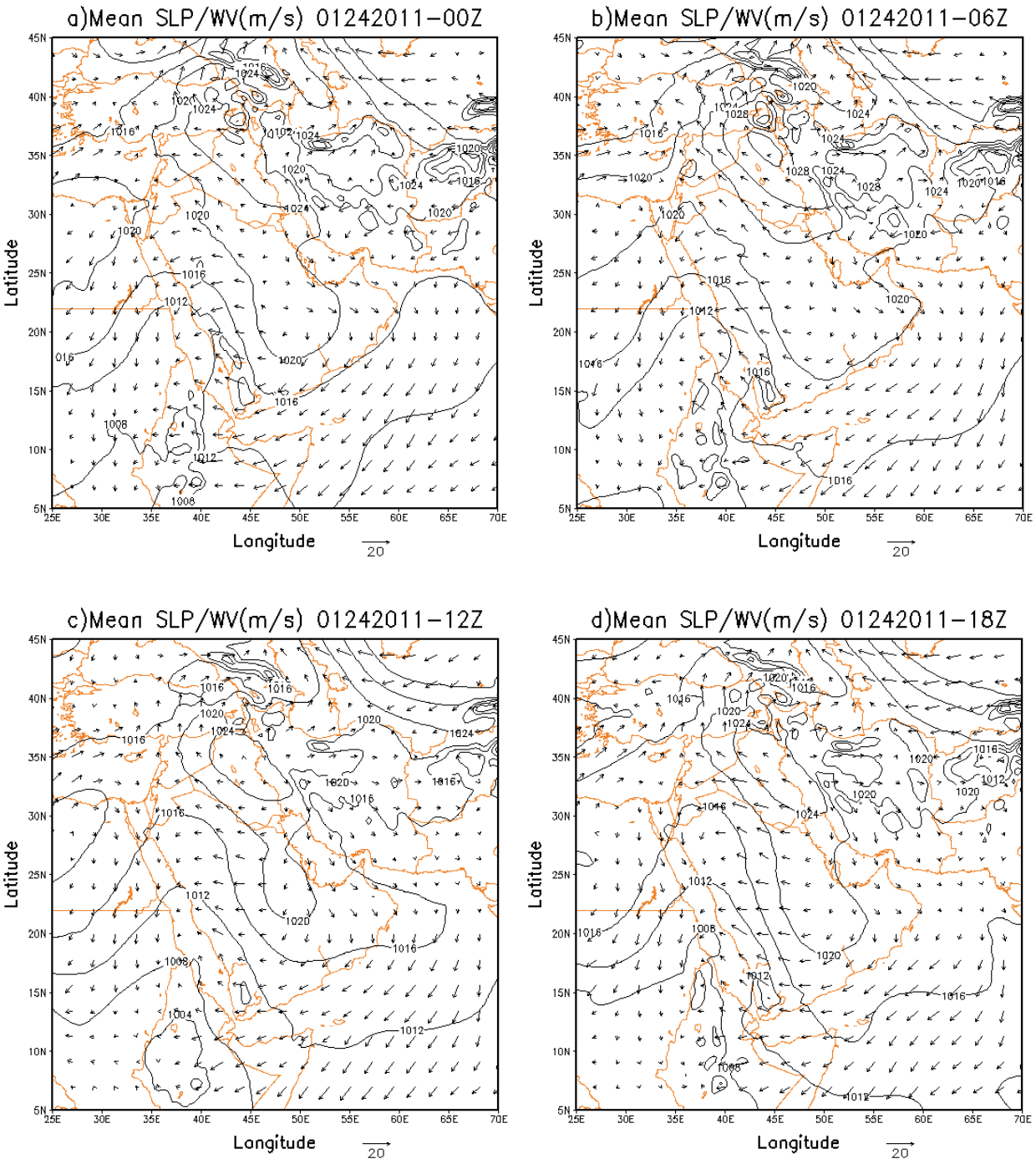

Fig 4.1: Mean Sea level pressure (contours) and wind vectors (m/s) for the 24th of January 2011 for 00Z, 06Z, 12Z, and 18Z.

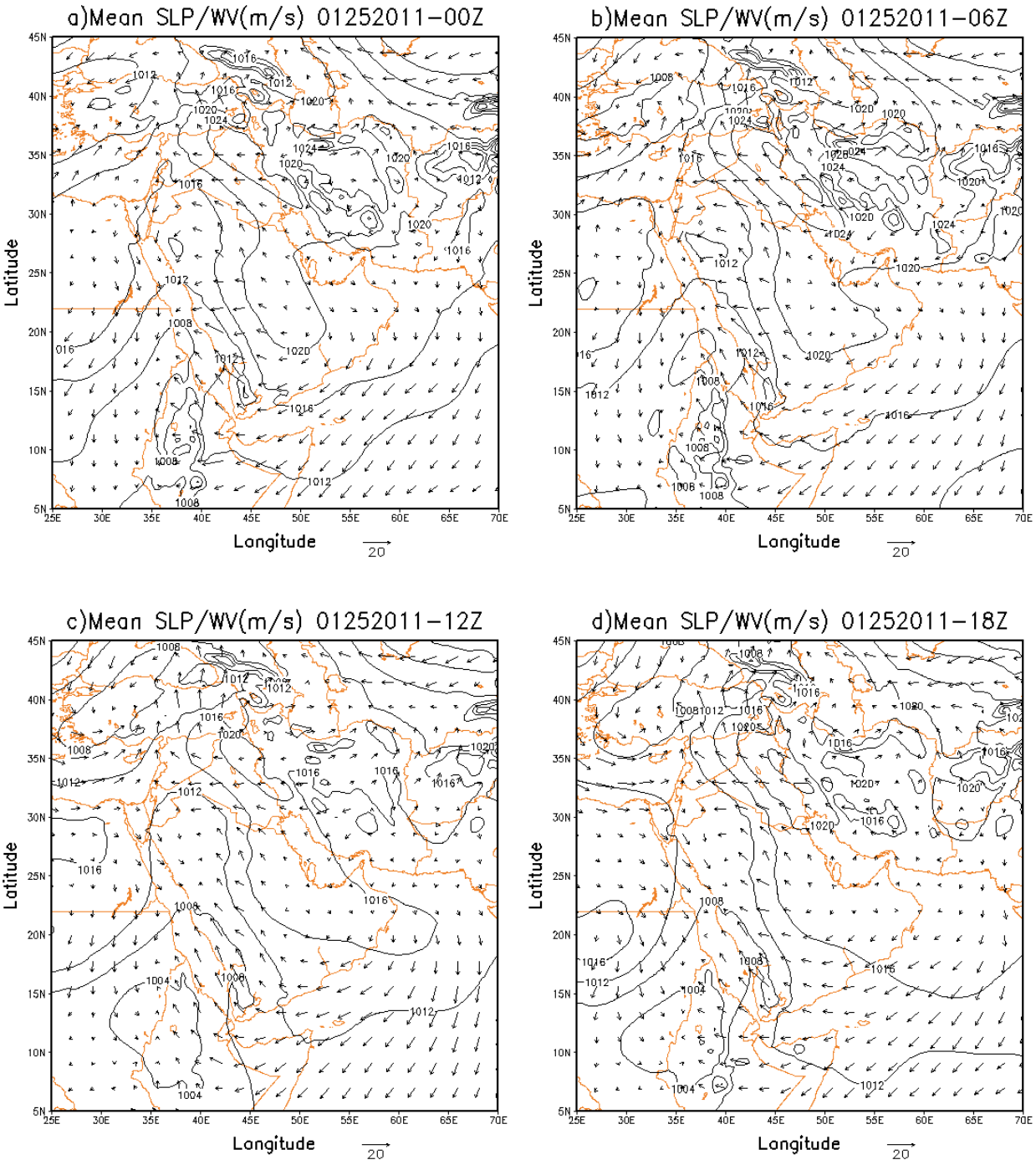

Fig 4.2: Same as in Figure 4.1, but for the 25th of January 2011.

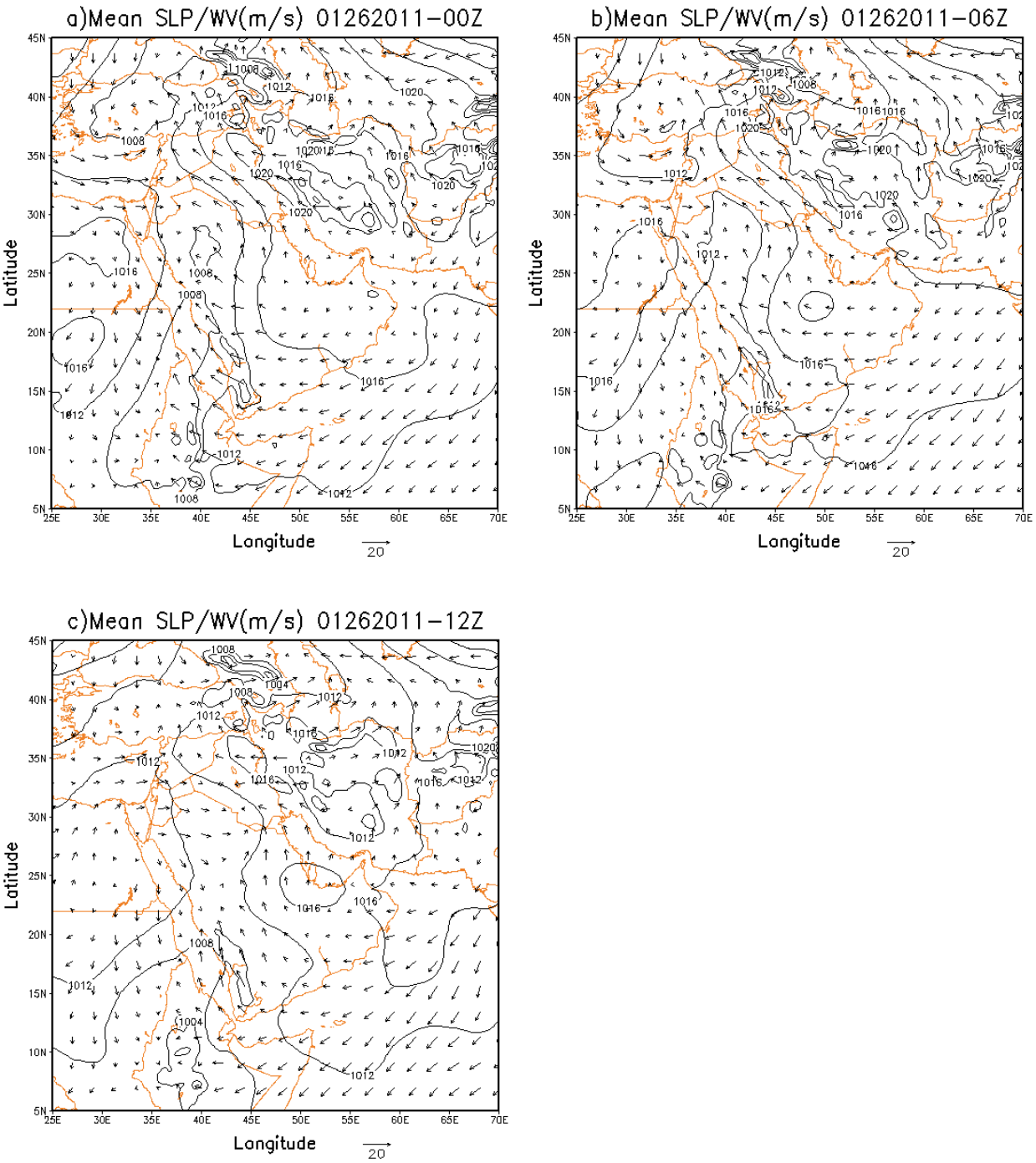

Fig 4.3: Same as in Figure 4.1, but for the 26th of January 2011.

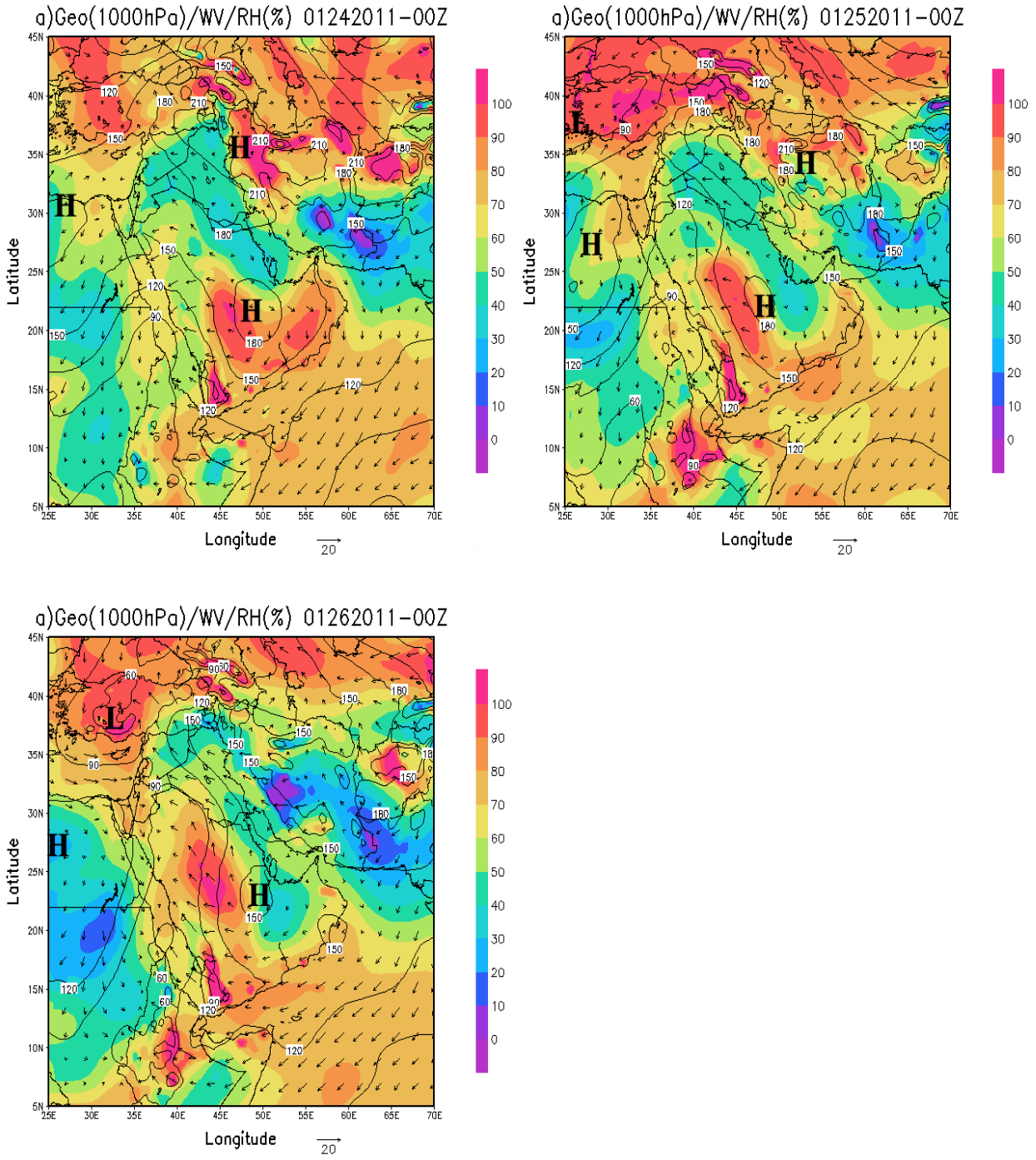

Fig 4.4: 1000hPa geopotential heights (contours), relative humidity (shaded), and wind vectors, a) for 00Z on the 24th of January 2011, b) for 00Z on the 25th of January 2011, c) for 00Z on the 26th of January 2011.

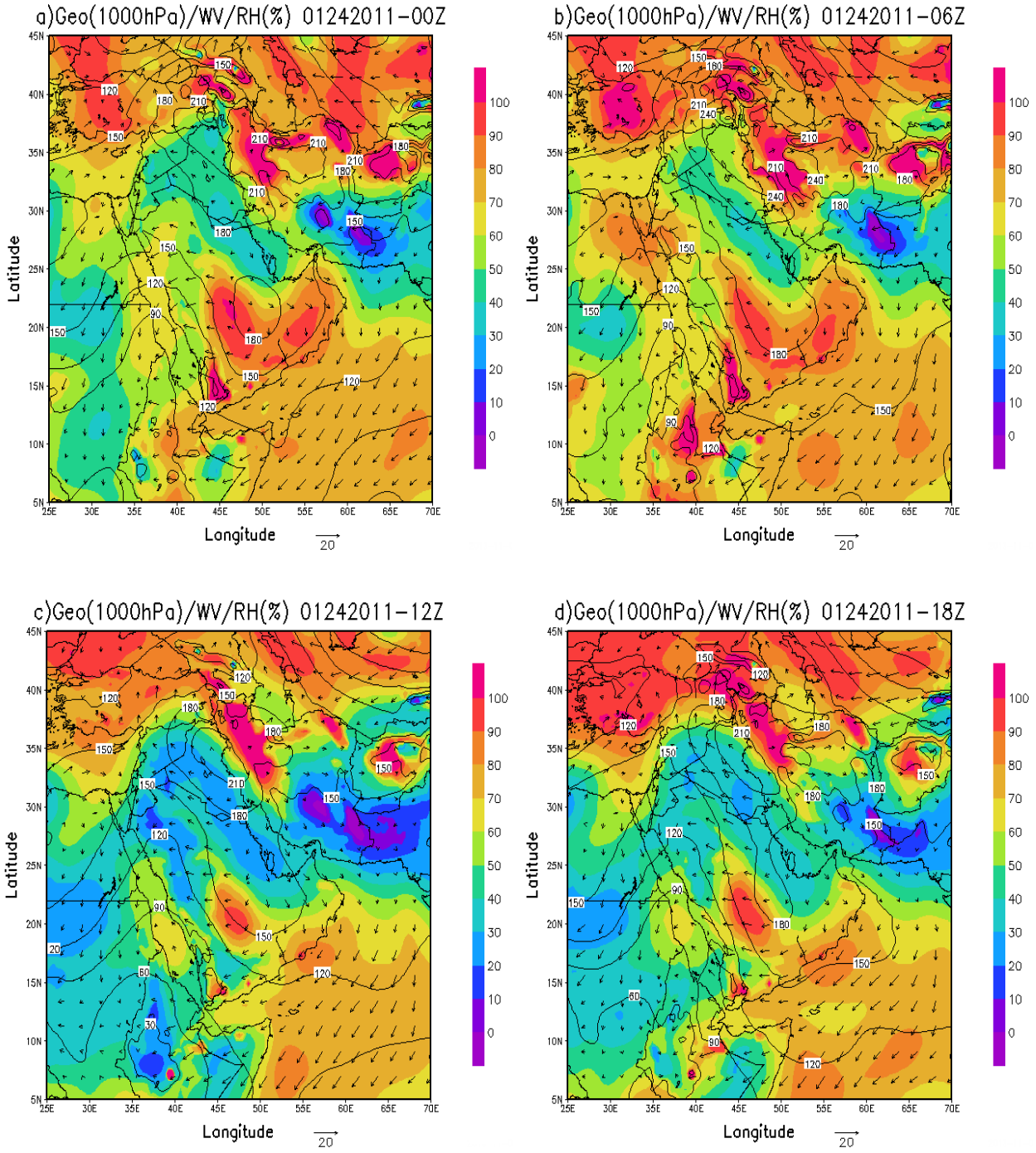

Fig 4.5: 1000hPa geopotential heights (contours), relative humidity (shaded), and wind vectors for the 24th of January 2011, a) 00Z, b) 06Z, c) 12Z, and d) 18Z.

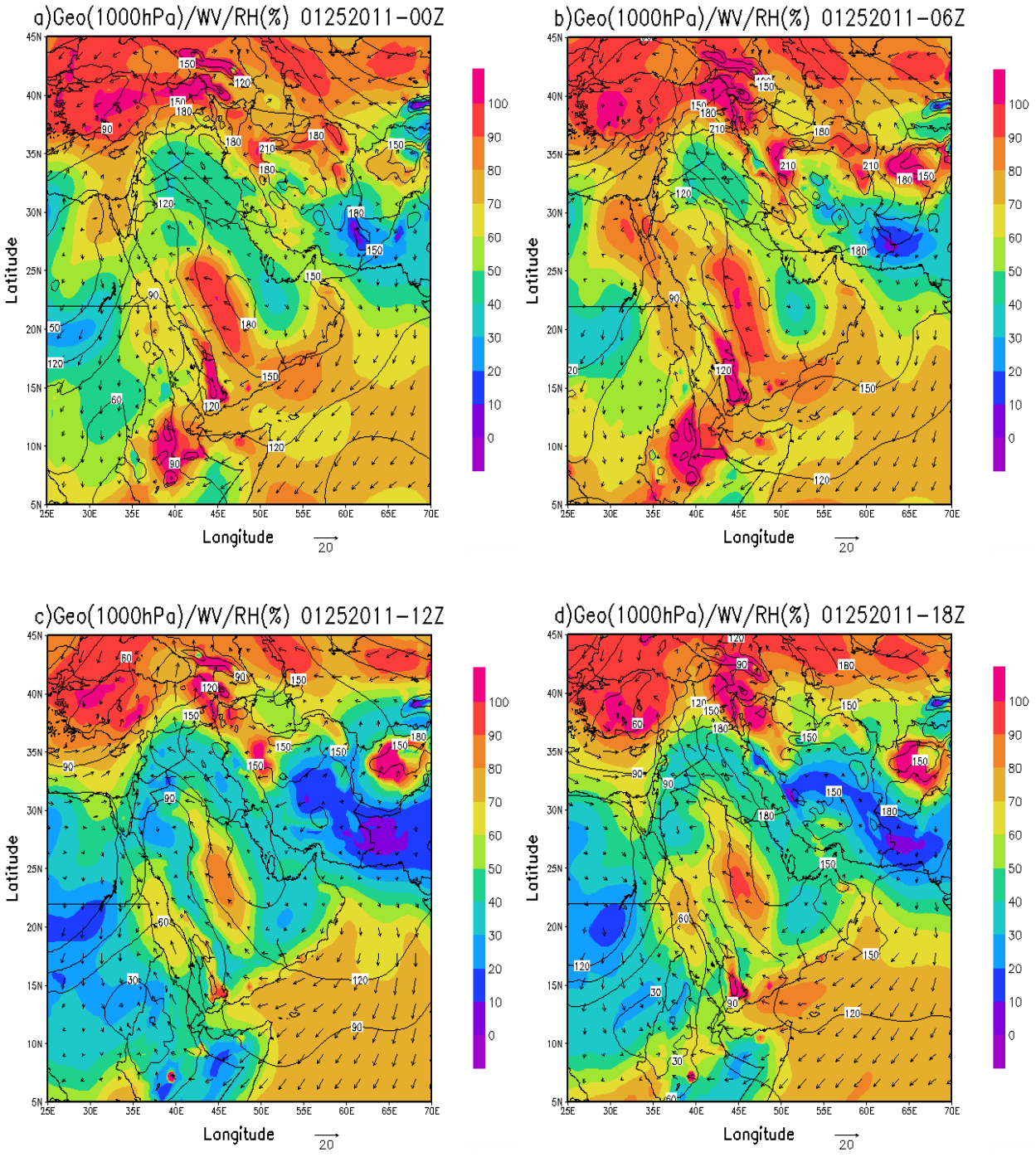

Fig 4.6: Same as in figure 4.5, but for the 25th of January 2011.

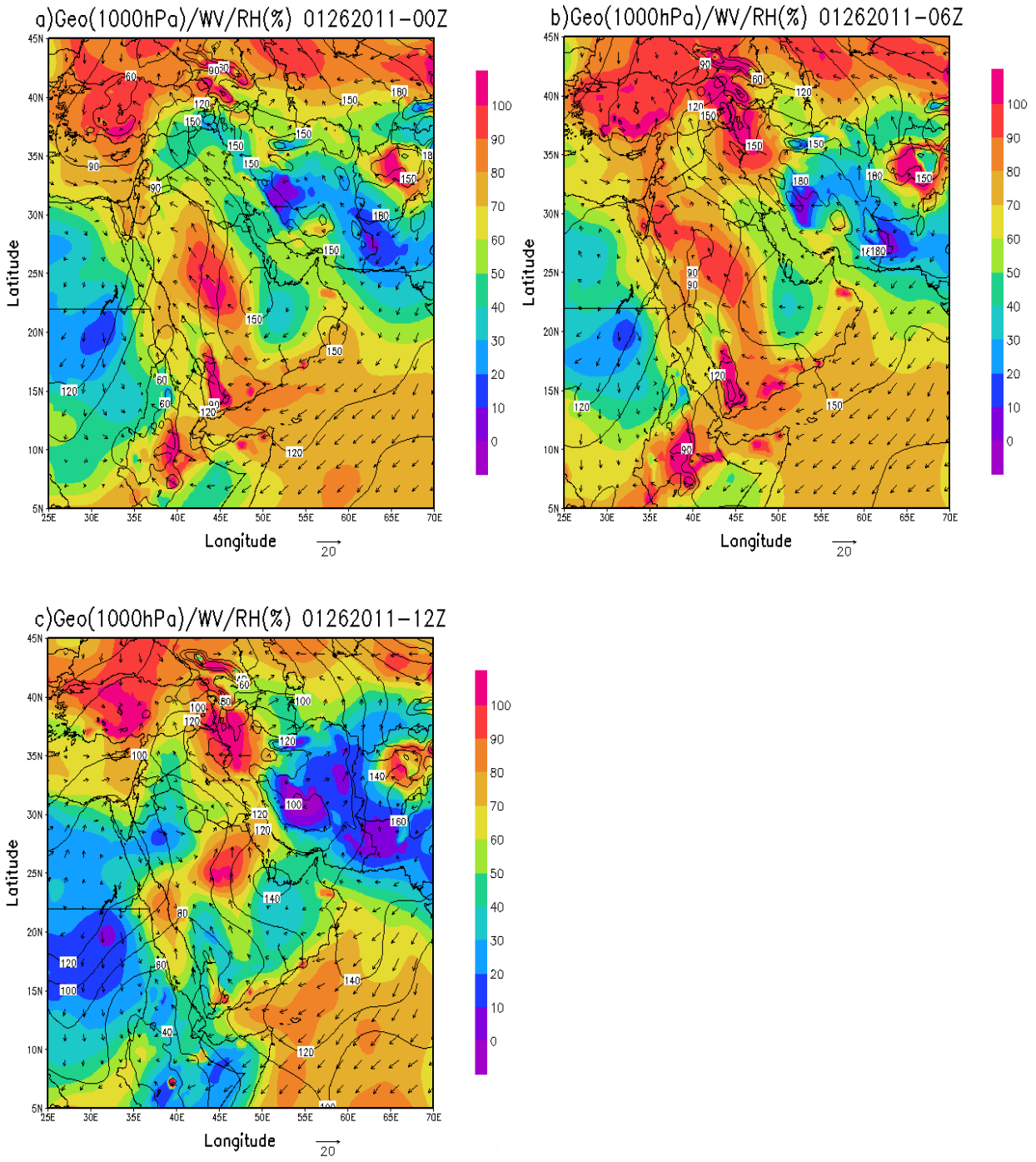

Fig 4.7: Same as in figure 4.5, but for the 26th of January 2011.

4.1.2. Low-level jet (LLJ) and moisture

Moisture is the main player in forming clouds, and hence, producing rain and causing precipitation. In order to have storm formation in a specific location, it is important to have an effective mechanism to transport moisture to that specific location. The LLJ is an ideally mechanism responsible for the transport of moisture in a short period of time. Figures 4.5, 4.6, and 4.7 show, in addition to the movement of the synoptic systems, the concentration of the moisture and how the moisture was transported to the central Red Sea area from the northern part of the Indian Ocean and the Arabian Sea. The charts indicate that an average relative humidity around 60% over the central Red Sea area on the 24th (Figures 4.5a, 4.5b, 4.5c, and 4.5d) increased to around 80% on the 25th (Figures 4.6a, 4.6b, 4.6c, and 4.6d), to reach high values on the storm day of around 90% on the 26th (Figures 4.7a, 4.7b, and 4.7c).

Generally, in this flash flood event, everything took place below the 500 hPa level. High moisture in the surface level associated with strong winds at the surface in the southern part of the Red Sea can be mainly considered the source of the huge amount of rain produced from the storm. The wind speed is shown in Figures 4.8, 4.9, and 4.10 for each of the three days, plotted along with 925 hPa geopotential heights, where the highest southerly wind over the southern Red Sea part is located. The elevation of the 925 hPa level varies between 780 m to 840 m above the surface. The wind speed over the southern Red Sea started from about 6 meter per second (11.6 knot) on the 24th (Figures 4.8a, 4.8b, 4.8c, and 4.8c). Then, the wind speed increased to strongly influence moisture transport and reach its maximum value during the three-day period. It was around 15 meter per second (29.1 knots) on the day before the storm on 25 January at 06Z and 12Z (Figures 4.9b and 4.9c). During the time before and on the storm day, there was a large anomaly in the meridional wind over the Arabian Peninsula, in general, and the southern part of

the Red Sea, in particular. Figure 4.11a shows an average composite mean meridional wind speed, and Figure 4.11b shows the meridional wind speed anomaly based on a climatological mean of a period from 1981 to 2010 for the same days of the year for the Arabian Peninsula and the Red Sea area in the 925 hPa level, where the fastest wind existed.

The composite mean of the meridional wind speed over the southern Red Sea was estimated to be about 8 meters per second. The meridional wind composite anomaly was more than 5 meters per second for the same area. This indicates that high wind speed forming a LLJ in the southern part of the Red Sea was well above average before and during the day of the storm, and this enhanced the transport of moisture to the central Red Sea where the storm formed. When the southerly LLJ, which transported the high moisture content in the area, confronted the northerly cold wind over the central Red Sea area west of Jeddah, strong frontogenesis and convergence formed, which resulted in forcing the air to rise and initiate and enhanced deep convection. Junker et al. (1999) found that the presence of a LLJ and a low-level boundary, or front, at a location that has strong low-level moisture leads to extreme rainfall events.

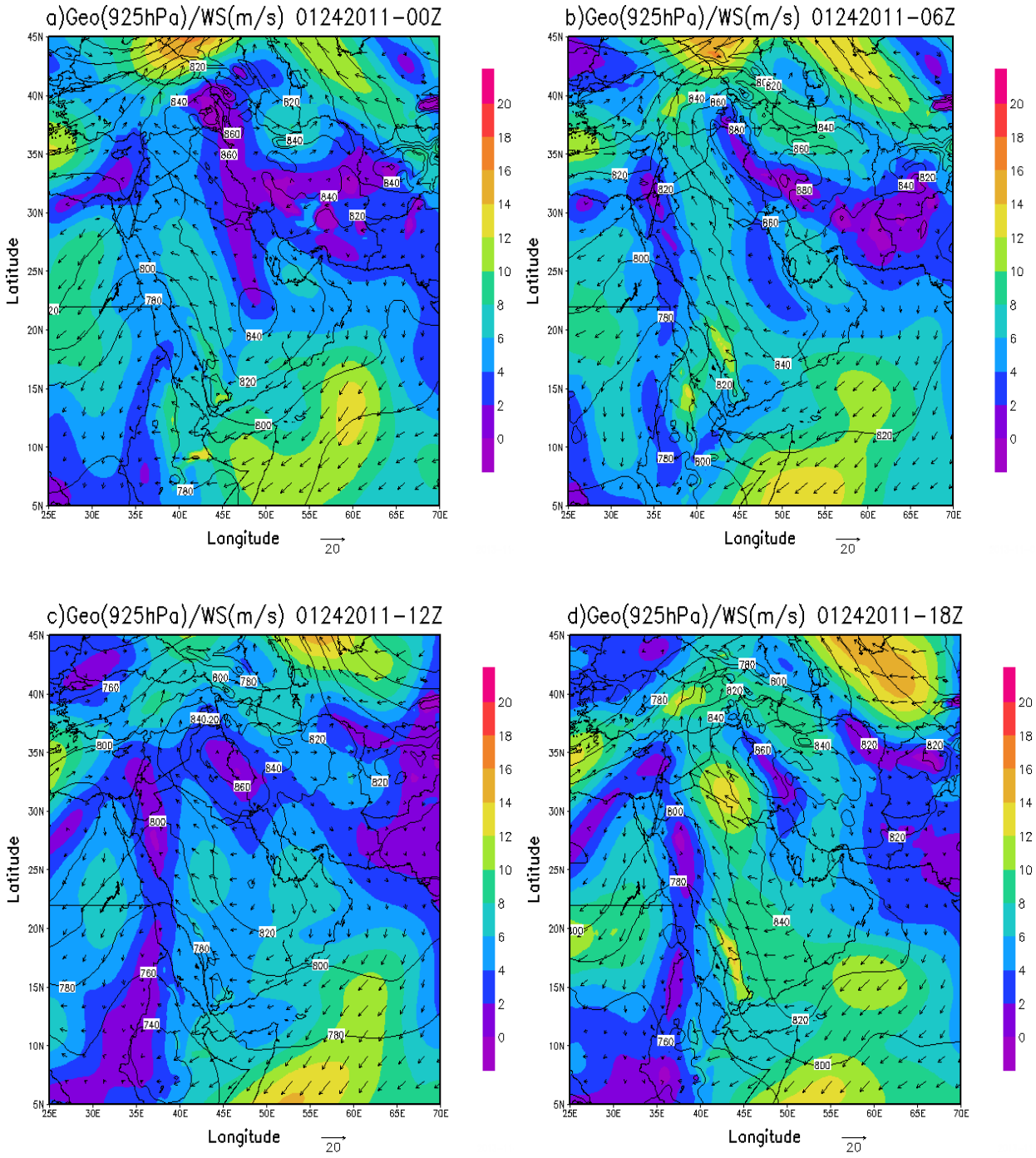

Fig 4.8: 925hPa geopotential heights (contours), wind speed (shaded), and wind vectors for the 24th of January 2011, a) 00Z, b) 06Z, c) 12Z, and d) 18Z.

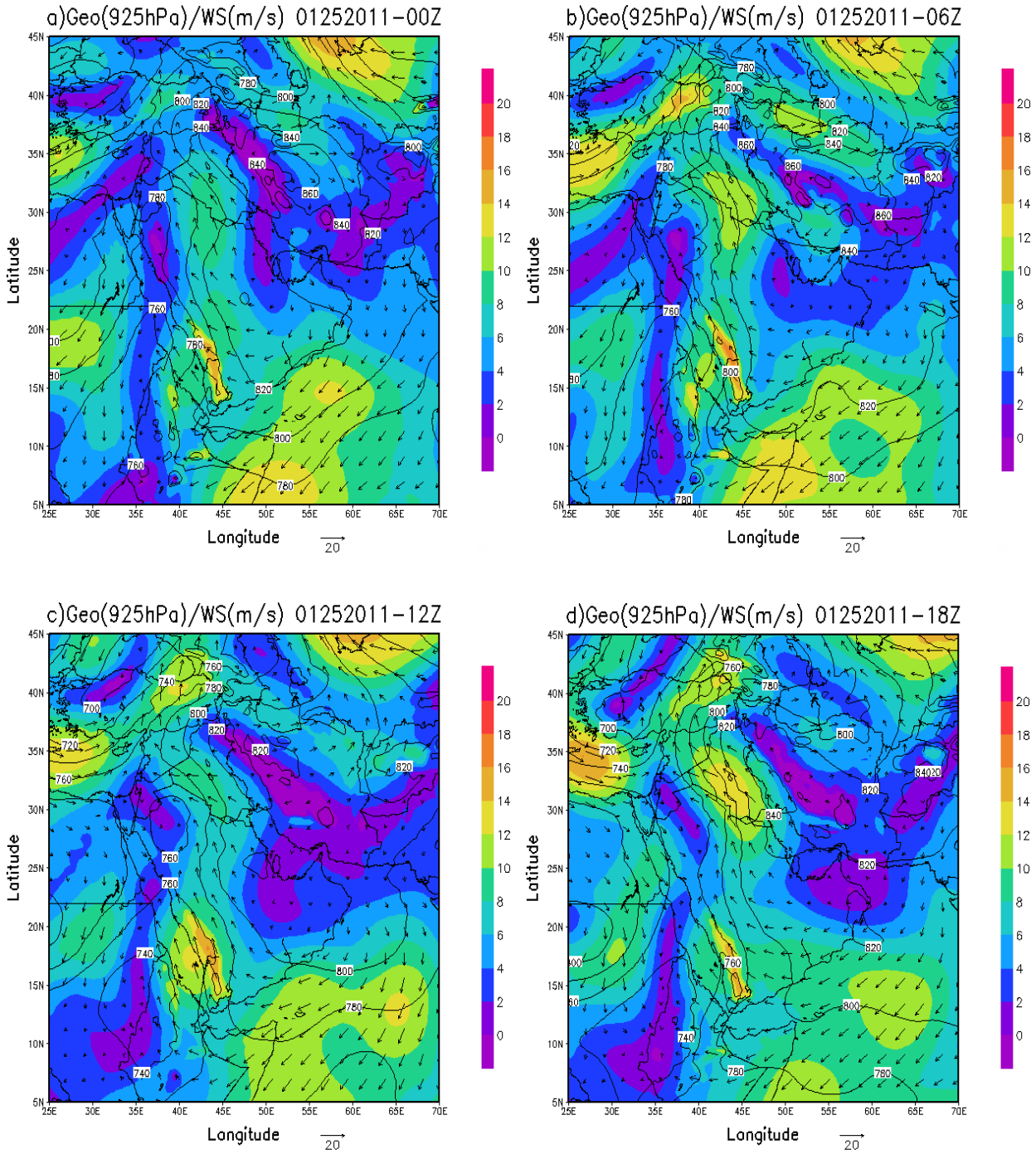

Fig 4.9: Same as in figure 4.8, but for the 25th of January 2011.

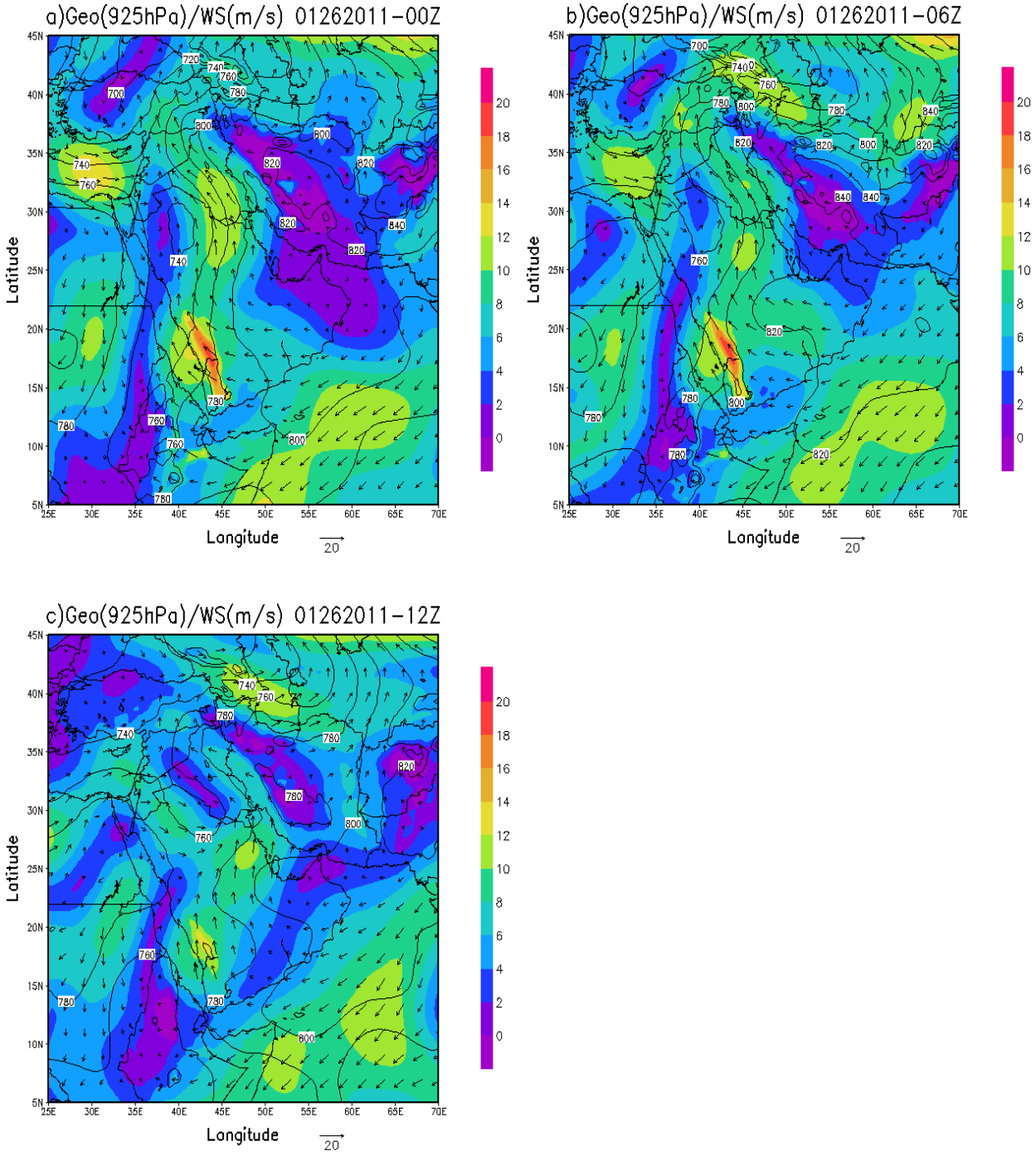

Fig 4.10: Same as in figure 4.8, but for the 26th of January 2011.

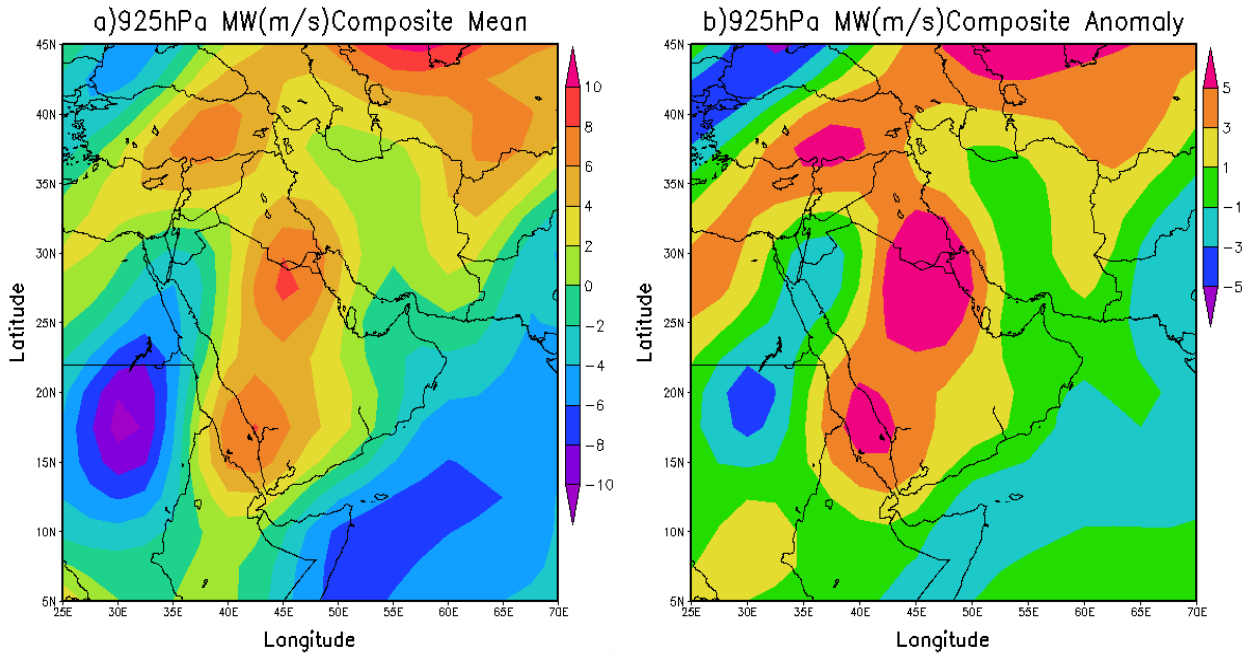

Fig 4.11: a) Composite mean of the meridional wind speed for 925hPa level, b) the meridional wind speed anomaly for 925hPa level based on a climatological mean of a period from 1981 to 2010 for the same days.

4.1.3. Upper level analysis

Figures 4.12, 4.13, and 4.14 show the 850 hPa geopotential heights and temperatures for each of the relevant three days in January. The charts of the 850 hPa level are usually used to show low-level air advection, which indicates the upward and downward motion of air in the troposphere. Warm air advection contributes to the rising motion of air, while cold air advection contributes to the sinking motion of air on the synoptic scale. Warm air advection started to take place over the Red Sea on 24 January at 12Z (Figure 4.12c), and then cold air advection from the north started to interfere due to the contribution of the subtropical anticyclone over northeastern Africa that started to shift easterly (Figure 4.12d).

On 25 January at 12Z and 18Z (Figure 4.13c and 4.13d), warm air advection over the southern part and cold air advection over the northern part of the Red Sea started to initiate

strong local frontogenesis and create high instability over the central Red Sea area to the west and over the city of Jeddah. As in this case, this frontogenesis and instability played an important role in starting a series of repeated convective events over a short period of time that formed a quasi-stationary MCS over the city of Jeddah.

Charts of 700 hPa geopotential heights are shown in Figures 4.15, 4.16, and 4.17 for each of the three days. These charts show an upper-level trough (short wave) started to form a little to the west over the central Red Sea, and was characterized by weaker winds on the 24th at 12Z (Figure 4.15c). The left side of the trough axis exhibits cold air advection, while the right side of the short wave axis exhibits warm air advection. In addition, wind speed increased on the right side of the trough axis, and hence it diverts and enhances rising motion along with the effect of warm air advection. The trough started to become more consistent, and the winds started to increase on 25 January at 18Z (Figure 4.16d).

When the storm was in its active phase between 00Z and 12Z on 26 January (Figures 4.17a, 4.17b, and 4.17c), the wind speed increased and the trough became stronger, which led to making the environment more suitable for enhancing convection. Jeddah, in this case, was affected by warm air advection because of the influence of the trough before the storm day on the 25th and during the storm day on the 26th. Since everything took place below the 500 hPa level, the short wave is present in the 500 hPa (Figures 4.18, 4.19, and 4.20) on the day of the storm. Jeddah was under the area of the right axis of the trough, where rising air and precipitation is favorable, but it is slightly weaker at this level than at the 700 hPa level. Mesoscale analysis of the environment over the Central Red Sea area and around the city of Jeddah will be discussed in the next section.

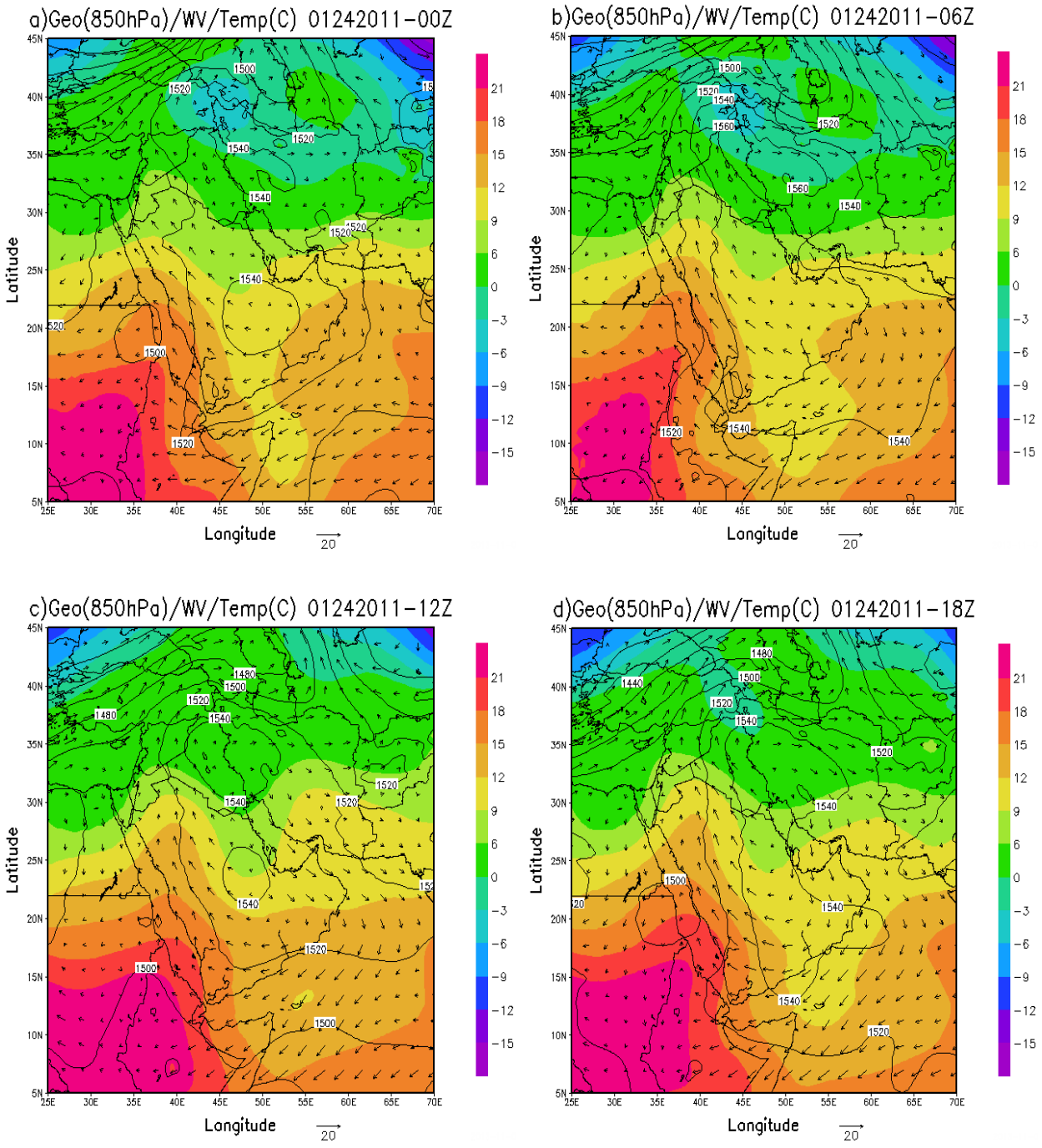

Fig 4.12: 850hPa geopotential heights (contours), temperature (shaded), and wind vectors for the 24th of January 2011, a) 00Z, b) 06Z, c) 12Z, and d) 18Z.

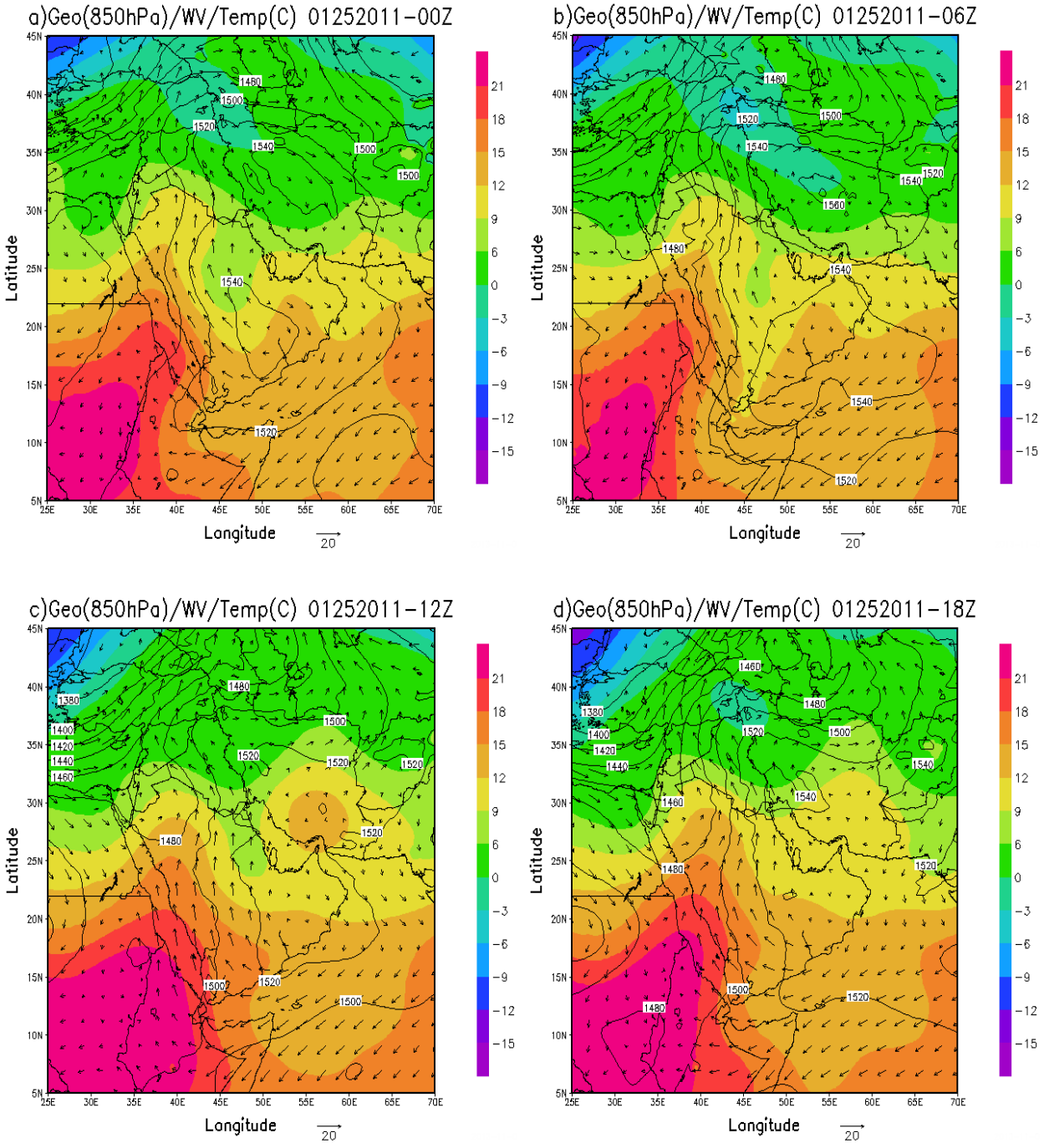

Fig 4.13: Same as in figure 4.12, but for the 25th of January 2011.

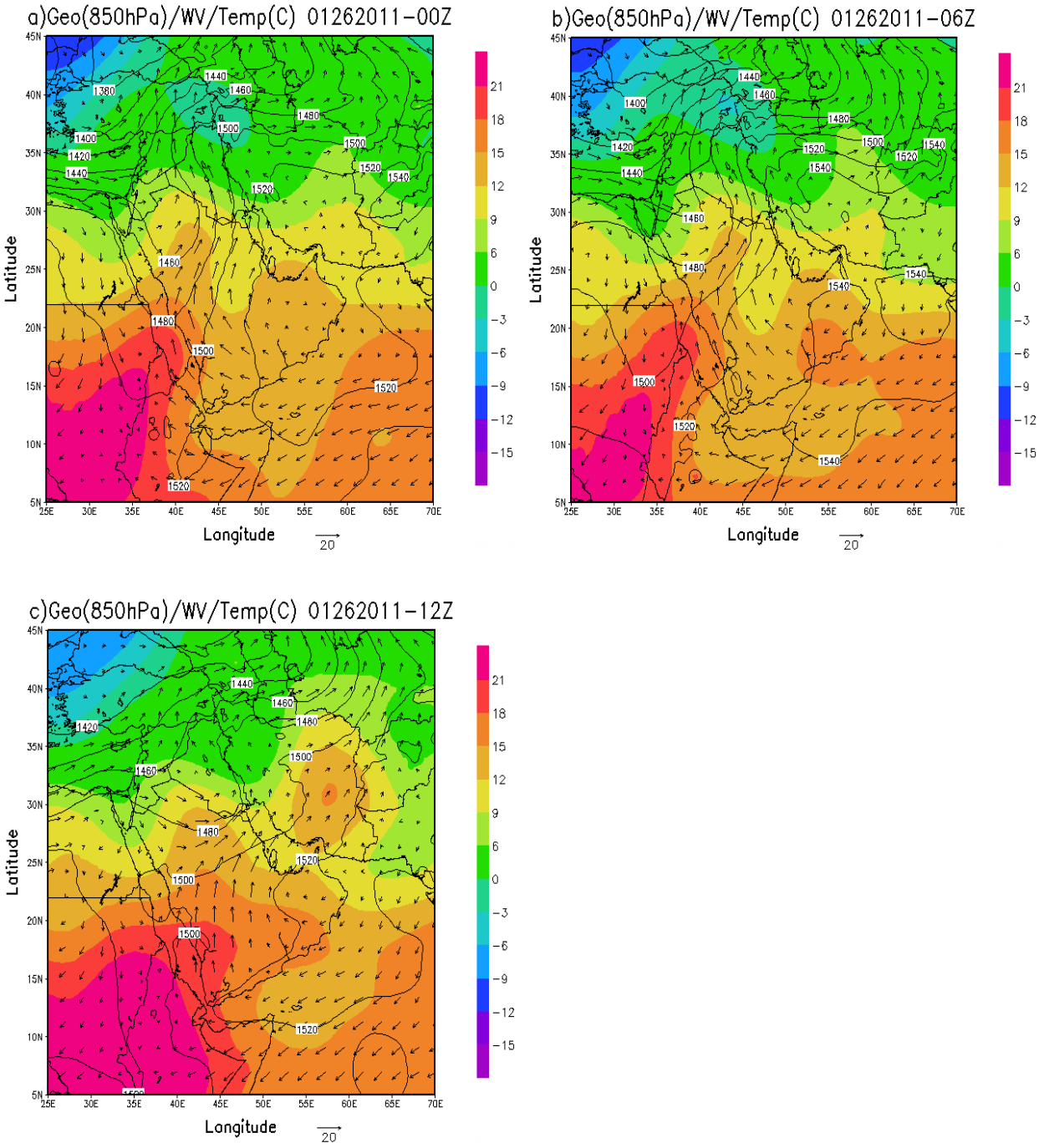

Fig 4.14: Same as in figure 4.12, but for the 26th of January 2011.

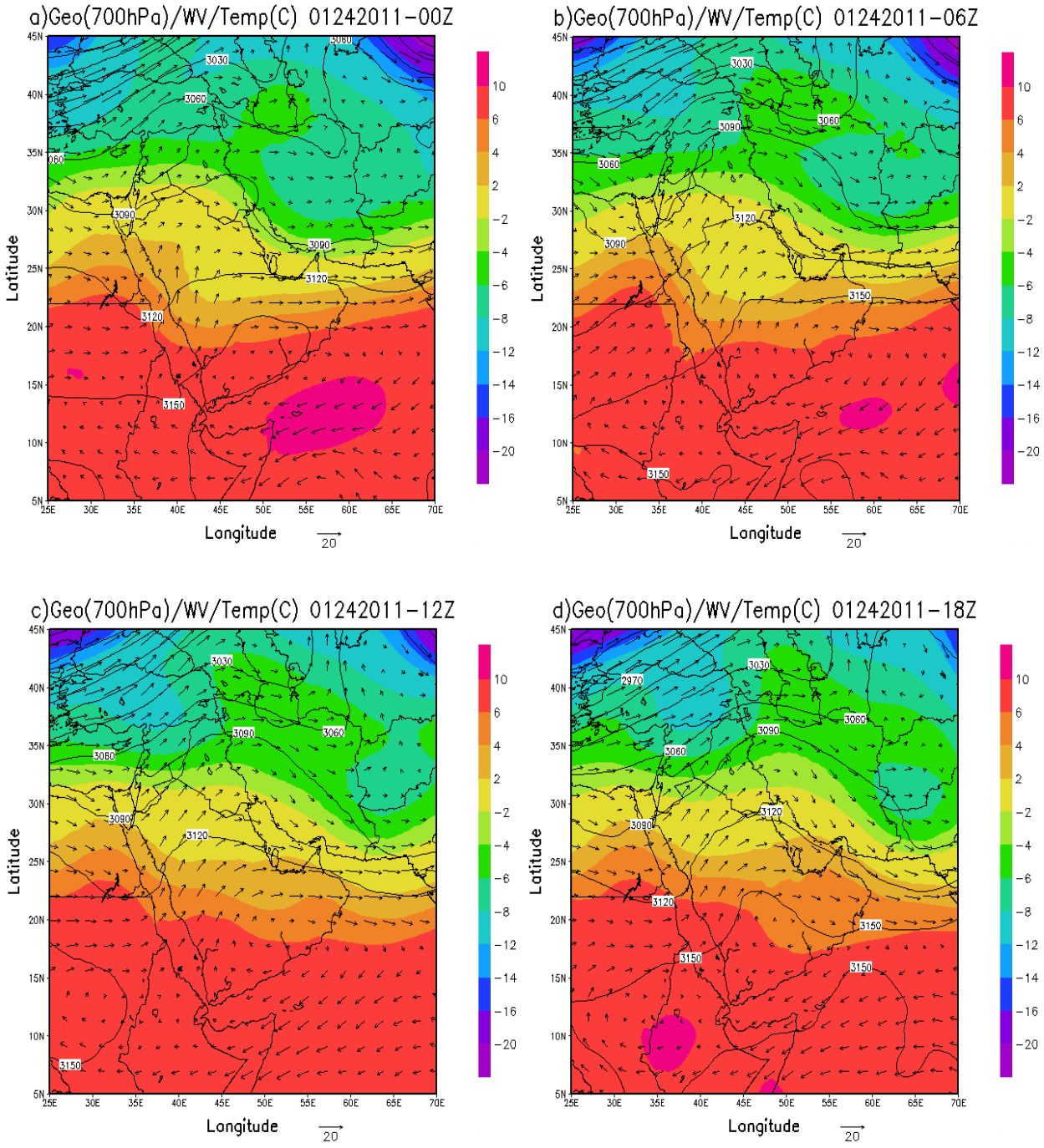

Fig 4.15: 700hPa geopotential heights (contours), temperature (shaded), and wind vectors for the 24th of January 2011, a) 00Z, b) 06Z, c) 12Z, and d) 18Z.

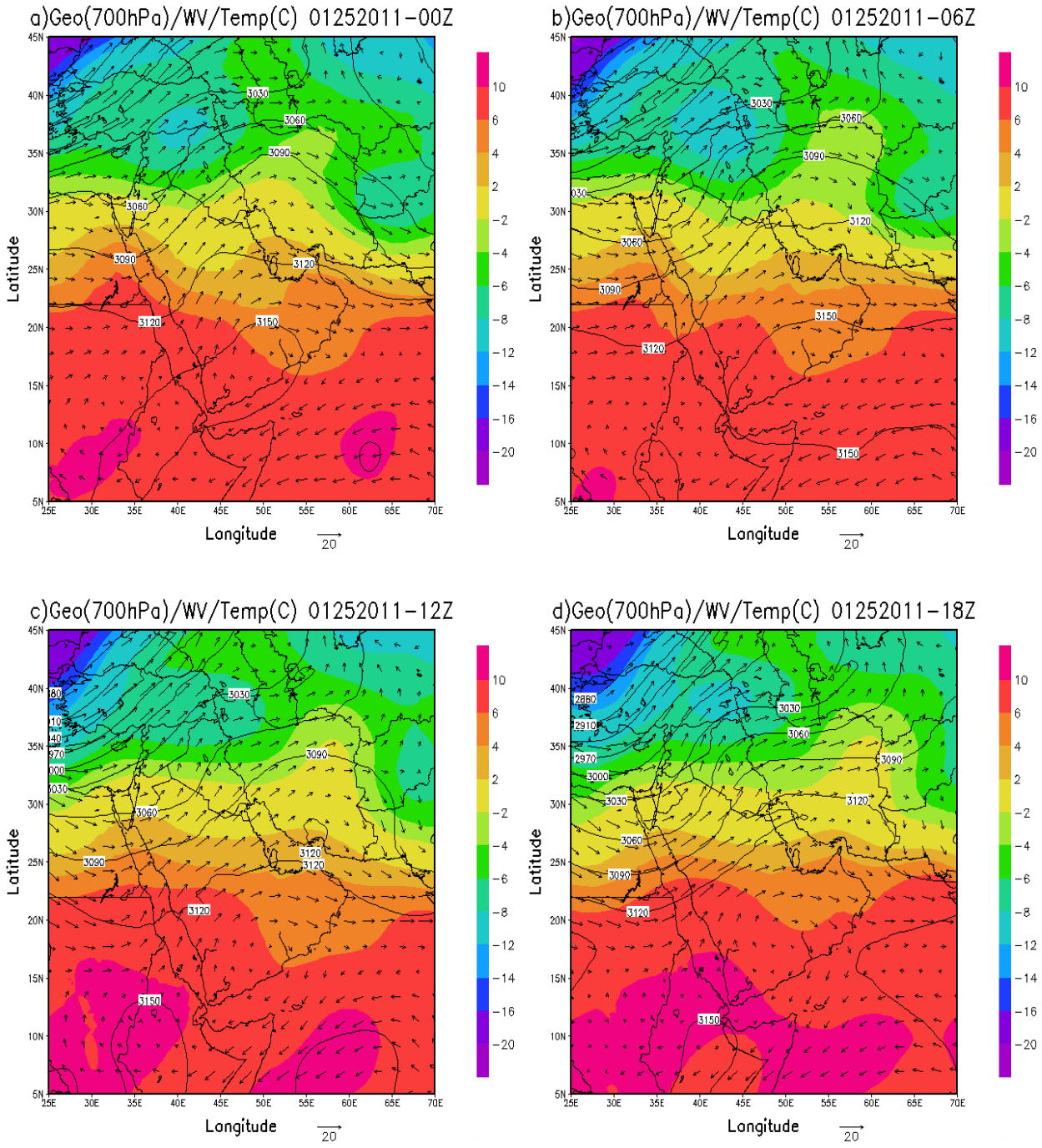

Fig 4.16: Same as in figure 4.15, but for the 25th of January 2011.

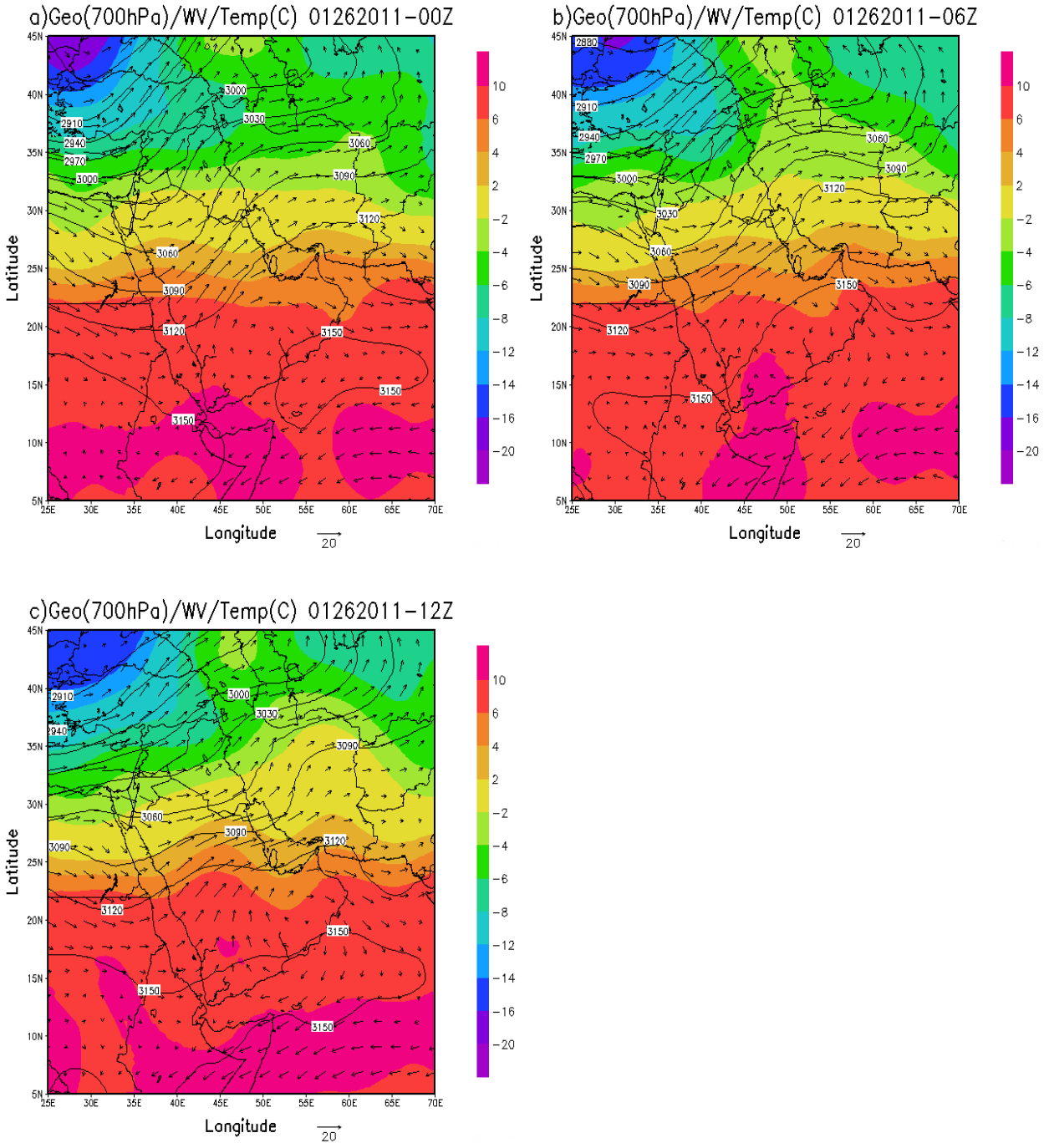

Fig 4.17: Same as in figure 4.15, but for the 26th of January 2011.

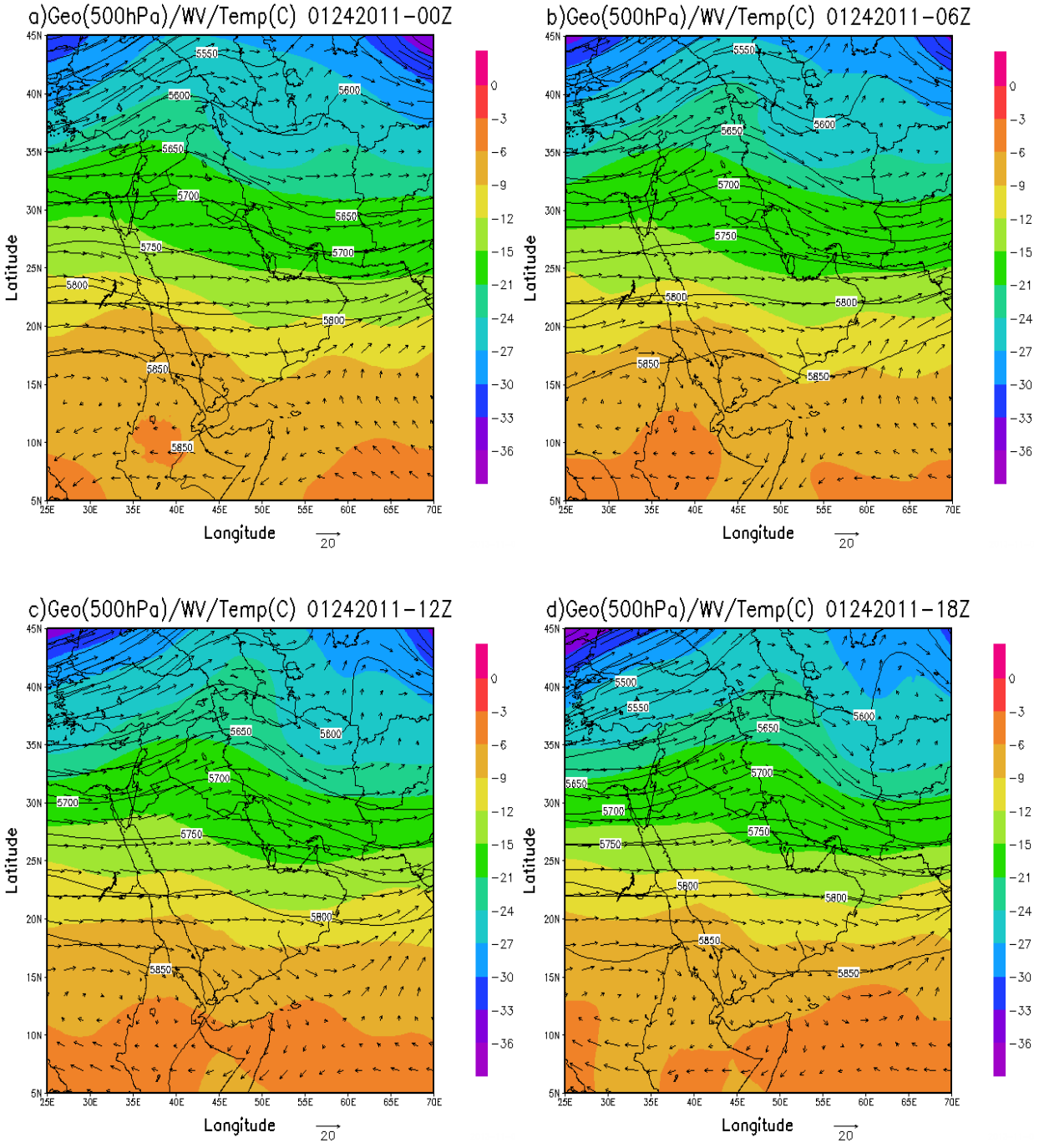

Fig 4.18: 500hPa geopotential heights (contours), temperature (shaded), and wind vectors for the 24th of January 2011, a) 00Z, b) 06Z, c) 12Z, and d) 18Z.

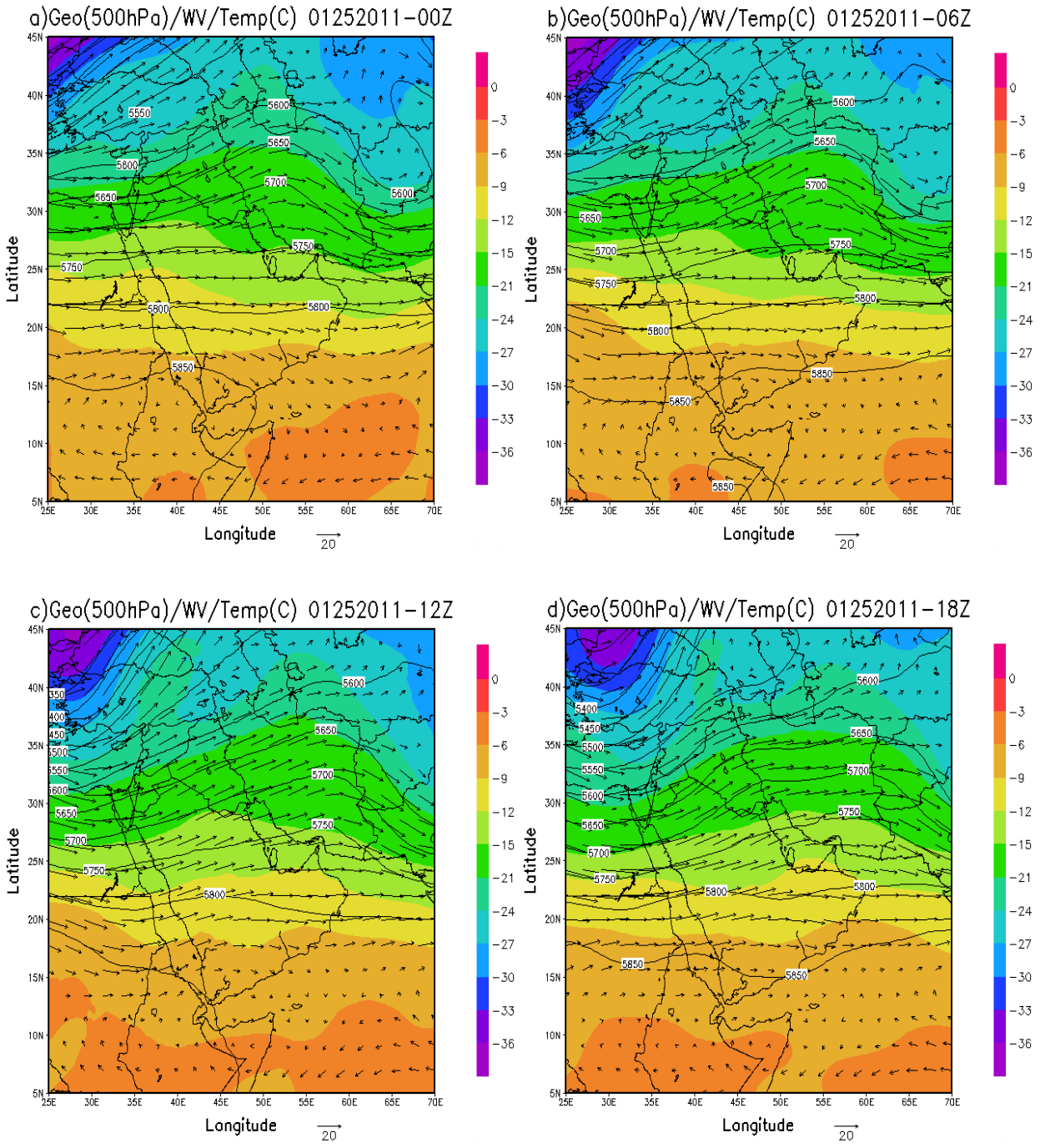

Fig 4.19: Same as in figure 4.18, but for the 25th of January 2011.

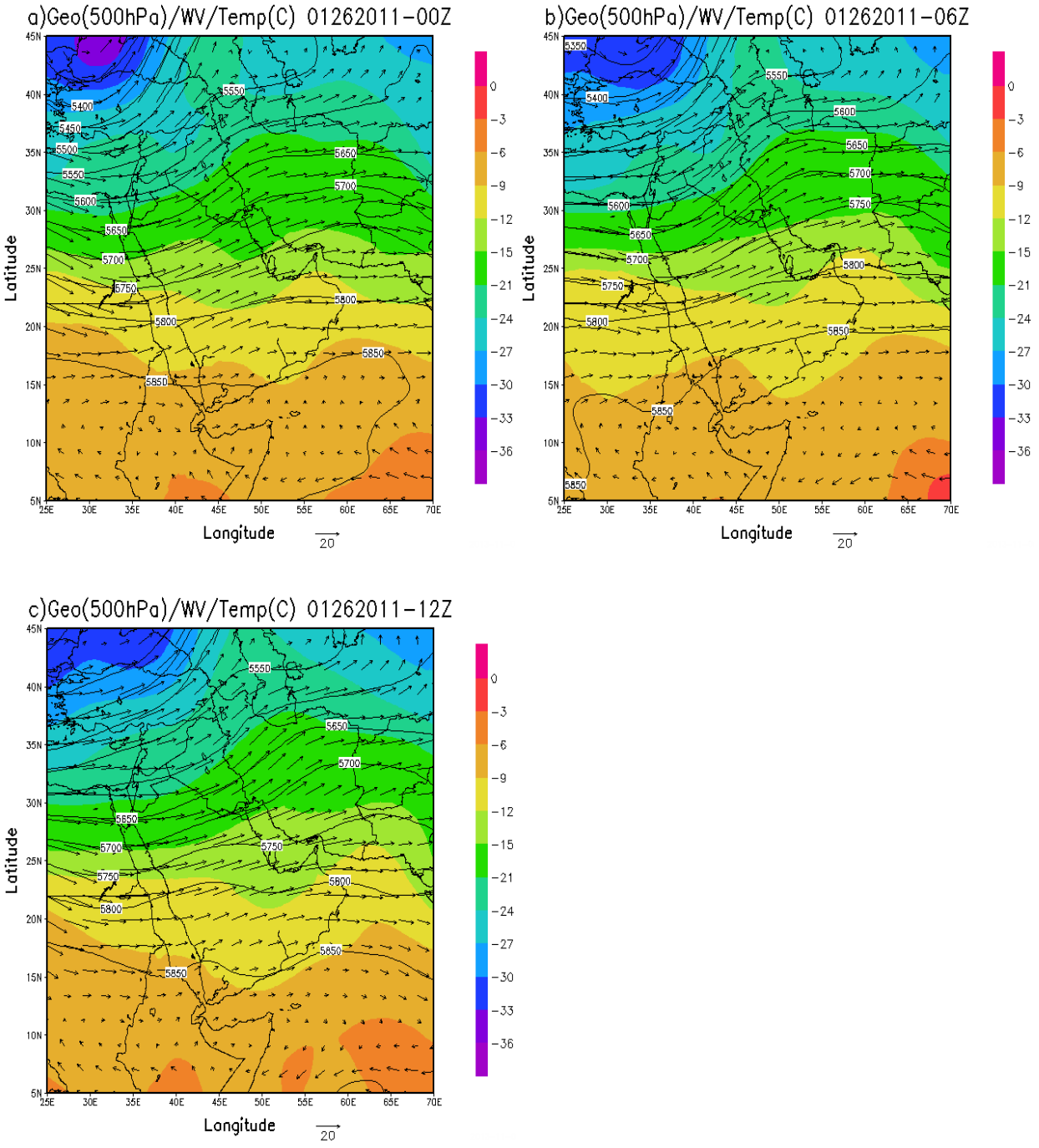

Fig 4.20: Same as in figure 4.18, but for the 26th of January 2011.

4.2. Mesoscale overview

4.2.1. Mesoscale analysis

As mentioned before, Jeddah is located on the west coast of Saudi Arabia, overlooking the Red Sea from the west. The Hijaz plateau and the Sarawat mountain range are located east of the city, which has an elevation varying southward from 800-3,200 km. Precipitation in Jeddah is affected by its location on the Red Sea based on the physical properties of the troposphere and the topographic features of the region. As described before, the interaction between the two different air masses causes strong convergence and instability over the central Red Sea area. The convective available potential energy (CAPE) was relatively high over Jeddah during the day of the storm. CAPE is an indicator of the instability of the atmosphere and if a parcel of air is positively buoyant.

Figure 4.21 shows the sounding from Jeddah for 00Z, 12Z. CAPE amount was calculated from the 00Z and 12Z sounding, and equals 1822 and 1062 joules per kilogram, respectively. The 00Z sounding was before the storm started, and the 12Z was after the storm. CAPE gives an indication of the possible intensity of convection. Moderate to strong convection usually ranges between 1,000 and 3,000 joules per kilogram, meaning the CAPE for Jeddah was noticeably high in the 00Z sounding.

In addition, the 00Z sounding shows a precipitable water of 40 kg per square meter, which indicates a large amount of moisture was available to fall as precipitation on the surface. Figure 4.22 illustrates the composite mean of the precipitable water and the composite anomaly based on climatological data from the period from 1981 to 2010 for the Arabian Peninsula and the Red Sea. The composite mean over the southern and the central parts of the Red Sea area is about 30-35 kilogram of water per square meter, and the composite anomaly over the central part

of the Red Sea is noticeably higher than its average of about 8-10 kilogram of water per square meter, which indicates a very high precipitable water in the area during the day of the event.

Davis (2001) presented a typical thermodynamic profile for a flash flooding case shown in Figure 4.23. He attributed the high precipitation efficiency and high rainfall rates to the rapid conversion of moisture to rain low in the cloud, which support warm rain processes. He identified the deep, warm cloud layer as the extended layer between the lifted condensation level (LCL) and the freezing level. Warm rain processes occur in the lower level of the convective storm where the air temperature is greater than 0 C. The deeper the warm cloud layer, the greater is the potential of heavy rainfall and flash flooding to occur (Davis 2001). Chappell (1993) indicated that in order to forecast the potential of high precipitation rate from a sounding, it should show a deep warm layer with high precipitable water, moderate CAPE (1,500-2,000 J/kg), low cloud base and high Equilibrium level, and relatively weak wind shear. This sounding of Jeddah in 00Z fulfilled all of these conditions and shows a profile that is relatively similar to the typical profile presented in Davis (2001). It showed a deep warm cloud layer extended from the LCL level in 976 hPa to the freezing level at about 550 hPa.

In addition, the soundings illustrate the presence of clockwise vertical wind shear (veering), which is associated with warm air advection and rising motion in the synoptic scale, as discussed in the previous section, when looking into the 700 hPa charts. This is because southerly wind at the surface usually transports moisture and warmer air towards the north in the northern hemisphere. Moreover, weak vertical wind shear is important to the storm development because entrainment rates are less, and precipitation efficiency is enhanced (Cotton et al., 2011). Furthermore, Davis (2001) and Miller et al. (1978) concluded that veering wind shear promotes long durational rainfall along the axis of the upper level flow. Miller et al. attributed continual

rainfall along the axis of the upper-level flow to the strong low-level convergence produced from the convective outflow initiated from precipitation (Figure 4.24). In Jeddah's case, strong frontogenesis already existed due to the synoptic forcing and the mechanism described by Miller et al. shown in Figure 4.24.

Consequently, based on the availability of high CAPE, the presence of weak vertical wind shear, and high precipitable water, the environment of Jeddah on 26 January was adequate for flash flooding. These physical factors played a very important role in initiating and enhancing the convection over Jeddah and in the persistence of precipitation.

High sea surface temperature might have an important role in forming the MCS. In a recent study conducted by Raitsos et al. (2011), the authors showed that based on satellite-derived sea surface temperatures and ground-based air temperatures, the average sea surface temperature of the Red Sea has increased since the mid-nineties and they have noticed a sudden increase by 0.7℃ during the last decade. This increase in sea surface temperature produces more moisture in the atmosphere. In addition, higher surface air temperature enhances sensible heat flux. Both make the atmosphere more suitable for convection by increasing the moisture and the amount of CAPE. Sea surface temperature of the Red Sea for the day of Jeddah's flash flood event is shown in Figure 4.25. The figure shows very high sea surface temperature (25-28 ℃) in the southern part of the Red Sea, which might have considerable impact on the development of the MCS over Jeddah.

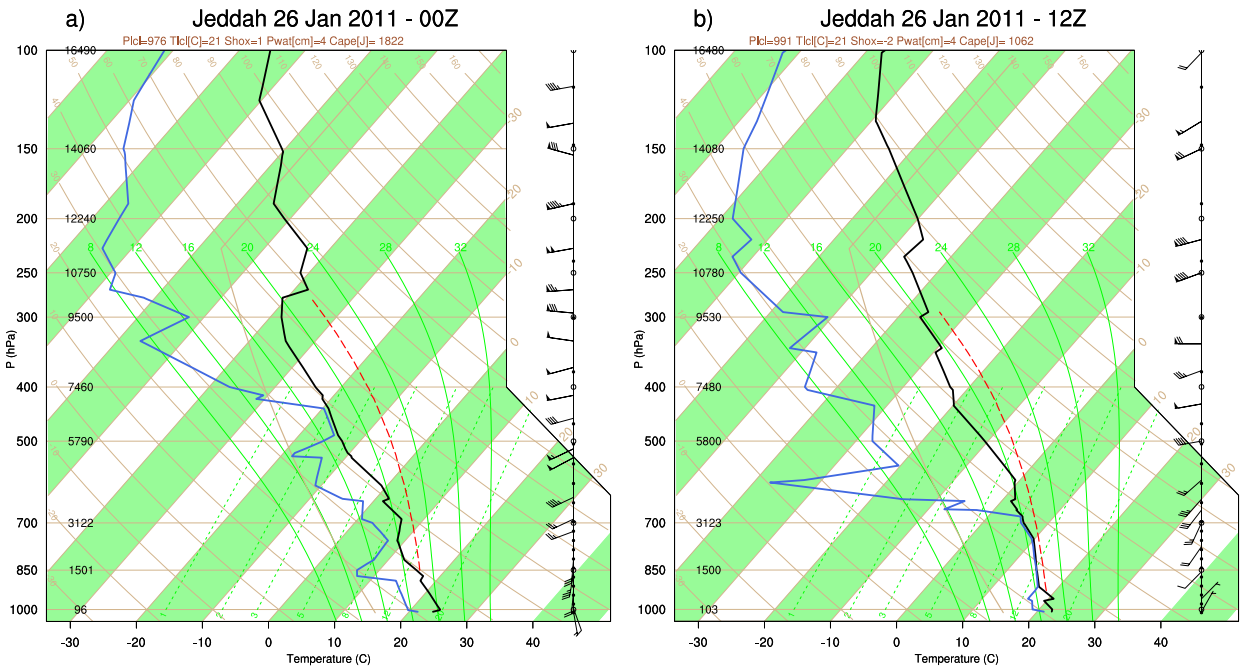

Fig 4.21: Thermodynamic profiles from Jeddah at a) 00Z on 26 January 2011, b) 12Z on 26 January 2011, a mixed parcel ascent are indicated in red in both soundings.

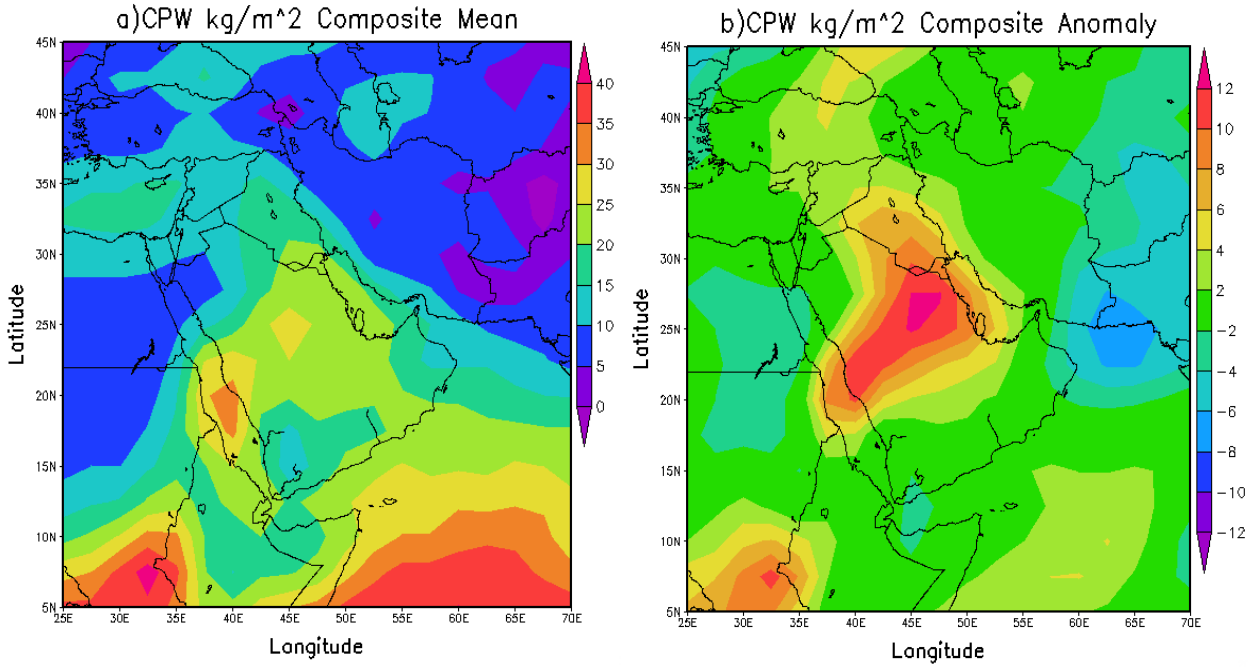

Fig 4.22: a) Composite mean of columnal precipitable water on 26 January 2011, b) the columnal precipitable water anomaly for on 26 January 2011 based on a climatological mean of a period from 1981 to 2010 for the same days.

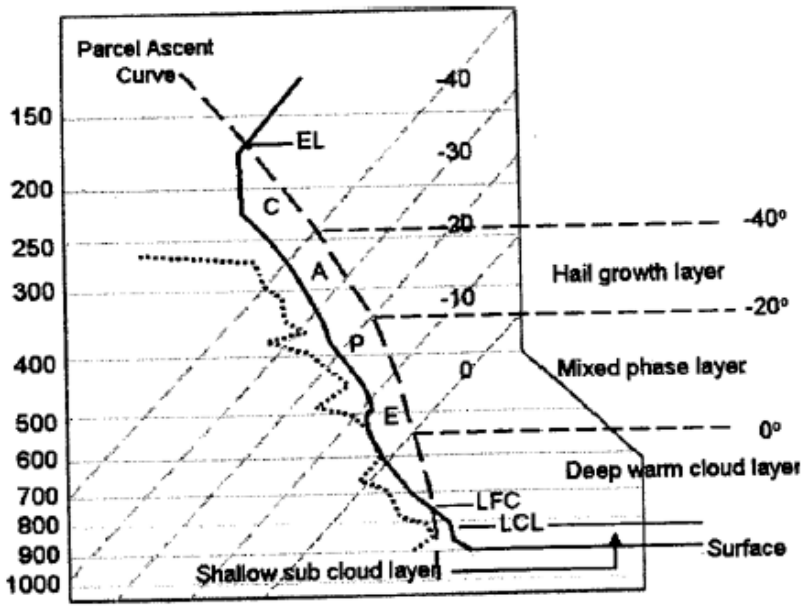

Fig 4.23: A representative flash flood sounding is broken down into layers based on the microphysical processes responsible for rain production. The depth of the subcloud layer, warm cloud layer, the mixed phase layer, and the hail growth layer can be important parameters for rain fall production with warm or cold rain processes. The mean precipitabe water, relative humidity, and CAPE in each layer also greatly impact the rainfall production processes. From Davis (2001).

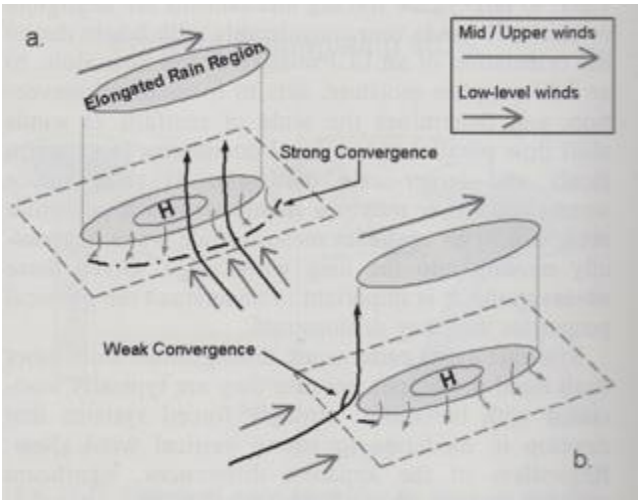

Fig 4.24: Illustration of a multicellular storm growing in an environment where (a) the low-level winds are perpendicular to the mid- and upper-level winds, (b) the low level winds are parallel to the mid- and upper-level winds. From Cotton (1990); adapted from Miller et al. (1978).

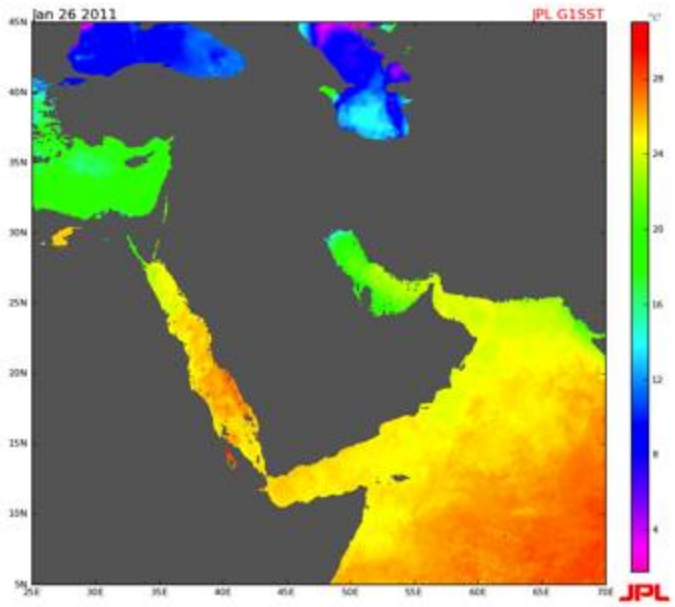

Fig 4.25: Average sea surface temperature on 26 January 2011. From (http://ourocean.jpl.nasa.gov/SST/).

4.2.2. Satellite and radar analysis

Infrared satellite images (Figure 4.26) were helpful in showing the location of the MCS and the storm location and cloud formation over the city, but generally, they were not helpful in determining storm properties. On the other hand, weather radar has proven its capability in detecting storm formation, propagation, and location. It also has proven its capability in detecting the motion of the storm, as well as the severity of the storm and the precipitation types.

Figure 4.27 shows a radar image in Jeddah during the peak of the storm on 26 January 2011 at 0939Z. The radar images illustrate clearly the MCS over Jeddah started early on the morning of 26 January. They also show that the convection started at about 06Z and continued to occur as the storm started to propagate over the city for about 5-6 hours. The radar image (Figure 4.27) illustrates a wide range of high reflectivity (shown in orange and yellow) over Jeddah. The color ranges indicate a reflectivity of about 50 to 55 dBZ. This gives an estimation of an average

precipitation rate between 50 and 100 millimeter per hour (mm/hr). This precipitation rate is considered high and can produce heavy rain and subsequently a flood, even if it lasted for only 1-2 hours.

Comparing these precipitation rates with the long-term average, the mean precipitation rate for this time of the year based on a climatological data for period from 1981 to 2010 is between 21 and 25 millimeters per day (Figure 4.28a), and the composite anomaly for the same day is around 25 millimeters per day (Figure 4.28b). This gives an indication of the severity of the storm and the huge amount of rain precipitated over Jeddah during that day.

Schumacher and Johnson (2005) conducted radar-based research to examine 116 extreme rainfall events in the United States over a three-year period from 1999 to 2001. They classified about 51% of the MCSs responsible for the extreme rainfall into two patterns. The first was called training line-adjoining stratiform (TL/AS) and the second was called backbuilding-quasi-stationary (BB) (Figure 4.29). The BB classification was applied when convective cells repeatedly form upstream of the MCS system, while decaying convective cells occurred downstream in the same location, leading to large total rainfall (Schumacher and Johnson 2005). The radar of Jeddah shows a precipitation pattern of the MCS that falls within the BB classification, where the convection occurs repeatedly over the same area and produces huge amounts of rainfall in a short time.

Results of a simulated storm will be presented and detailed structures of the simulated quasi-Stationary MCS will be analyzed and discussed in the next chapter.

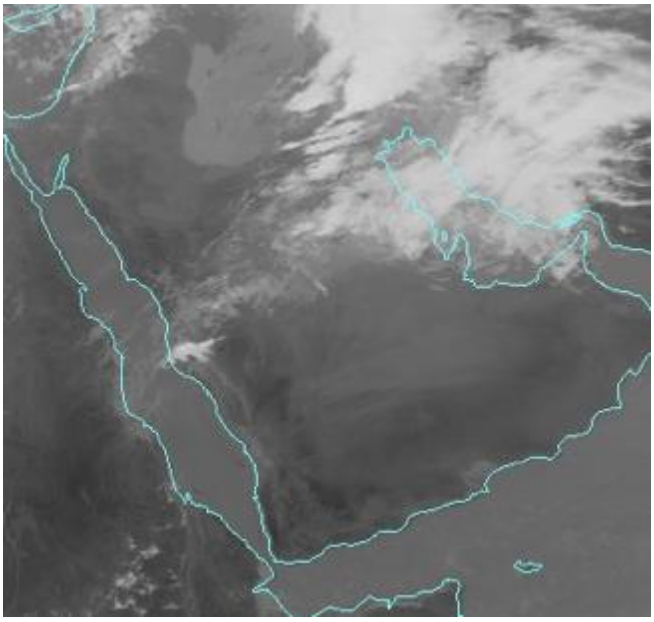

Fig 4.26: A satellite image of the Arabian Peninsula and the Red Sea on 26 January 2011 at 06Z.

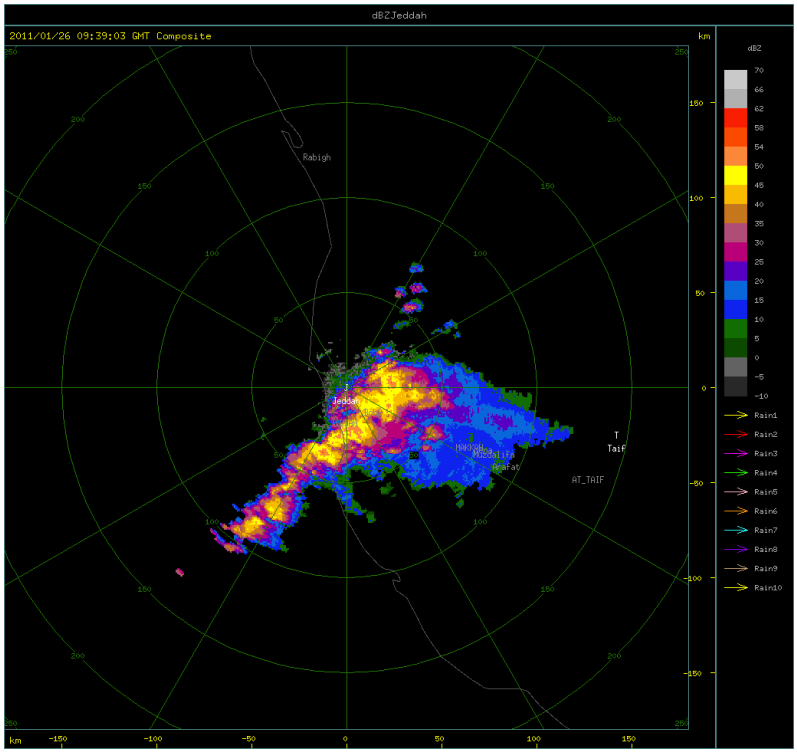

Fig 4.27: A radar image for Jeddah at 0939Z showing a quasi-stationary MCS.

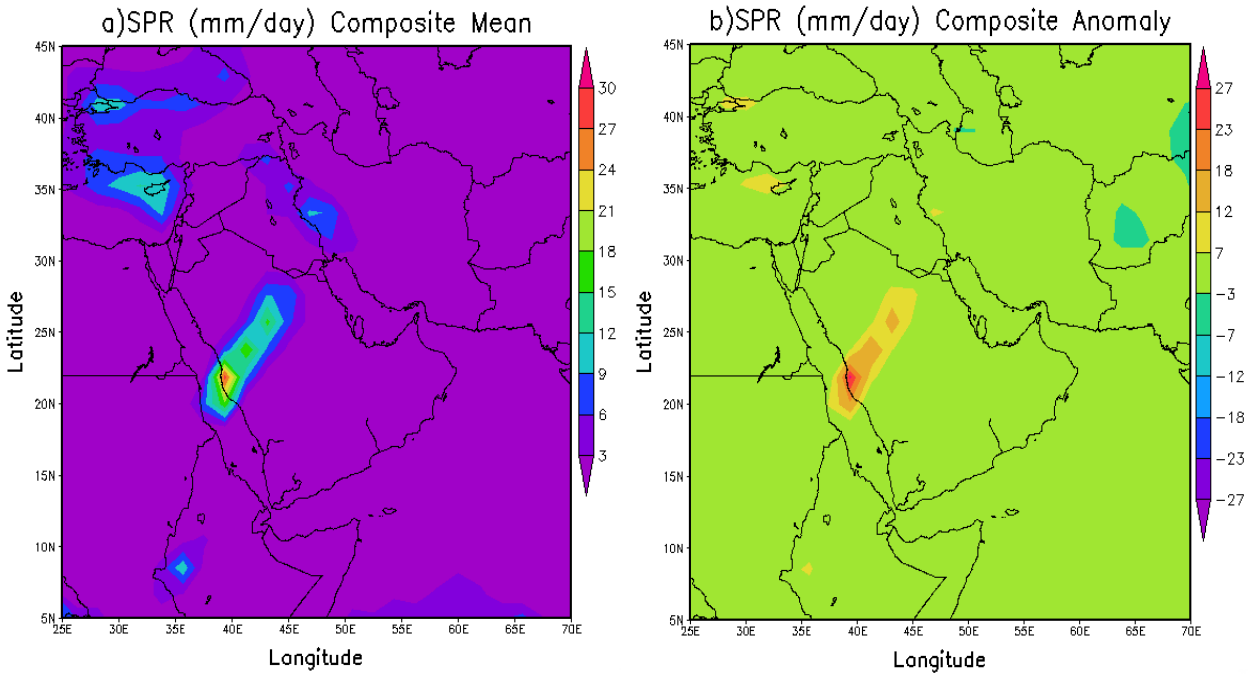

Fig 4.28: a) Composite mean of surface precipitation rate on 26 January 2011, b) the surface precipitation rate anomaly for on 26 January 2011 based on a climatological mean of a period from 1981 to 2010 for the same days.

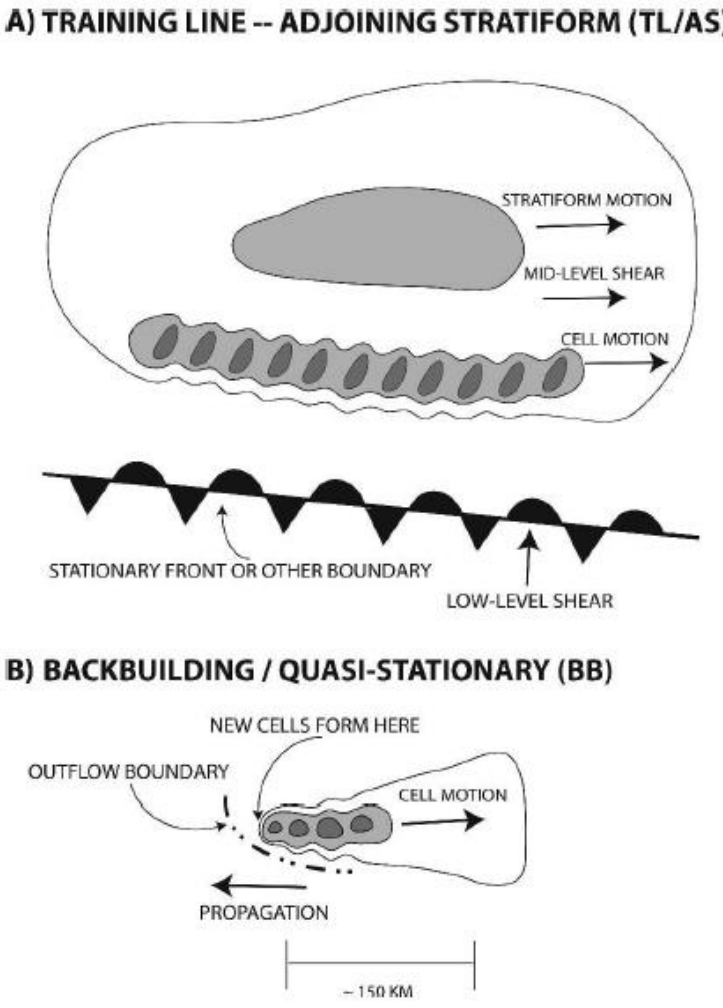

Fig 4.29: Schematic diagram of the radar-observed features of the (a) TL/AS and (b) BB patterns of extreme-rain-producing MCSs. Contours (and shading) represent approximate radar reflectivity values of 20, 40, and 50 dBZ. In (a), the low-level and midlevel shear arrows refer to the shear in the surface-to-925-hPa and 925–500-hPa layers, respectively, as discussed in section 4. The dash–dot line in (b) represents an outflow boundary; such boundaries were observed in many of the BB MCS cases. The length scale at the bottom is approximate and can vary substantially, especially for BB systems, depending on the number of mature convective cells present at a given time. From Schumacher and Johnson (2005).

CHAPTER 5: SIMULATION RESULTS

5.1. Rainfall simulation

Due to the scarcity of meteorological observation in KSA, proving or disproving the modeling study is a difficult task. In this study, compares the model results with King Abdul Aziz International Airport (KAIA) weather station rain gauge, TRMM 3B42 data, and the radar images of the rainfall event. The KAIA weather station rain gauge recorded an accumulated rainfall of 19 mm on 26 January. This rainfall amount doesn't reflect the severity of the storm due to the location of KAIA north of Jeddah (39.15°E, 21.70°N). The MCS formed over the southern part of Jeddah where the flooding occurred.

The model was successful in predicting the location of the MCS over the southern part of Jeddah, but it produced the rainfall about three hours earlier than observed. The distribution of the computed rainfall total in the fine model grid (grid3) is shown in Figure 5.1. The computed rainfall distribution over Jeddah was not uniform and had high variability. Most of the precipitation occurred over the southern areas. The rainfall ranged from about 20 mm in the north to about 120 mm over the south of Jeddah. This variability could be due to the location of the surface front and the effect of the topography, as well as the urban heat island effect due to anthropogenic activities. As mentioned before, Jeddah is located west of the Al-Hijaz escarpment, and the slope of the escarpment could have played a role in enhancing the storm over the south of Jeddah, as well as most of the urban land located in the southern part of the city.

The model computed a rainfall total of 110 mm south of Jeddah during the simulated 12 hours. The simulation showed that precipitation started around 05Z and lasted until the end of the

simulation time at 12Z. The simulation showed a peak in the total hourly rainfall and in the precipitation rate between 05Z and 07Z, with a maximum precipitation rate of 180 mm per hour.

Two locations in the south of Jeddah were selected to represent the southern area and to investigate these peaks. The first location, labeled A in Figure 5.2, has coordinates 39.3°E and 21.3°N, and the second location, labeled B, has coordinates 39.5°E and 21.3°N. Figure 5.2a and Figure 5.2b show the hourly-accumulated rainfall total for 06Z and 07Z, respectively. The first location (point A) in the south received a rainfall total of more than 55 mm at 06Z, and the second location (point B) in the southeast received about the same rainfall total in the following hour at 07Z. This is a consequence of the storm propagation toward the northeast, where the maximum intensity of the precipitation shifted from location A to location B in the two-hour period.

Figure 5.3 shows the accumulated rainfall and the instantaneous precipitation rates for these locations in addition to KAIA. As shown in Figure 5.3a, the KAIA observation was about 19 mm and the model computed a rainfall total of 15.68 mm. TRMM 3B42 underestimated the total rainfall for the same location and recorded 11.98 mm. The model computed a total rainfall of 112 mm and 102 mm for the locations A and B, respectively (Figures 5.3b and 5.3c). TRMM 3B42 shifted the precipitation toward the north of Jeddah and had an unrealistic estimation for total rainfall in these locations (Figure 5.4). As mentioned by Haggag and El-Badry (2013), many studies have shown an underestimation of the rainfall events estimated by TRMM for extreme events. In this study, TRMM was not a reliable tool to evaluate simulation results.

Figure 5.3b shows the starting time of the precipitation and indicates the maximum instantaneous precipitation rate at 0550Z for location A. The simulation maintains relatively higher precipitation rates, ranging from 20 to 60 millimeters per hour between 05Z and 07Z.

Recalling what Doswell et al. (1996) mentioned about high rainfall rates and long duration, they defined that about 25 mm/hr is considered a high precipitation rate with the precipitation lasting for 1 hour. The figure shows a sudden increase in the accumulated rainfall between 05Z and 07Z due to the high precipitation rates at this time, and then maintains a smooth increase until the end of the simulation time at 12Z.

For location B, Figure 5.3c shows two high-instantaneous precipitation rates, one is equal to 125 mm/hr at 0510Z, and the other is around 80 mm/hr at 0630Z. As for the accumulated rainfall, the same sudden increase between 05Z and 07Z is shown in Figure 5.3c. The accumulated rain smoothly increased after 07Z. This localized precipitation over the southern part of Jeddah, represented by locations A and B, and determined the severity of the MCS and contributed to the flash flood occurrence.

In addition, the severity of the MCS can be seen from the radar reflectivity. As discussed in the previous chapter, the radar image shows a maximum reflectivity range between 50-55 dBZ, and this indicates a precipitation rate between 50 and 100 mm/hr. This compares quite well with the model computation of the hourly rainfall total during the storm peak. In order to calculate the model derived reflectivity to compare the rainfall simulation with the realtime radar observations, the instantaneous model reflectivity was calculated using a given drop size distribution of a sample of rain, and the sixth power of the average diameter of drops contained in a unit volume. The equation utilized was ($Z = N \times D^6$), where Z is the reflectivity in mm^6m^{-3} unit, N is the number of distribution for the raindrops in cubic meters m^{-3}, and D is the average diameter of the raindrop in millimeter mm. Then, the reflectivity in the dBZ unit is calculated taking the logarithmic scale of Z, where ($Z_{dBZ} = 10 \times log_{10} Z_{mm^6m^{-3}}$).

The model calculated a widely spread reflectivity field. It gives a reflectivity range between 45 and 50 dBZ, and a peak of about 55 dBZ over location A, where the maximum accumulated precipitation is calculated. Meanwhile, the model calculated about 40-45 dBZ reflectivity in the north and northeastern parts of Jeddah. Figure 5.5 shows the simulated model reflectivity during the peak of the storm intensity and the radar reflectivity at 0930Z. The figure indicates the location of the storm using the model derived reflectivity field and the real-time radar reflectivity. RAMS provided a good indication about the location and the lifetime of the MCS, even though it produced high reflectivity fields in other areas that were not observed by the radar. Importantly, the model performed well in the prediction of the maximum precipitation that was responsible for this flash flood event.

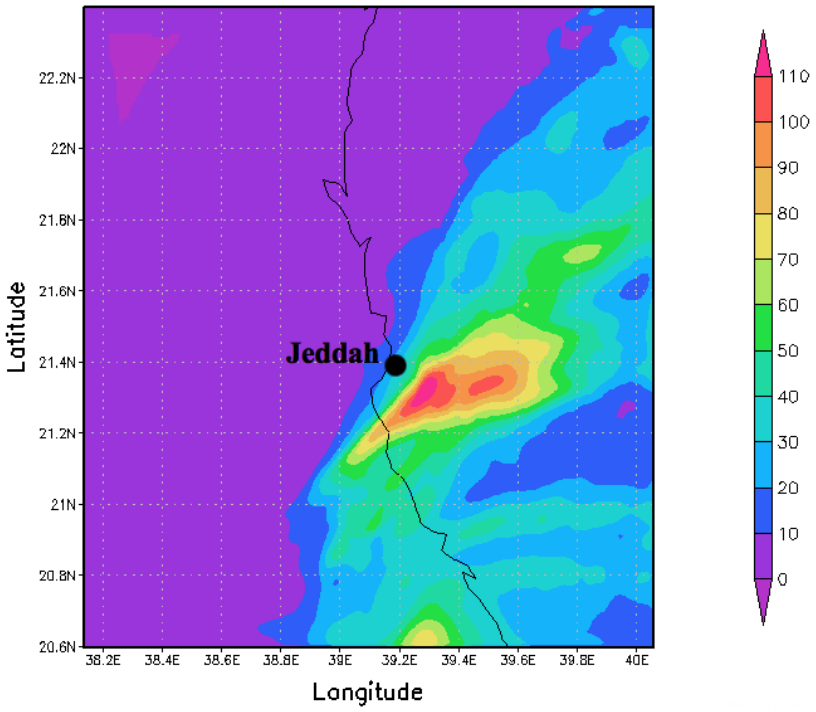

Fig. 5.1: Computed accumulated rainfall [mm] calculated from grid3 for the 12 hours simulation on 26 January 2011.

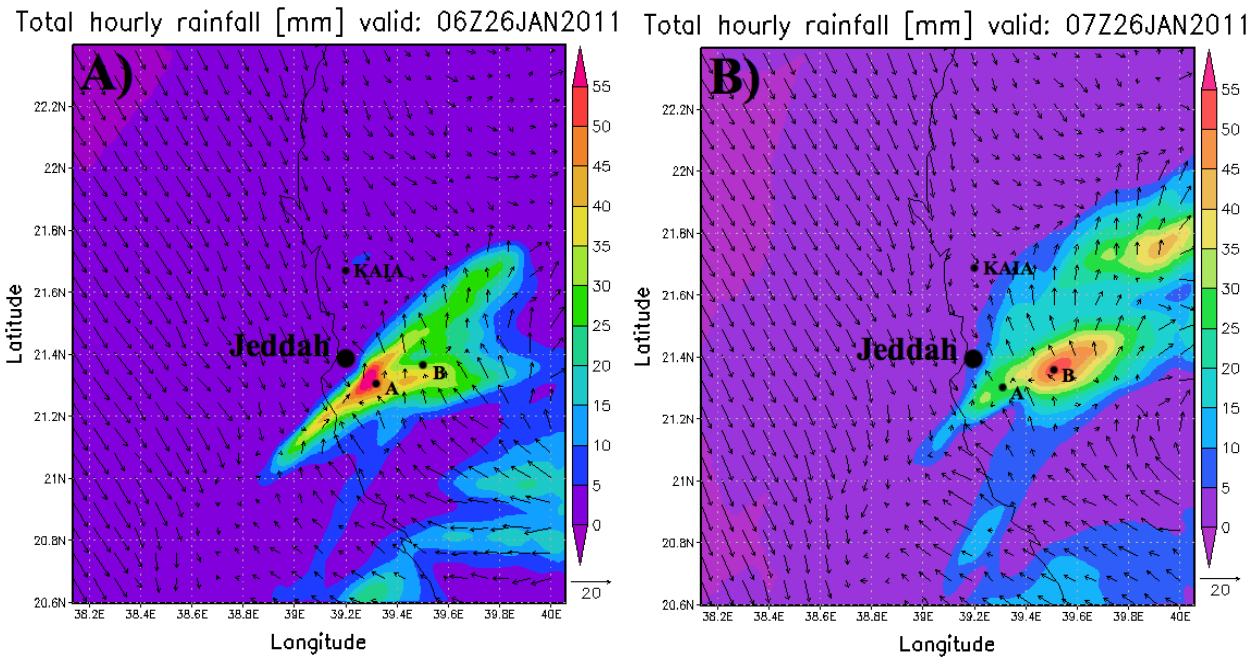

Fig. 5.2: Model simulated total hourly-accumulated rainfall [mm] and horizontal surface wind vectors, a) for 06Z, b) for 07Z.

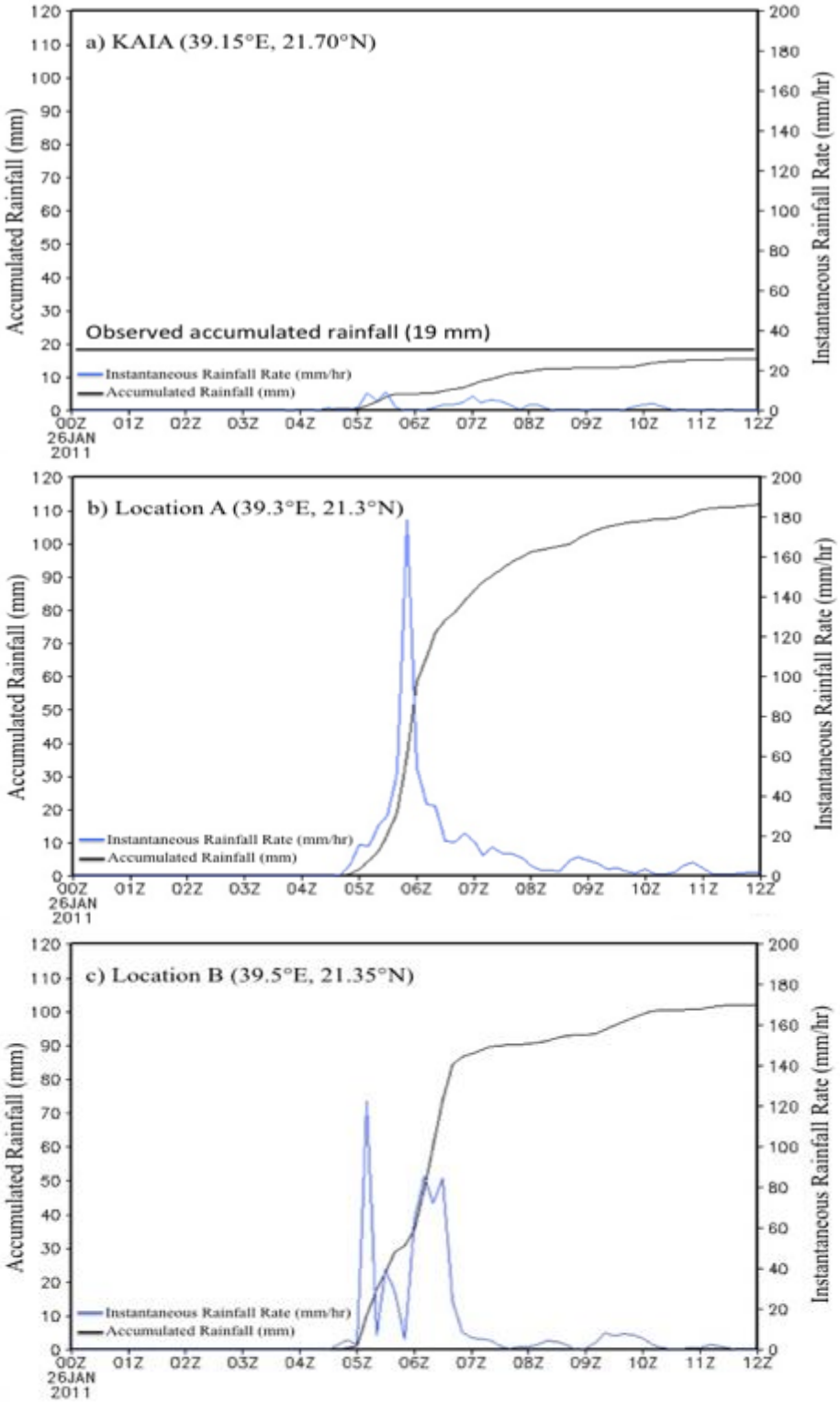

Fig. 5.3: Time series of accumulated rainfall and instantaneous precipitation rates (from grid3) at several locations near Jeddah on 26 January 2011 from 00Z to 12Z. The black line represents the computed hourly rainfall and the blue line represents the instantaneous precipitation rates. a) For KAIA, the solid line shows the observed accumulated rainfall. b) For location A. c) For location B.

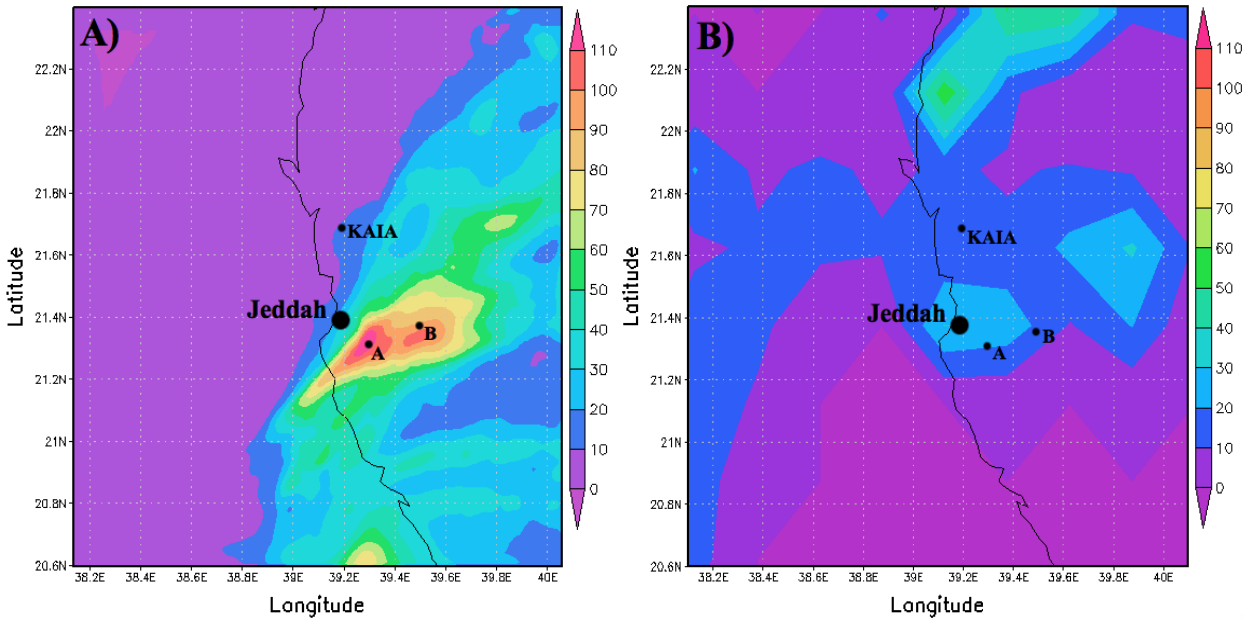

Fig. 5.4: Comparison of a) computed total accumulated rainfall from RAMS (grid3) and b) TRMM's accumulated rainfall for 26 January in 2011 over western KSA.

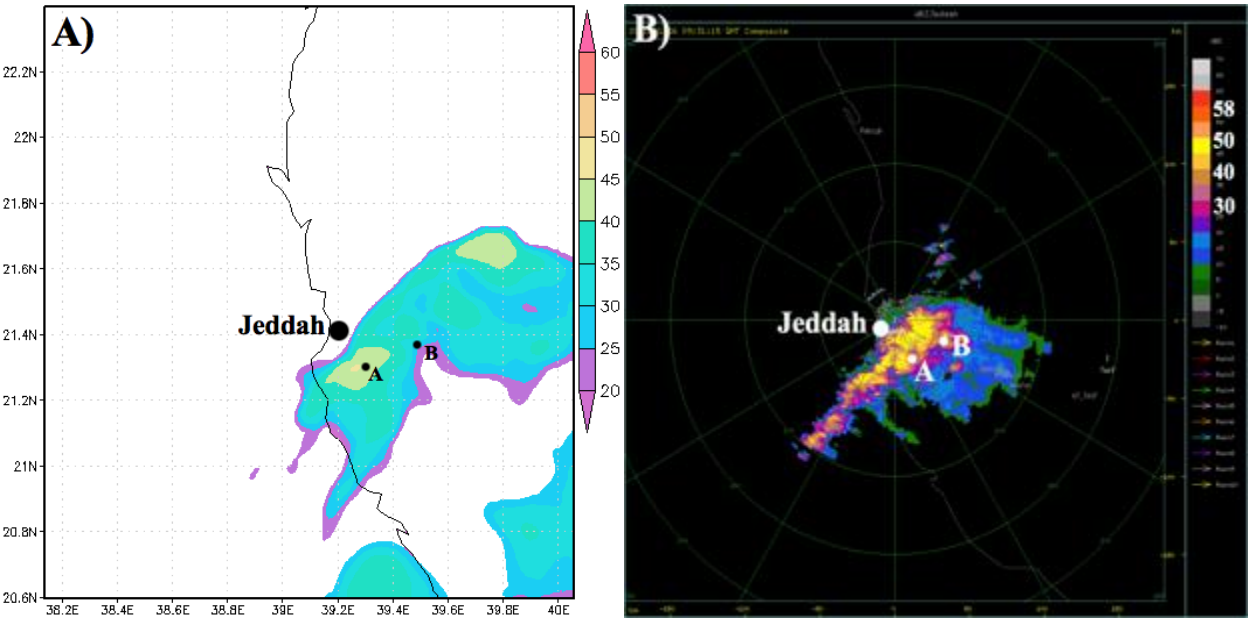

Fig. 5.5: A) Instantaneous model reflectivity [dBZ] computed by RAMS using the relation ($Z = N \times D^6$), B) Jeddah's rainfall radar reflectivity on at 0930Z on 26 January 2011.

5.2 Simulation of the surface field

The previous section showed that RAMS was able to predict quite accurately the location and the lifetime of the heavy rainfall event over Jeddah. However, it is important to note that the synoptic patterns were a major player in providing the ingredients for the MCS to form and last for several hours. The model's ability to predict the location and the duration of the storm seems to be associated with its accurate prediction of the synoptic patterns, which is represented by the reanalysis data that is used for initial and lateral boundary conditions. Moisture transport associated with the LLJ was the main factor responsible for supporting the storm and feeding the area with a large amount of water vapor. The strong surface front resulted in strong convergence forced raising air over Jeddah as shown in Figure 5.2.

In addition, Figure 5.6a illustrates that at the 925 hPa level (the level of the LLJ) high values of meridional moisture flux occurred over the central Red Sea area where the convergence was initiated by surface frontogeneses. The meridional moisture flux is calculated as the mixing ratio (q, <g/kg>) times the meridional component of the horizontal wind (v, <m/s>) at the 925 hPa level. Figure 5.8 illustrates a vertical south-north cross-section taken at the center of the MCS from Grid1. The figure shows strong meridional moisture flux, units shown in Figure 5.8, at the 925 hPa level over the southern Jeddah area, plotted along with the equivalent potential temperature, which indicates the upward motion of the southerly surface flow. The figure shows the two different air masses clearly, where southerly flow has equivalent potential temperature higher than the northerly, and the strong frontogenesis directly over southern Jeddah between 21°N and 22°N.

Figure 5.8 also shows the instability, updraft, and the cold pool in the area of the study. The instability is indicated in the figure directly where the near vertical contour exists, and the

updraft is located between 20°N and 21.5°N, where the equivalent potential temperature contour of 336 K shifted up and vertical shape between 20°N and 21.5°N, while the cold pool is obviously seen between 21°N and 21.5°N. The continuity of strong meridional moisture flux associated with the LLJ in the presence of the surface front produced a strong updraft over the southern Jeddah area (Figure 5.9), which contributed to the flash flood.

Doswell et al. (1996) discussed that the presence of low-level moisture as well as the upward motion is the main cause of deep, moist convection. It can be represented by vertical moisture flux, and can be useful in predicting a flash flood. High vertical moisture flux values over southern Jeddah shown in Figure 5.6b were calculated as the summation of the vertical moisture flux over the intervals 1000-925, 925-850, and 850-700 using a finite centered difference. The vertical moisture flux was calculated as the mixing ratio times of the vertical wind component in each level below 700 hPa, since most water vapor exists below 700 hPa. Moreover, Figure 5.7 illustrates strong convective instability, represented by CAPE calculated for the fine domain (Grid 3) over Jeddah and it's surrounding area. The figure shows high values of CAPE in some parts over the sea as well as over the Jeddah area ranging from 2,200 J/kg to 2,600 J/kg. These high values have a significant affect on the convection in these areas due to the high sea surface temperature and surface temperature resulting from the urban environment.

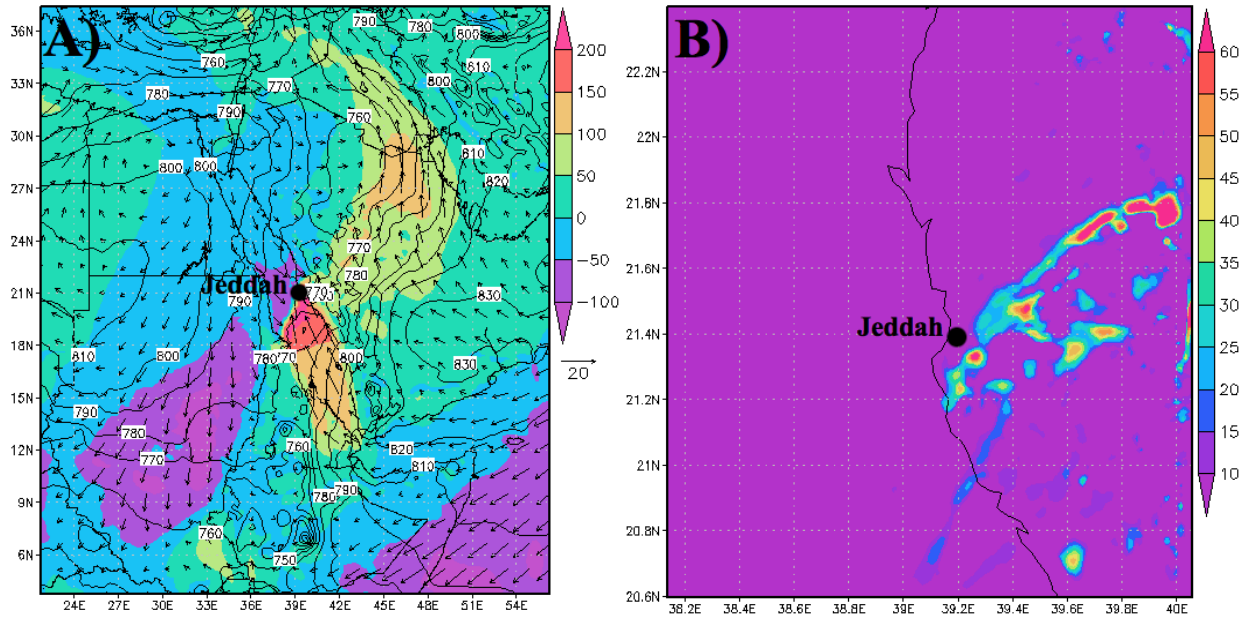

Fig. 5.6: A) Meridional moisture flux (shaded) (g/kg*m/s) at 925 hPa, 925 hPa geopotential heights (contours), and wind vectors (m/s). B) Vertical moisture flux convergence in the 1000-700 hPa (shaded with values greater than 10 g/kg*m/s). Valid at 06Z in 26 January 2011.

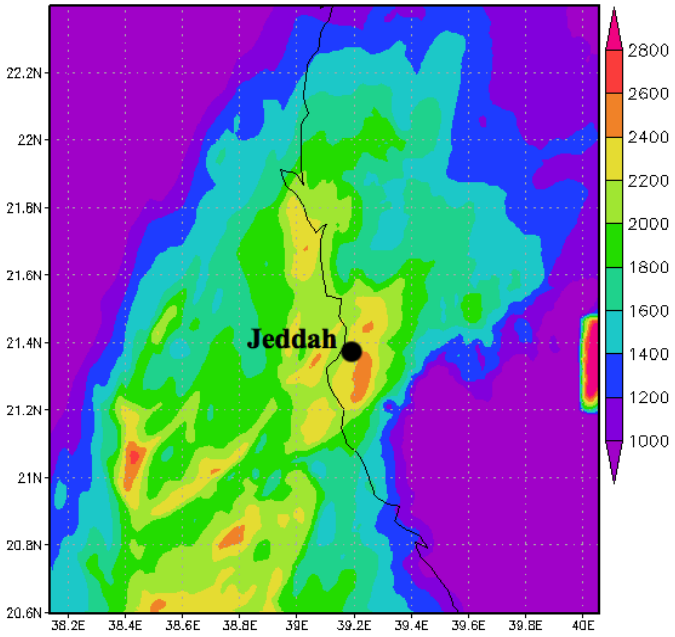

Fig. 5.7: Surface-based CAPE in the unit [J/kg] calculated from the fine domain (Grid3) Valid at 06Z in 26 January 2011.

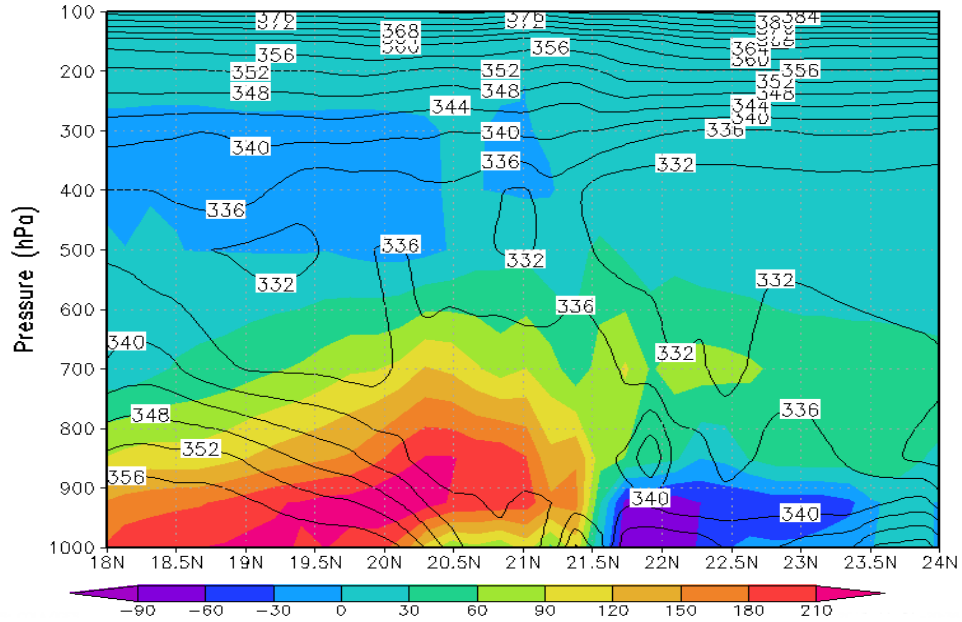

Fig 5.8: South-north cross-section from Grid1, equivalent potential temperature (contour interval of 4 K), meridional moisture flux in g/kg*m/s (shaded), valid at 06Z in 26 January 2011.

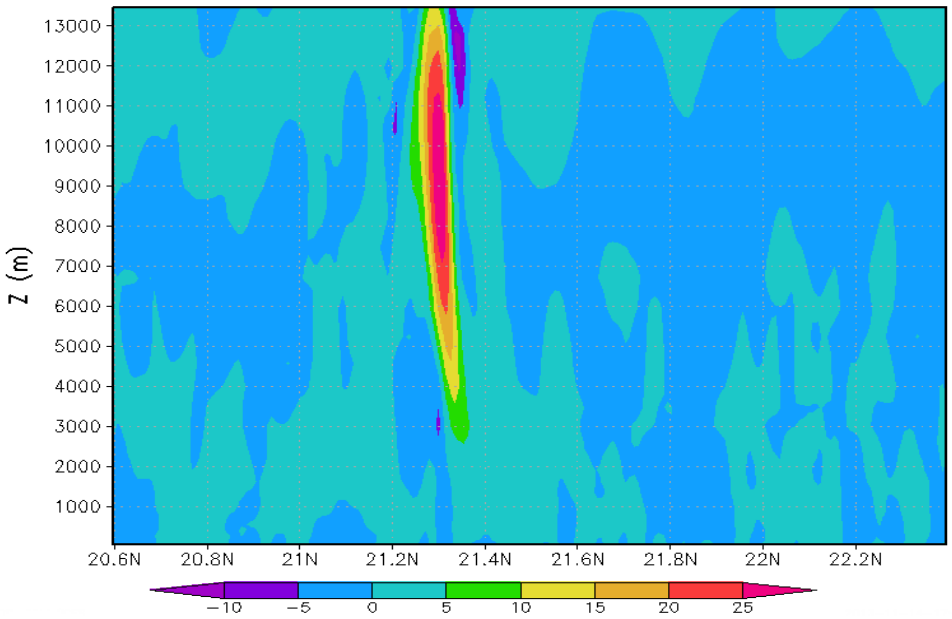

Fig 5.9: South-north cross-section from the fine domain (Grid3), showing vertical velocity shaded (w, m/s), valid at 06Z in 26 January 2011.

5.3. Results of the sensitivity experiment

5.3.1. Sensitivity of precipitation to the removal of water surfaces

The role of the Indian Ocean as well as the Red Sea in enhancing the storm and the production of large amounts of heavy rainfall was investigated. A simulation using the same model set up, initial and boundary conditions using the NCEP reanalysis data, and duration was conducted, but in this case, the ocean and the sea was removed from the model and replaced with land surface. The model computed total precipitation volume (integrated from grid3) of $701{,}917.10^6$ kg for the control case. The total precipitation volume reduced to $539{,}428.10^6$ kg when the water surfaces were removed from the model. This indicates that the total precipitation amount reduced about 23%. The distribution of precipitation did not change that much, and the maximum accumulated precipitation location still remained over the southern and southeastern parts of Jeddah (Figure 5.10b).

Recalling the point of interest where maximum accumulated precipitation was located, (point A, 39.3°E and 21.3°N), the peak of the instantaneous precipitation rate reduced to about 110 mm/hr from about 180 mm/hr when the water surfaces were removed from the model, and the accumulated precipitation computed by RAMS reduced to 67 mm from 112 mm (Figure 5.11a and 5.11b). However, it was expected that the effects of the water surfaces contributed by adding more moisture to the atmosphere, and thereby enhances convection. Based on this concept, the precipitation amount was expected to have a large reduction, but the model still computed a relatively high-accumulated rainfall. Other factors might have played a role to enhance convection. Sensible heat flux resulted in increased air temperature as well as increased instability, seem to have had a major influence on storm formation and enhancing the convection. In addition, the simulation showed that water surfaces had no effect on the

distribution and the location of the precipitation, while it does affect the severity and the amount of precipitation.

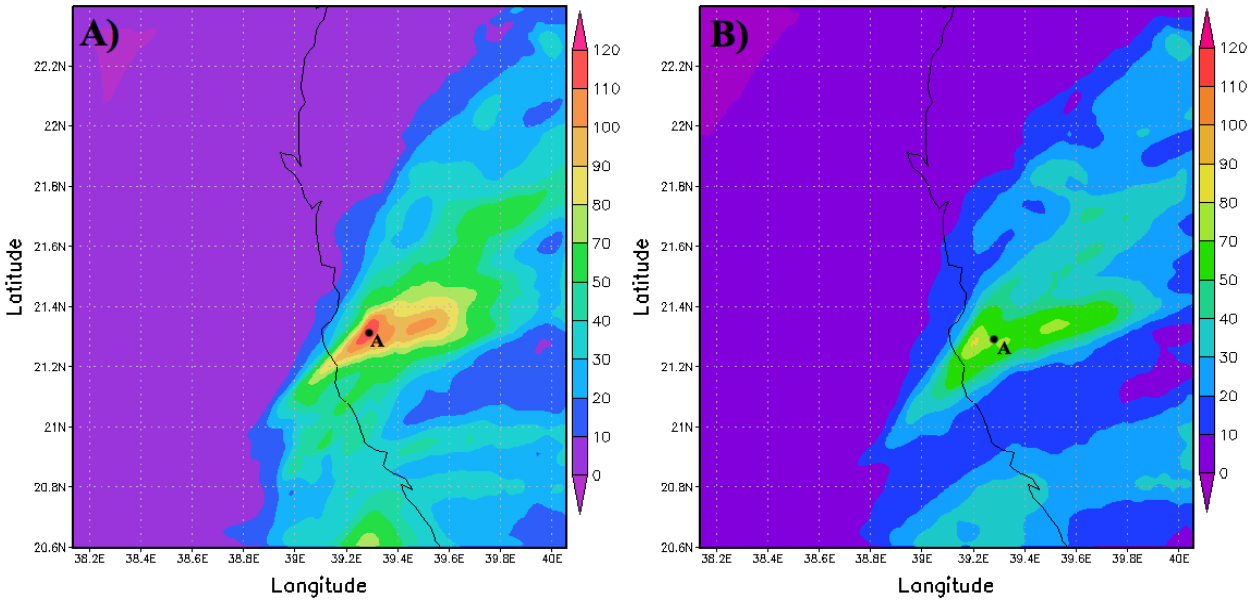

Fig. 5.10: Computed accumulated precipitation, A) Water surface embedded in the model. B) Water surfaces removed from the model.

5.3.2. Sensitivity of precipitation to the concentration of CCN

Atmospheric particles have direct and indirect influences on the weather by acting as cloud condensation nuclei (CCN). These particles have many different types, which can have different influences on cloud formation and precipitation. Several studies have investigated the CCN types and sizes influence on cloud formation and precipitation amounts. Mineral dust could work as a good CCN as it can absorb water on its surface (Karydis et al., 2011). Dust can also function at giant CCN (GCCN) and as ice nuclei (IN) (van den Heever et al., 2006). This study only examined the impacts of the CCN activity of the dust.

Karydis et al. (2011) showed that mineral dust has a large contribution to CCN concentrations in North Africa and the Arabian Peninsula, with a percentage estimated at 40%.

On January 26th, a large concentration of dust was observed over the southern Red Sea using a satellite product provided through the Naval Research Lab. Figure 5.12 shows an enhanced satellite image of the Red Sea during the storm on 26 January on 1145Z during the decay stage of Jeddah's storm. This visible satellite image is a NexSat product described by Miller et al. (2006). The spatial distribution of the mineral dust is shown in pink, and the darker color indicates higher concentrations. The image showed a significant dust concentration around the west coast of the southwestern region of Saudi Arabia and the east coast of Sudan. The warm and moist southerly flow from the south could easily transport dust to the central Red Sea area and alter cloud microphysical processes by increasing the number concentration of CCN.

In addition to dust, anthropogenic emissions associated with human activities; especially in big-economy cities like Jeddah are considered as significant contributors to the CCN concentrations in the atmosphere. The industrial portions of the city are located in the south and extend for an area of about 13 km^2, and might also contribute to increasing the CCN concentration in the atmosphere over Jeddah by producing several pollutants.

Wang (2005) conducted 90 numerical simulations to investigate the role of increased aerosols concentration in enhancing tropical deep convection, and the results suggested that increasing aerosol concentrations could lead to strong convection in the presence of the appropriate thermodynamic and dynamic mechanisms. However, this study investigated the influence of the number concentration of CCN on precipitation by varying the number concentration of CCN in RAMS. Figure 5.13 shows the accumulated precipitation distributions calculated by RAMS for varying CCN number of concentration. Values of 300, 600, 1,000, and 1,500/cc CCN concentrations were selected. The lower value of CCN concentration was 300/cm^3 (Figure 5.13a) and it produced a maximum total rainfall of more than 130 mm east of Jeddah.

The model computed total precipitation volume (integrated from grid3) of 713,346.10^6 kg or 1% greater than the control simulation, which used a moderate value of 600 cm^{-3} concentration of CCN.

The spatial distribution of the accumulated rainfall shifted to the south with about the same total precipitation when using 1000 CCN cm^{-3} concentration (Figure 5.13c) and the model produced a larger amount of total precipitation volume, which was 720711X4.10^{10} kg or 2.6 % greater than the control simulation. Using a CCN concentration of 1500 cm^{-3} (Figure 5.13d) intensifies the precipitation in narrow swaths, but the total precipitation volume for the fine domain computed by the model reduced to 676047X4.10^{10} kg or 3.6 % less than the control simulation. The simulation shows two locations of locally high-accumulated precipitation between 21N and 21.2N where it computed over 110 mm, and over 130 mm between 20.6N and 20.8N.

Enhancing CCN concentration can speed up the formation of small droplets and ice species and slow down the formation of rain droplets which then enhances the updraft and intensifies the storm (Khain, 2005; Koren et al., 2005; Rosenfeld et al., 2008; Rosenfeld et al., 2012; van den Heever et al., 2007). Then, the earlier formation of enhanced surface precipitation will produce stronger downdrafts and intensify the cold pool, which could form new cells. The total precipitation volume initially increased by 2.6% when CCN concentration was enhanced from 600 cm^{-3} to 1000 cm^{-3}. Then, it decreased by 3.6% when CCN concentration is further enhanced to 1500 cm^{-3}. In the first case, enhancing CCN concentration results in more supercooled water transported aloft which invigorates the convection and increases precipitation.

Carrio and Cotton (2011) found a “tipping point” where very high CCN concentrations reduced the total precipitation volume relative to more moderate increases in CCN by reducing

riming efficiency of ice. Thus more water substance is thrust into anvil levels rather than increasing surface precipitation amounts.

Location A was used again to investigate the effect of CCN concentration on the severity of the storm over the area of the study. For this location, the precipitation started at 05Z for all CCN concentrations (Figure 5.14). Then the accumulated precipitation increased rapidly to reach over 90 mm and 60 mm when using moderate CCN concentrations of 600 cm^{-3} and 1000 cm^{-3} respectively after two hours, which indicates higher precipitation rates for this scenario. Using a lower CCN concentration of 300 cm^{-3} shows relatively high precipitation rate in the first two hours and moderate in the following 3 hours, and the computed accumulated precipitation was 81 mm. The model computed accumulated precipitation of 32 mm for the very high CCN concentration of 1500 cm^{-3} in the area of our interest over Jeddah. We speculate the actual values of CCN are moderate values 300 and 1000/cc because they produced the more accurate spatial distribution of accumulated rainfall in Jeddah.

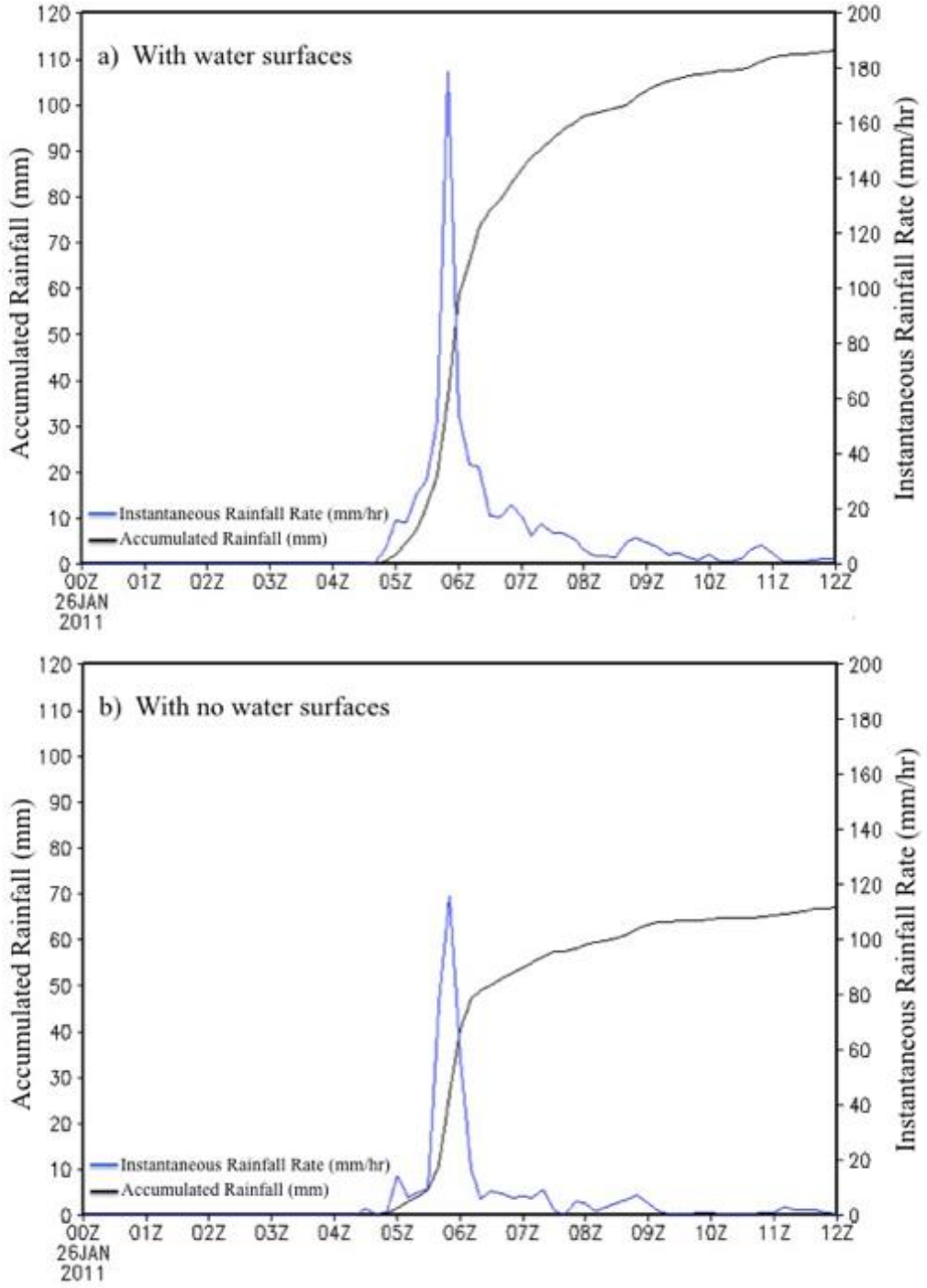

Fig. 5.11: Time series of accumulated rainfall and instantaneous precipitation rates (from grid3) at location A (39.3°E and 21.3°N) near Jeddah on 26 January 2011 from 00Z to 12Z. The black line represents the computed hourly rainfall and the blue line represents the instantaneous precipitation rates. a) With water surfaces embedded in the model. b) Water surfaces removed from the model.

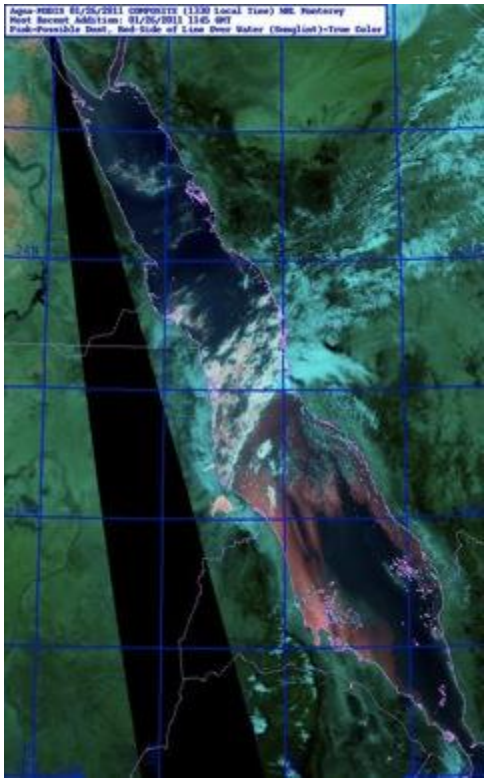

Fig. 5.12: An enhanced satellite image showing the dust distribution and location over the Red Sea. Valid at 1145Z on 26 January 2011.

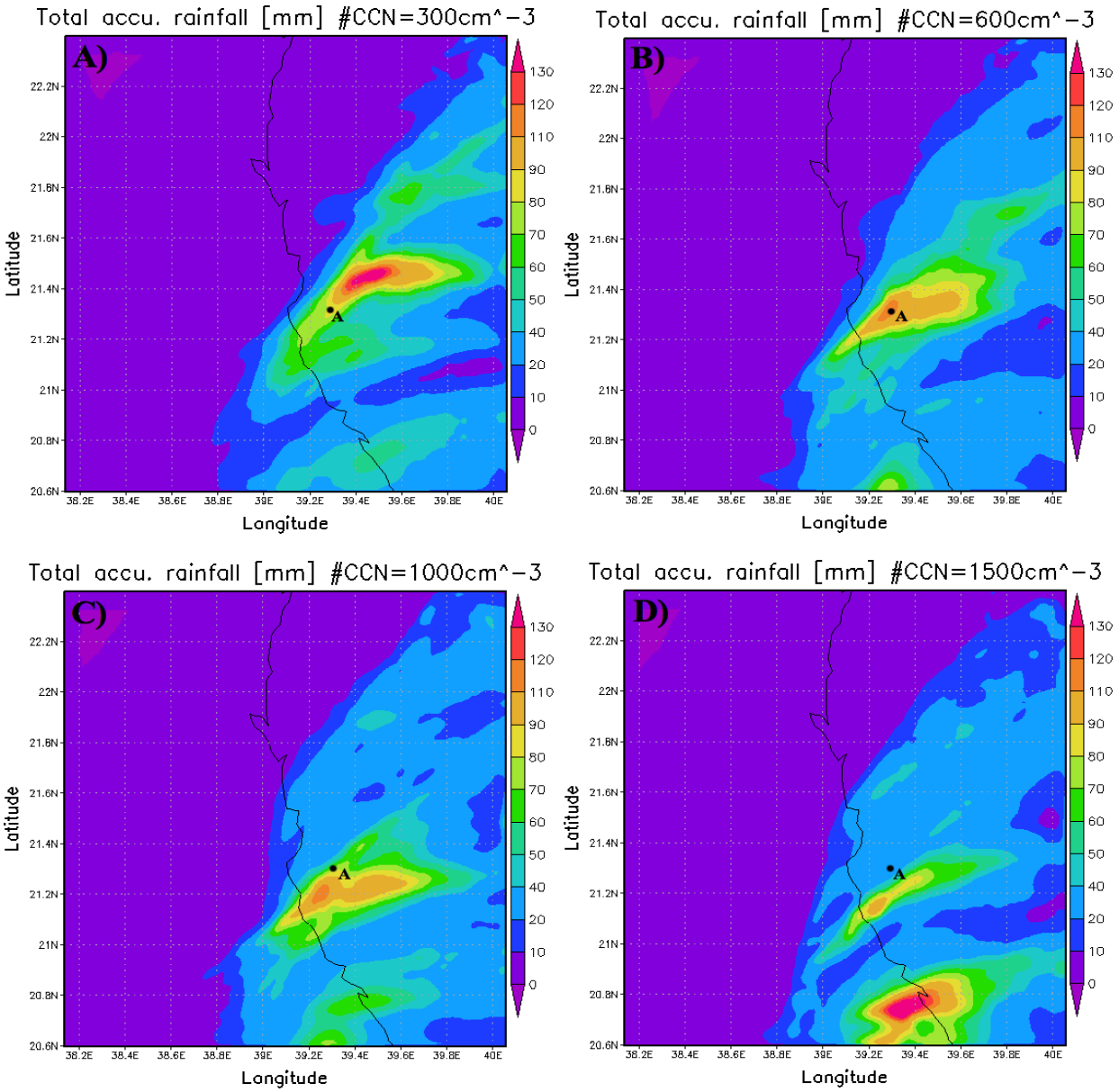

Fig. 5.13: Fig. 5.1: Computed accumulated rainfall [mm] calculated from grid3 for varying CCN concentration. A) Using CCN concentration of 300 cm^{-3}. B) Using CCN concentration of 600 cm^{-3}. C) Using CCN concentration of 1000 cm^{-3}. D) Using CCN concentration of 1500 cm^{-3}.

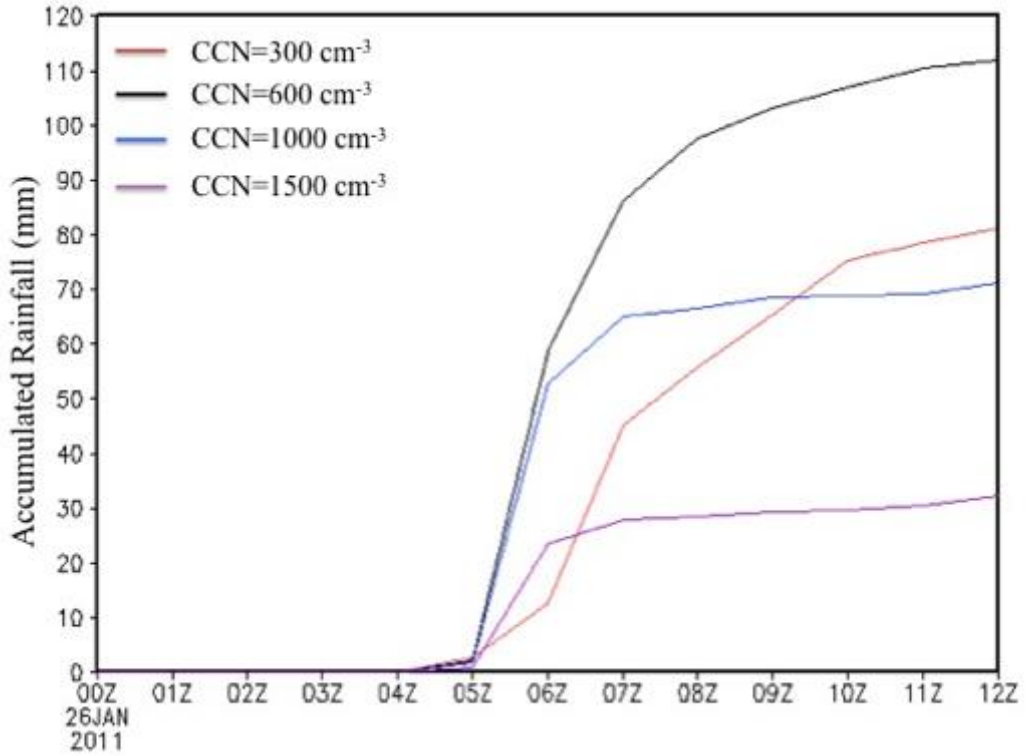

Fig 5.14: Time series of accumulated rainfall (from grid3) at location A (39.3°E and 21.3°N) near Jeddah on 26 January 2011 from 00Z to 12Z for different CCN concentration.

5.3.3. Sensitivity to the urban heat island effect

In this section, the urban heat island (UHI) effect on the precipitation in Jeddah during the flash flood event is investigated. UHI is an area of densely developed land that is warmer than the surrounding rural area due to anthropogenic activities. This heat is a consequence of concrete, asphalt, and buildings storing the energy absorbed from the shortwave radiation during the day due to their high heat capacity. Unlike the rural and suburban areas, urban areas release this energy slowly as long wave radiation resulting in maintaining high temperatures. UHI can impact the weather by providing low pressure over the city due to the warmer temperature and enhance the convergence of low-level air, which can be moist and thus can provide an environment suitable for cloud formation and increase precipitation.

Jeddah is a big city that has an area of 5,460 km^2, and it mostly consists of an urban environment. The UHI effect likely contributed to the storm severity and precipitation over Jeddah due to the higher sensible heat it produces, and hence enhanced the instability of the atmosphere. In addition, based on Section 5.2, the environment over Jeddah had very high values of CAPE, which also indicates strong instability. In all of the simulations in the previous sections, the simulations were conducted taking into account that Jeddah is defined as an urban area in the model using the Town Energy Budget (TEB) urban model (Masson 2000; Masson et al. 2002). In this section, a simulation of the storm and precipitation was conducted by removing the effect of the city and defined the location of Jeddah as if the city did not exist.

In the *no city* simulation, the model predicted the same spatial distribution of the precipitation over Jeddah and computed total accumulated rainfall of about 90 mm over southern Jeddah. Even though the computed total precipitation volume from the fine domain in the *no city* run was higher than one in the run with the city, the latter produced more intense localized precipitation over the city due to enhanced convection and trigger mechanisms resulting from the UHI effect. However, no significant change in the nature of the flow around the city was observed in the simulation due to the dominant role of the synoptic features. The computed accumulated precipitation over southern part of Jeddah (Location A) increased by 44% when UHI effect is present. The effect of the urban area provided favorable ingredients to start and intensify the convection potentially earlier over the urban and downwind areas. The simulation showed that the presence of the city rarely modify significantly the precipitation over a larger region (grid3). The main effect concluded from this simulation is to localize the storm and increase precipitation over the city and a small area downwind of the city. The change in the total precipitation volume is linked to the change in the precipitation area. The precipitation

covered larger area in the no city run than in the city run. Figure 5.15 shows how the precipitation amount decreased from about 110 mm to about 90 mm over the southern part of Jeddah when the UHI effects were removed from the model for the *no city* run. The figure also shows the widely spread precipitation that covered larger areas in the domain, which resulted in total precipitation volume greater than the control simulation.

Carrio et al. (2010) conducted similar simulations to investigate UHI effect on convection and they showed that the total volume of precipitation monotonically increased when they ran simulations with the city and embedded higher CCN concentrations. Likewise, van den Heever and Cotton (2006) concluded that the UHI effect enhances the interaction between microphysical and dynamical processes and increases surface precipitation. This suggests that UHI effects in Jeddah had an impact on the precipitation and contributed to enhanced total precipitation over the urban areas. The simulation showed that the precipitation in Jeddah increased by 22.2% when taking UHI effects into account.

Summary

The sensitivity experiments have shown that storm formation and severity over Jeddah on 26 January 2011 was sensitive to several factors. There is no doubt that water surfaces played a major role in producing more moisture to the atmosphere and hence had an impact on the storm severity and the precipitation amount. In addition, the concentration of the CCN controlled the location of the precipitation as well as the total amount of precipitation in the area of study. Furthermore, based on the simulations, the UHI effect had a relatively important influence on the severity of the storms and hence on the precipitation. Table 5.1 summarizes the total rainfall for the area of study for selected locations in Jeddah for the conducted sensitivity experiments.

Table 5.1: Computed total precipitation volume (integrated from domain 3) and local accumulated rainfall in several locations in Jeddah for the different sensitivity experiments.

Sensitivity tests	**Model inputs**	**Total volume of precipitation (integrated over domain3) X($4X10^{10}$)kg**	**Accumulated precipitation at**		
			KAIA (39.15°E, 21.70°N).	**Location A South of Jeddah (39.3°E, 21.3°N).**	**Location B Southeast of Jeddah (39.5°E, 21.35°N).**
Optimal case	Sea: yes CCN=600 cm^{-3} UHI effect: yes	701917	19 mm	112 mm	102 mm
Water surface	Sea: removed CCN=600 cm^{-3} UHI effect: yes	539428	23.73 mm	67 mm	69.5 mm
CCN concentration	Sea: yes CCN=300 cm^{-3} UHI effect: yes	713345	14.68 mm	81.14 mm	52.31 mm
	Sea: yes CCN=1000 cm^{-3} UHI effect: yes	720711	32.98 mm	71.19 mm	58.28 mm
	Sea: yes CCN=1500 cm^{-3} UHI effect: yes	676047	31.71 mm	32.22 mm	50 mm
UHI effect	Sea: yes CCN=600 cm^{-3} UHI effect: no	728676	24.61 mm	77.53 mm	69 mm

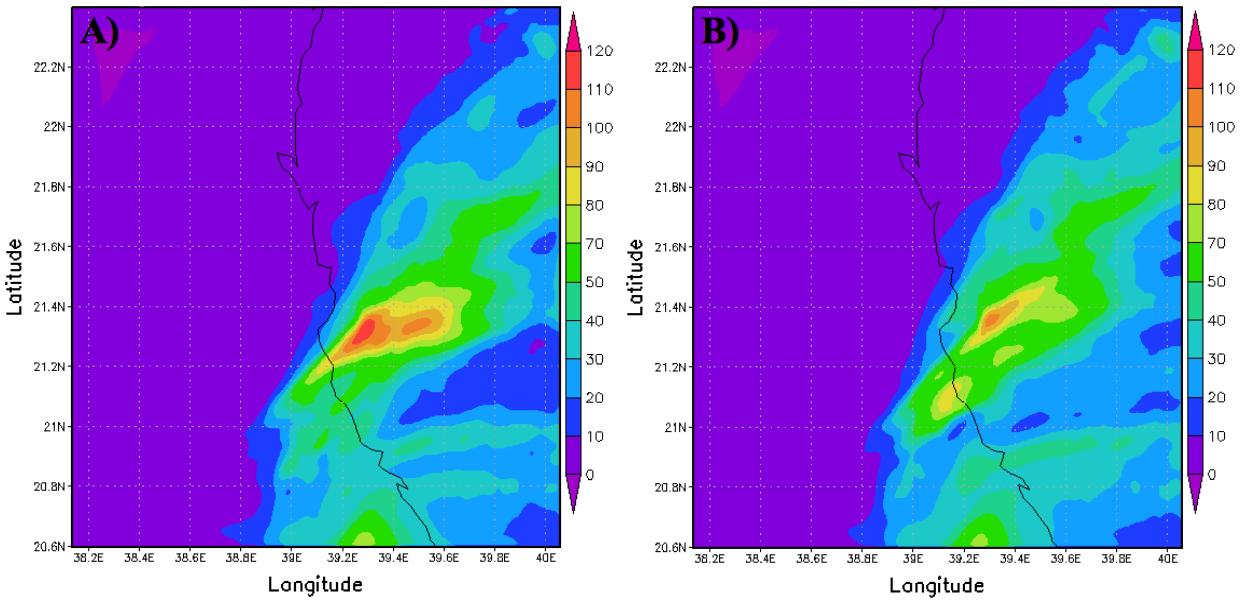

Fig 5.15: Computed accumulated rainfall [mm] calculated from grid3 for the 12 hours simulation on 26 January 2011. A) Simulation of control run (city run). B) Simulation with *no city*.

CHAPTER 6: CONCLUSIONS AND SUGGESTIONS FOR FUTURE RESEARCH

6.1. Conclusion

The goal of this study was to provide greater understanding of the mechanisms responsible for the severe precipitation that resulted in a flash flood event on 26 January 2011 in Jeddah, Saudi Arabia. This event caused at least 11 fatalities and more than 114 were injured and the city of Jeddah was turned into a disaster zone after the flood. The precipitation amount exceeded the total annual rainfall for Jeddah for the entire year, and this event was the heaviest rainfall event in KSA in the current decade. In this study, the results from numerical simulations using the Regional Atmospheric Modeling System (RAMS) and diagnostic analysis of the storm were presented.

As noted by Doswell et al. (1996), in heavy precipitation prediction it is useful to use an ingredients-basis concept as well as a quantitative precipitation forecast scheme. Jeddah's case study was investigated in order to understand and identify the ingredients that were responsible for the MCS formation and the heavy precipitation. The main ingredient indicated from the analysis is the presence of proper synoptic scale features that occurred simultaneously leading to strong interaction between different air masses over Jeddah. The presence of the Mediterranean cyclone beside the subtropical anticyclone over northeastern Africa contributed to bringing cold air to the northern area of the Red Sea. On the other hand, the presence of a quasi-stationary anticyclone contributed to advecting warm and moist air from the Indian Ocean and Arabian Sea toward the southern Red Sea area. Consequently, strong frontogenesis and convergence resulted from the interaction between the cold air advection and the warm moist air over the central Red Sea area. This is basically the main mechanism responsible for Jeddah's storm formation and

development, taking into account that any shifting in one of the three systems would obstruct the storm formation in that particular region.

In addition to the synoptic features, the presence of a LLJ associated with the quasi-stationary anticyclone (blocking high) over the Arabian Peninsula, as well as the high moisture at the surface in the southern part of the Red Sea was another ingredient. This mechanism basically maintained the water vapor transport and the meridional moisture flux over Jeddah for a longer time and enhanced the convection and precipitation. Additionally, the presence of a 700 hPa upper-level trough provided warm air advection over Jeddah and supported the upward motion.

The analysis also indicated the presence of suitable mesoscale ingredients leading to an enhanced vertical motion, vertical moisture flux, and convection. The results indicated that high CAPE and high sea surface temperature in the study area provided strong instability, and the presence of veering wind shear, as well as a deep warm cloud layer in the convective storm, maintained and intensified the convection and the precipitation over Jeddah due to the enhanced latent heat released and large precipitation efficiency.

The simulations exhibited accumulated precipitation maxima greater than 110 mm over the southern part of Jeddah. Lack of ground observations was an obstacle in the approach to verify the simulation results. The rain gauge data obtained from KAIA weather station compared quite well with the model calculations of the precipitation over the north of Jeddah, demonstrating the outstanding performance of the model. Furthermore, the location of the consequence damages and losses south of the city were associated with the model's forecast of the spatial distribution of the precipitation, where it calculated an accumulated precipitation greater than 110 mm. The model's capability in reproducing the spatial and temporal distribution

of the precipitation over the southern part of Jeddah also was shown through an image from Jeddah's rainfall radar.

Several sensitivity experiment simulations were conducted on this heavy precipitation event in order to understand the influence of the water surfaces, concentration of CCN, and UHI effect on the storm formation and severity. The simulations showed that water surfaces had no significant effect on the distribution and the location of the precipitation, while it did affect the severity and the amount of precipitation. The results suggested that moderate CCN concentration values between 300 and 1,000 cm^{-3} produced the best representation of the spatial distribution of the accumulated rainfall in Jeddah. The results indicated that the total precipitation volume initially increased when CCN concentration was enhanced, but it decreased when the CCN concentration was further enhanced. The UHI sensitivity experiment simulation showed that the UHI effect produced more intense and localized precipitation over the city. The *no city* simulation showed that the model predicted the same spatial distribution of the precipitation without the UHI, but with reduced precipitation efficiency and accumulated precipitation.

6.2. Suggestions for future research

Suggestions for future work include several different ideas. First, an interesting research could be conducted by focusing on the CCN and GCCN percentages. Investigating the source of the aerosols in the area by simulating the dominant flows that contribute in providing the region with different aerosol types and properties in order to understand their effect on the storm evolution. For example, whether high sand or dust concentrations are expected to be associated with the southeasterly flow and greater concentrations of sea salt when the flow comes from the south or the southwest. Moreover, explicit representation of pollution sources of CCN over

Jeddah would be useful in investigating their impact on precipitation for the event. Hence, conducting a microphysical study and numerical simulations by dealing with these different particles due to their different nucleation properties to investigate the effect of these particles on the storm location and severity would be motivating and valuable.

It would also be interesting to conduct a study focusing on the UHI effect, perhaps by doubling the urban area in the model north of the city and investigate the difference that this could make in the spatial and temporal distribution of the storm, assuming that the urban land expansion in Jeddah is increasing rapidly. In addition, it would be interesting to focus more on the role of the sea breeze and the downwind effects in the convective enhancement as well as making future urban map projections of the city and studying the hydrological implications. Furthermore, the study of convection in this area could include investigating the seawater circulation of the Red Sea and the change in sea surface temperature as well as varying water vapor amounts in the region.

From a larger scale point of view, future work should include study the frequency of the formation of the Mediterranean cyclones and their propagation in addition to the subtropical anticyclones in the regions, as well as studying the general circulation patterns predicted by global climate models. As a result of global warming effects, would extreme rainfall events intensify and occur more frequently in regions that are known for low precipitation?

REFERENCES

Abdullah, M. A., & Al-Mazroui, M. A. (1998). Climatological study of the southwestern region of Saudi Arabia- I. Rainfall analysis. *Climate Research, 9*(3), 213-223.

Akaeda, K., Reisner, J., & Parsons, D. (1995). The role of mesoscale and topographically induced circulations in initiating a flash flood observed during the TAMEX project. *Monthly Weather Review, 113*, 1720-1739.

Alateeq, B. (2011). 10 deaths and 114 injured in jeddah flood and search for 3 missing, *Alwatan*. Retrieved from http://www.alwatan.com.sa/local/News_Detail.aspx?ArticleID=39514&CategoryID=5

AlKhalaf, A., & Basset, H. A. (2013). Diagnostic Study of a Severe Thunderstorm over Jeddah. *Diagnostic Study of a Severe Thunderstorm over Jeddah, 3*(1), 150-164. doi: 10.4236/acs.2013.31017

Almazroui, M. (2011a). Calibration of TRMM rainfall climatology over Saudi Arabia during 1998–2009. *Atmospheric Research, 99*(3-4), 155-165.

Almazroui, M. (2011b). Sensitivity of a regional climate model on the simulation of high intensity rainfall events over the Arabian Peninsula and around Jeddah (Saudi Arabia). *Theoretical and Applied Climatology, 104*(1), 261-276.

Almazroui, M. (2012). The life cycle of extreme rainfall events over western Saudi Arabia simulated by a regional climate model: Case study of November 1996. *Atmósfera, 25*(1).

Amengual, A., Romero, R., Gomez, M., & Alonso, S. (2007). A Hydrometeorological Modeling Study of a Flash-Flood Event over Catalonia, Spain. *Journal of Hydrometeor, 8*(3), 282-303.

Bryan, G. H., Wyngaard, J. C., & Fritsch, J. M. (2003). Resolution requirements for the simulation of deep moist convection. *Monthly Weather Review, 131*(10).

Caracena, F., Maddox, R. A., Hoxit, L. R., & Chappell, C. F. (1979). Mesoanalysis of the Big Thompson storm. *Monthly Weather Review, 107*, 1-17.

Carrió, G. G., Cotton, W. R., & Cheng. (2010). Effects of the Urban growth of Houston on convection and precipitation. Part I: the August 2000 case. *Atmospheric Research, 96*, 560-574.

Carrió, G. G., & Cotton, W. R. (2011). Effects of the Urban growth of Houston on convection and precipitation. Part II: Their dependence on instability. *Atmospheric Research, 102*, 167-174.

Chappell, C. F. (1993). Dissecting the flash flood forecasting problem. Post-prints, Third Heavy Precipitation Workshop (Vol. NOAA Tech Memo NWS ER-87, 293-297). Pittsburgh, PA: National Weather Service.

Cotton, W. R. (1990). *Storms* (Vol. 1). Fort Collins, CO: Aster Press.

Cotton, W. R., Bryan, G. H., & van-den-Heever, S. C. (2011). *Storm and Cloud Dynamics* (2nd ed.): Academic Press.

Cotton, W. R., G.Thompson, & Mielke, P. W. J. (1994). Real-time mesoscale prediction on workstations. *Bulletin of the American Meteorological society, 75*, 349-362.

Cotton, W. R., McAnelly, R. L., & Ashby, C. T. (2002, June). In John Horel (Chair). Simulation of extreme precipitation events in the colorado rocky mountains. 10th conference on mountain meteorology and map meeting 2002, Park City, UT. Retrieved from https://ams.confex.com/ams/10Mountain/techprogram/paper_35491.htm

Cotton, W. R., Pielke-Sr., R. A., Walko, R. L., Liston, G. E., Tremback, C. J., Jiang, H., . . . McFadden, J. P. (2003). Rams 2001: Current status and future directions. *Meteorology and Atmospheric Physics, 82*, 5-29.

Davis, R. S. (2001). Flash Flood Forecast and Detection Methods. *Meteorological Monographs, 28*, 481-526.

De Pauw, E. (2002). *An Agroecological Exploration of the Arabian Peninsula*. Aleppo, Syria: ICARDA.

Doswell, C. A., Brooks, H. E., & Maddox, R. A. (1996). Flash flood forecasting: an ingredients-based methodology *Weather Forecasting, 11*, 560-581.

Ducrocq, V., Ricard, D., Lafore, J. P., & Orain, F. (2002). Storm-scale numerical rainfall prediction for five precipitating events over France - On the importance of the initial humidity field. *Weather Forecasting, 17,* 1236-1256.

El-Sammany, M. S. (2010). Forecasting of Flash Floods over Wadi Watier – Sinai Peninsula Using the Weather Research and Forecasting (WRF) Model. *World Academy of Science, Engineering and Technology, 46*, 996-1000.

Federico, S., Avolio, E., Bellecci, C., Lavagnini, A., Colacino, M., & Walko, R. L. (2008). Numerical analysis of an intense rainstorm occurred in southern Italy. *Natural Hazards Earth System Science, 8*, 19-35. doi: 10.5194/nhess-8-19-2008

Ghazanfar, S. A., & Fisher, M. (1998). *Vegetation of the Arabian Peninsula*. Netherlands: Kluwer Academic Publishers.

Haggag, M., & El-Badry, H. (2013). Mesoscale Numerical Study of Quasi-Stationary Convective System over Jeddah in November 2009. *Atmospheric and Climate Sciences, 3*(1), 76-86. doi: 10.4236/acs.2013.31010

Harrington, J. (1997). *The effects of radiative and microphysical processes on simulated warm and transition season arctic stratus.* (Ph.D. Dissertation), Colorado State University, Fort Collins.

Junker, N. W., Schneider, R. S., & Fauver, S. L. (1999). A Study of Heavy Rainfall Events during the Great Midwest Flood of 1993. *Weather Forecasting, 14*, 701-712.

Kain, J., & Fritsch, J. (1990). A one-dimensional entraining/detraining plume model and its application in convective parameterization. *Journal of Atmospheric Science, 47*, 2784-2802.

Kalnay, E., Kanamitsu, M., Kistler, R., Collins, W., Deaven, D., Gandin, L., ... & Joseph, D. (1996). The NCEP/NCAR 40-year reanalysis project. *Bulletin of the American meteorological Society, 77(3)*, 437-471.

Karydis, V. A., Kumar, P., Barahona, D., Sokolik, I. N., & Nenes, A. (2011). On the effect of dust particles on global cloud condensation nuclei and cloud droplet number. *Journal of geophysical research, 16*, 116. doi: D23204

Khain, A. P., Rosenfeld, D., & Pokrovsky, A. (2005). Aerosol impact on the dynamics and microphysics of convective clouds. *Q. J. Roy. Meteor. Soc. 131*, 2639-2663.

Klemp, J. B., & Wilhelmson, R. B. (1978). The simulation of three-dimensional convective storm dynamics. *Journal of Atmospheric Science, 35*, 1070-1096.

Koren I., Kaufmann, Y.J., Rosenfeld, D., Remer, L. A., & Rudich, Y., (2005). Aerosol invigoration and restructuring of Atlantic convective clouds, *GRL, 32*, L14828, doi:10.1029/2005GL023187.

Kuo, H. (1974). Further studies of the parameterization of the influence of cumulus convection on large scale flow. *Journal of Atmospheric Science, 31*, 1232-1240.

Lawrence, M. G. (2005). The relationship between relative humidity and the dew point temperature in moist air: A simple conversion and applications. *Bulletin of the American Meteorological society, 86*, 225-233.

Lerach, D. G. (2012). *SIMULATING SOUTHWESTERN U.S. DESERT DUST INFLUENCES ON SEVERE, TORNADIC STORMS.* (PhD Dissertation), Colorado State University, Fort Collins.

Li, J., Maddox, R. A., Gao, X., Sorooshian, S., & Hsu, K. (2003). A Numerical Investigation of Storm Structure and Evolution during the July 1999 Las Vegas Flash Flood. *Monthly Weather Review, 131*, 2038-2059.

Lin, X. (1999). Flash floods in arid and semi-arid zones. *IHP-V Technical Documents in Hydrology, 23*.

Maddox, R. A., Canova, F., & Hoxit, L. R. (1980). Meteorological characteristics of flash flood events over the western United States. *Monthly Weather Review, 108*, 1866-1877.

Maddox, R. A., Caracena, F., Hoxit, L. R., & Chappell, C. F. (1977). Meteorological aspects of the Big Thompson Flash Flood of 31 July 1976: U.S. Department of Commerce, National Oceanic and Atmospheric Administration Environmental research Lab.

Maddox, R. A., Chappell, C. F., & Hoxit, L. R. (1979). Synoptic and Meso-α Scale Aspects of Flash Flood Events 1. *Bulletin of the American Meteorological society, 60*, 115-123.

Mahrer, Y., & Pielke, R. A. (1977). A numerical study of the airflow over irregular terrain. *Beitr€age zur Physik der Atmosph€are, 50*, 98-113.

Masson, V., (2000). A physically-based scheme for the urban energy budget in atmospheric models. *Boundary-Layer Meteorology*, 94, 357–397.

Masson, V., Grimmond, C. S. B., & Oke, T. R. (2002). Evaluation of the Town Energy Budget (TEB) scheme with direct measurements from dry districts in two cities. *Journal of Applied Meteorology*, 41, 1011–1026.

Miller, M. J. (1978). The Hampstead storm: A numerical simulation of a quasi-stationary cumulonimbus system. *Quarterly Journal of the Royal Meteorological Society, 104*, 413-427. doi: 10.1002/qj.49710444014

Miller, S. D., Hawkins, J. D., Kent, J., Turk, F. J., Lee, T. F., Kuciauskas, A. P., . . . Hoffman, C. (2006). NexSat - Previewing NPOESS/VIIRS imagery capabilities. *Bulletin of the American Meteorological society, 87*(4), 433.

Nair, U. S., Hjelmfelt, M. R., & Pielke, R. A. (1997). Numerical Simulation of the 9–10 June 1972 Black Hills Storm Using CSU RAMS. *Monthly Weather Review, 125*, 1753-1766.

NOAA. (2012). Natural hazard statistics. from http://www.nws.noaa.gov/om/hazstats.shtml

Parker, M. D., & Johnson, R. H. (2000). Organizational modes of midlatitude mesoscale convective systems. *Monthly Weather Review, 128*(3413-3436).

Pielke, R. A., Cotton, W. R., Walko, R. L., Tremback, C. J., Lyons, W. A., Grasso, L. D., . . . Copeland, J. H. (1992). A comprehensive meteorological modeling system—RAMS. *Meteorology and Atmospheric Physics, 49*, 69-91.

Qari, M. H. T. (2009). Geomorphology of Jeddah Governorate, with Emphasis on Drainage Systems. *Journal of King Abdulaziz University: Earth Sciences, 20*(1), 93-116.

Raitsos, D. E., & Hoteit, I., Prihartato, P. K., Chronis, T., Triantafyllou, G., & Abualnaja, Y. (2011). Abrupt Warming of the Red Sea. *Geophysical Research Letters, 38*(5), L14601.

Romero, R., Doswell, C. A., & Ramis, C. (2000). Mesoscale Numerical Study of Two Cases of Long-Lived Quasi-Stationary Convective Systems over Eastern Spain. *Monthly Weather Review, 128*(11), 3731-3751.

Rosenfeld D., Lohmann, U., Raga, G.B., O'Dowd, C. D., Kulmala, M., Fuzzi, S., Reissell, A., & Andreae, M. O., (2008). Flood or Drought: How Do Aerosols Affect Precipitation? *Science, 321*, 1309-1313.

Rosenfeld D., Woodley, W. L., Khain, A., Cotton, W. R., Carrió, G., Ginis, I., & Golden, J. H., (2012). Aerosol effects on Microstructure and Intensity of Tropical Cyclones. *Bulletin of the American meteorological Society*, 2012, 987-1001.

S., N. U., Hjelmfelt, M. R., & Pielke-Sr., R. A. (1997). Numerical simulation of the 9-10 June 1972 Black Hills Storm using CSU RAMS. *Monthly Weather Review, 125*, 1753-1766.

Schumacher, R. S., & Johnson, R. H. (2005). Organization and Environmental Properties of Extreme-Rain-Producing Mesoscale Convective Systems. *Monthly Weather Review, 133*(4), 961-976.

Schwartz, C. S., Kain, J. S., Weiss, S. J., Xue, M., Bright, D. R., Kong, F., Kevin, T. W., Levit, J. J., & Coniglio, M. C. (2009). Next-day convection-allowing WRF model guidance: A second look at 2-km versus 4-km grid spacing. *Monthly Weather Review, 137*(10).

Sénési, S., Bougeault, P., Chèze, J. L., Cosentino, P., & Thépenier, R. (1996). The Vaison-la Romaine flash flood: meso-scale analysis and predictability issues. *Weather Forecasting, 11*(417-442).

Shmida, A. (1985). *Biogeography of the desert flora*. Amsterdam: Elsevier Science Publishers.

Smith, K., & Ward, R. (1998). *Floods – physical processes and human impacts*. Chichester, UK: John Wiley & Sons Ltd.

Subyani, A. M. (1999). Topographic and seasonal influences on precipitation variability in southwest Saudi Arabia. *Journal of King Abdulaziz University, 11*, 89-102.

Subyani, A. M. (2009). Hydrologic Behavior and Flood Probability for Selected Arid Basins in Makkah area, Western Saudi Arabia. *Arabian Journal of Geosciences, 4*(5-6), 817-824. doi: 10.1007/s12517-009-0098-1

Tremback, C. J. (1990). *Numerical simulation of a mesoscale convective complex: Model development and numerical results.* (PhD Diss.), Colorado State University, Fort Collins. (Atmospheric Science Paper No. 465)

Tripoli, G. J., & Cotton, W. R. (1982). The Colorado State University three-dimensional cloud=mesoscale model – 1982. Part I: General theoretical framework and sensitivity experiments. *Journal de recherches atmosphérique, 16*, 185-220.

van den Heever, S. C., Carrió, G. G., Cotton, W. R., DeMott, P. J., & Prenni, A. J. (2006). Impacts of nucleating aerosol on Florida storms. Part I: Mesoscale simulations. *Journal of Atmospheric Science, 63*, 1752-1775.

van den Heever, S. C., & Cotton, W. R. (2004). The impact of hail size on simulated supercell storms. *Journal of Atmospheric Science*, *61*, 1596-1609.

van den Heever, S. C., & Cotton, W. R. (2007). Urban Aerosol Impacts on Downwind Convective Storms. *Journal of Applied Meteorology and Climatology, 46*, 828-850.

Wang, C. (2005). A modeling study of the response of tropical deep convection to the increase of cloud condensation nuclei concentration: 1. Dynamics and microphysics. *Journal of geophysical research*. doi: 10.1029/2004JD005720

Weisman, M. L., Skamarock, W. C., & Klemp, J. B. (1997). The resolution dependence of explicitly modeled convective systems. *Monthly Weather Review, 125*(4).